Chapter 10

LOW PRANDTL NUMBER THERMAL-HYDRAULICS*

10.1 Introduction

This chapter is an introduction into the field of momentum and heat transfer in low Prandtl number fluids. In order to read this chapter a basic knowledge in fluid dynamics and thermodynamics is required. To limit the content not all formulas for technical configurations are listed; therefore much better literature sources are available in engineering libraries or other specific sources.

The first section illuminates the specific characteristics of the liquid metals, which represent the largest class of low Prandtl number fluids. Rather specific low Prandtl number fluids like ferromagnetic fluids or metal/oil suspensions are not considered in this context. It is clearly dedicated to the single phase thermal-hydraulics of liquid metals obeying the Newtonian law. The terminology used in this report as well as the conservation equations are part of Chapter 2.

In the sections three and four are restricted to the laminar momentum and heat transfer although they are not of major importance in technical applications they act in many situations as the upper or lower limit appearing in a technical set-up. Here, first the momentum transfer is described, because the convective heat transport is always coupled with the simultaneously appearing momentum transport. Analytic solutions like for tube or plate flow as well as self-similar solutions of the boundary layer equations and coupled approximate solutions are sketched. Especially the latter can be used to perform technically relevant problem solutions. For some technical configurations formulas or literature sources are given. Both paragraphs deal solely with the technically most relevant case, namely the forced convective flow, in which the flow is controlled by a shaping of the duct or by a supplied pressure gradient.

The sections five and six deal with the turbulent momentum and energy transport through channels and ducts. Due to the importance of this field most of the space is dedicated to it. Natural or buoyant convection are in many applications superposed to the forced convective thermal energy transport phenomena. These types of flows are called mixed convective flows and are analytically not accessible and even a numerical treatment requires a lot of effort. Hence, within the section six the author tries to indicate for which dimensionless parameter set a forced turbulent thermal energy transport exists and where the transition region starts. Buoyant or natural convection both for the laminar and the turbulent energy exchange are not considered in this context. Although two-phase flows as well as free surface flows gain more and more importance in technical applications this rather specific topic is also not treated in the framework of this collection.

* *Chapter lead: Robert Stieglitz (FZK, Germany). Thanks are due to the many researchers within the FZK (in expressis Dr. G. Grötzbach, Dr. U. Müller, Dr. H. Hoffmann, Prof. K. Rehme) and from outside (Prof. V. Sobolev, Dr. C.B. Reed) who helped by providing literature or allowing access to rare papers, and to Dr. Takizuka for the helpful discussion concerning this chapter.*

10.2 Specific features of liquid metals

Liquid metals are considered in many nuclear and non-nuclear processes associated with thermal-hydraulic aspects. In the nuclear field liquid metals are both used in fission and fusion concept studies. While in the nuclear fusion lithium or lithium alloys allow to merge the fuel generation problem with the heat removal from the fusion reaction, see e.g. [Malang, *et al*., 1992] in the nuclear fission the use of liquid metals is much broader. In the fast breeder concept for instance sodium is used as coolant while in newer breeder concepts often lead or lead alloys are used, since they ensure compared to sodium in any case that no positive void coefficient appears. A comprehensive study on the fuel and coolant aspects as well as their advantages and disadvantages may be taken from [David, 2005]. Also in the non-nuclear energy generation liquid metals are used as heat transfer medium in solar plants, where the sunlight is reflected by numerous mirrors onto a heat exchanger operated with liquid metals, see [Benemann, 1996]. In refinery and casting processes of metals like steel, copper, tin, aluminium etc., as well as glasses, which behave in the molten condition similar like liquid metals, the same heat transfer problems appear as in the power generation field.

The main difference between the metals and the other media is that they have a significantly higher thermal conductivity λ(W/mK) and lower specific heat capacity c_p [J/(kgK)]. In case of the heavy liquid metals like lead, lead-alloys or mercury often the kinematic viscosity ν (m^2/s) is considerably smaller than that of e.g. air or water. The thermal conductivity combined with the specific heat capacity can be compressed in a characteristic number the so-called Prandtl number *Pr*. The Prandtl number is an essential non-dimensional parameter in convective heat transfer problems. The physical sense of the Prandtl number is that it weights the transport coefficients of momentum to that of thermal energy. Thus, the Prandtl number describes the ratio of momentum diffusion to the thermal transport in the fluid and it is defined as:

$$Pr = \frac{\rho \nu c_p}{\lambda} = \frac{\nu}{\kappa} \quad \text{with} \quad \kappa = \frac{\lambda}{\rho c_p} \tag{10.1}$$

where c_p is the specific heat capacity, ρ the density (kg/m^3) and λ the thermal conductivity. κ is often called in textbooks the temperature conductivity or thermal diffusivity. In contrast to gases or light liquid the heat capacity hardly depends on the pressure.

While engine oils have usually Prandtl number of the order $O(10^2\text{-}10^6)$ and "conventional" media like air or water reveal an order of O(1) Prandtl number the liquid metals exhibits significantly smaller Prandtl numbers in the range $Pr = 10^{-3}\text{-}10^{-2}$. Table 10.2.1 shows the Prandtl number of e.g. mercury compared to air water or engine oil for different temperatures. There exists no Newtonian fluid in the range between the liquid metals and the gases for e.g. $0.05 < Pr < 0.5$.

Table 10.2.1. Typical Prandtl number for different fluids from [Beitz & Küttner, 1986]

Temperature	Mercury	Air	Water	Engine oil
0°C	0.0288	0.72	13.6	$4.7 \cdot 10^4$
20°C	0.0249	0.71	7.02	$1.0 \cdot 10^4$
100°C	0.0162	0.70	1.74	$2.6 \cdot 10^2$

Let us consider a flow of a Newtonian fluid with the temperature T_0 over a semi-infinite plate with the constant temperature T_w. In Figure 10.2.1 such a configuration is illustrated for fluids with $Pr << 1$, $Pr \sim 1$ and $Pr >> 1$. Case (a) refers to liquid metals, which have good conductivity and a low viscosity, it is $Pr << 1$. Here the thickness of the viscous boundary layer δ_v is negligibly small and to

Figure 10.2.1. Illustration of the influence of the Prandtl number on the magnitude of the viscous and thermal boundary layers in a two-dimensional flow over plate with the constant wall temperature T_w

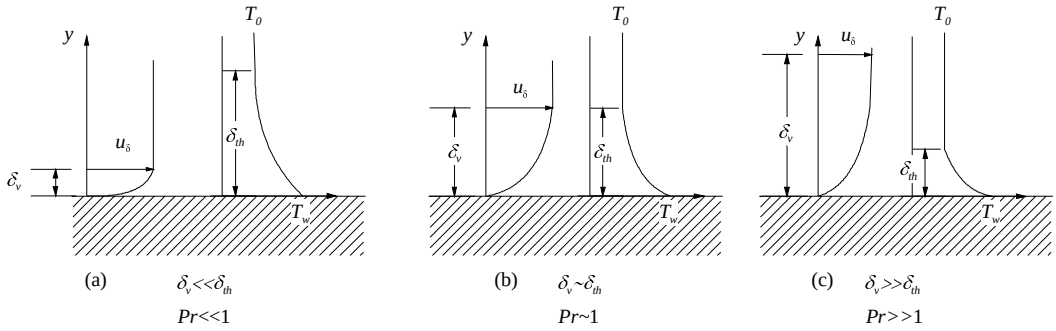

estimate the temperature boundary layer the velocity profile can be replaced by $u_\delta(x)$. In gas or water flows the thickness of the thermal and the viscous boundary layer are of the same order of magnitude, it is $Pr \sim 1$. Liquid like cool water (<20°C) and especially oils have poor thermal conductivity but their viscosity is relatively large, as shown in case (c). Here the viscous boundary determines almost the whole flow field.

In forced convective systems under laminar flow conditions, molecular conduction of heat expressed by the Prandtl number controls the thermal energy transfer process, irrespective of whether the coolant is a liquid metal or any other Newtonian fluid. Hence, there is no fundamental difference between the thermal behaviour of the three types of fluids described above under these conditions. And accordingly non-dimensional correlations developed to describe the heat transfer performance can be generally applied equally well to liquid metals in spite of their low Prandtl number.

Under turbulent flow conditions, however, eddy conduction of heat becomes important and the process of heat transfer is determined by both molecular and eddy conduction over the various flow regions in the fluid stream. While in ordinary fluids like air and water molecular conduction is only of importance near the wall (in the viscous sublayer), in a liquid metal the magnitude of the molecular conductivity is of the same order as that of the eddy conductivity. Thus, the molecular conduction is felt by the flow not only in the boundary layer but also to a significant extend in the turbulent core of the fluid stream. Therefore, the fundamental details of the heat transfer mechanism in liquid metals differ significantly from those observed for instance in air and as a result relationships (or correlations) developed to determine the heat transfer coefficients for turbulent flows obtained in those fluids cannot be used.

A further consequence of the even greater importance of molecular conduction of thermal energy in turbulent liquid metal flow is that the concept of the hydraulic diameter cannot be used so freely to correlate heat transfer data from systems which differ in configuration but retain a similar basic flow pattern. As an example in $Pr \sim 1$ fluids basic heat transfer data for flow through circular pipes can be used to predict Nusselt numbers (Nu) for flow parallel to a rod bundle by evaluating the hydraulic diameter for the latter and using this in the non-dimensional correlations for the circular tube. Such methods are found to be invalid for liquid metal systems, and accordingly theoretical, numerical or experimental heat transfer relationships must be developed to deal with each specific configuration, see [Reed, 1987] or [Dwyer, 1976].

Also a lot of effort has been dedicated to evaluate heat transfer coefficients in standard geometries in the recent years the available liquid metal heat transfer data show quite a bit of scatter. Several phenomena have been proposed to explain the scatter and the corresponding lack of correlation with

numerical predictions or theoretical approximations. They include: non-wetting or partial wetting of the fluid-solid interface, gas entrainment, the possibility of oxide formation or other surface contaminants, and mixed convection effects. Especially, the latter three influences the heat transfer considerably and by tracking numerous literature sources published in the past decades it turned out that they are mostly responsible for the existence of the large scatter. In this context it should be mentioned that for many liquid metal experiments a detailed description of the thermal and viscous boundary conditions is incomplete, which makes it difficult to judge about the applicability of the obtained data to draw estimation to more general geometries. And, even if great care is take on the boundary conditions in a pre- and post-test analyses of the experiment, in the heated state asymmetries in the set-up may appear leading to a co-existence between mixed and forced convection suggesting different heat transfer coefficients than under "clean" conditions, see [Lefhalm, *et al*., 2004].

Following an extensive amount of experimental investigations on the effects of wetting on the liquid metal heat transfer a general consensus has been reached on the subject. This is that wetting or lack of wetting, in or of itself, does not significantly affect liquid metal heat transfer. However, non-wetting combinations of liquid metals and solid surfaces can suffer more readily from gas entrainment problems and at elevated temperatures of oxidation at the solid liquid interface; impurities and particles can more easily become trapped at a non-wetting solid-liquid interface, thus reducing heat transfer. Hence care should be taken to avoid these problems in system designs. Finally, in liquid metal systems, uniform wall temperature boundary conditions (although difficult to obtain in the experiment) yield lower Nusselt numbers than constant wall heat flux boundary conditions for the same Peclet number. This is in contrast to $Pr \sim 1$-fluids, in which the two boundary conditions make only a little difference in the Nusselt number.

Related to the heavy liquid metals for many thermal-hydraulic configurations often no Nusselt number correlation exists. However, a lot of experiments in rather generic geometries were conducted for the sodium cooled fast breeder and in the context of the fusion engineering community using alkali metals as operation fluid. In many cases the Prandtl number of the individual fluids is close to the heavy liquid metals as shown in Figure 10.2.2. Nevertheless, great care has to be taken on the validity of the chosen heat transfer correlation even if the Prandtl number matches the heavy liquid metal considered, because the viscosity of the heavy liquid metals is considerably smaller than that of the alkali metals.

Figure 10.2.2. Molecular Prandtl number as a function of temperature in [°C] for different fluids

The thermophysical data for lead and lead-bismuth are taken from this book, while the data for sodium, the eutectic sodium-potassium alloy ($Na^{22}K^{78}$) are from [Foust, 1972], mercury (Hg) from [Lyon, 1952], lithium from [Addison, 1984], lead-lithium ($Pb^{83}Li^{17}$) from [Schulz, 1986] and [Smith, et al., 1984] and gallium-indium-tin from [Barleon, et al., 1996]

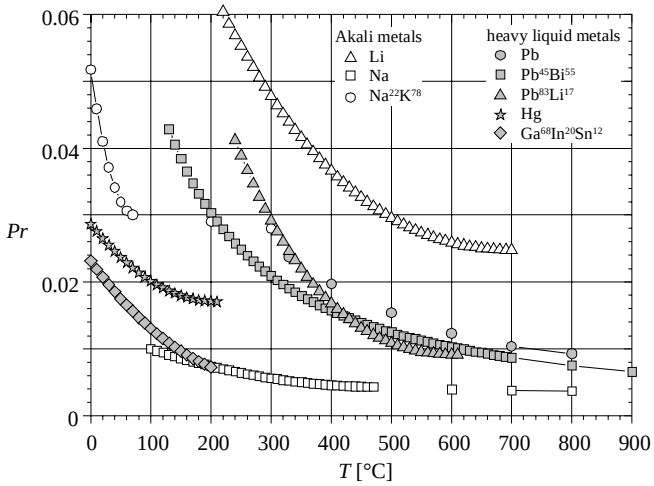

By multiplying the hydraulic Reynolds number *Re* with the Prandtl number *Pr* the Peclet number *Pe* is obtained which can be conceived as the ratio of the convective heat transport versus the molecular conduction. Both the Reynolds number and the Peclet number are defined as:

$$Re = \frac{u_0\, d}{\nu} \quad \text{and} \quad Pe = Re\, Pr = \frac{u_0\, d}{\kappa} \tag{10.2}$$

where u_0 is a characteristic velocity of the flow configuration considered and d a characteristic length scale of the problem. The Nusselt number correlations experimentally obtained can only then used for a heat transfer assessment or a transfer from an alkali metal to the heavy liquid metals if both Prandtl number and the valid Peclet number regime coincide.

10.3 The conservation equations

Within the context of this chapter we restrict ourselves to the consideration of flows in channels or closed cavities without the entrainment of an additional mass source or a mass transfer between different species.

Consider the flow of a single phase and single component fluid in a fixed control volume, then whole mass flow entering the volume must leave the volume. This is expressed by the continuity equation, which describes the conservation of mass. Because liquid metals below their boiling point are almost incompressible (ρ = const.) the continuity equation for them can be expressed by

$$\nabla \cdot \vec{u} = 0 \quad \text{or vectorial} \quad \frac{\partial u}{\partial x} + \frac{\partial v}{\partial y} + \frac{\partial w}{\partial z} = 0 \tag{10.3}$$

where $\vec{u}$ is the velocity vector composed of the velocity components (u,v,w) in x, y, and z-direction respectively and ($\nabla\cdot$) is the divergence operator.

The dynamic behaviour of fluid motion is governed by a set of equations called the momentum equations or the equation of motion. The derivation considering a defined control volume is similar to that of the continuity equations. The momentum equations can be written in the following form:

$$\begin{aligned}
\rho\left(\frac{\partial u}{\partial t} + u\frac{\partial u}{\partial x} + v\frac{\partial u}{\partial y} + w\frac{\partial u}{\partial z}\right) &= \rho\, f_x + \frac{\partial \sigma_{xx}}{\partial x} + \frac{\partial \tau_{yx}}{\partial y} + \frac{\partial \tau_{zx}}{\partial z} \\
\rho\left(\frac{\partial v}{\partial t} + u\frac{\partial v}{\partial x} + v\frac{\partial v}{\partial y} + w\frac{\partial v}{\partial z}\right) &= \rho\, f_y + \frac{\partial \tau_{xy}}{\partial x} + \frac{\partial \sigma_{yy}}{\partial y} + \frac{\partial \tau_{zy}}{\partial z} \\
\rho\left(\frac{\partial w}{\partial t} + u\frac{\partial w}{\partial x} + v\frac{\partial w}{\partial y} + w\frac{\partial w}{\partial z}\right) &= \rho\, f_z + \frac{\partial \tau_{xz}}{\partial x} + \frac{\partial \tau_{yz}}{\partial y} + \frac{\partial \sigma_{zz}}{\partial z}
\end{aligned} \tag{10.4}$$

where $f = (f_x, f_y, f_z)$ is a body force being of gravitational, electrical or magnetic origin, σ is the stress normal to the surface and τ the shear stress tangential to the sides of the control volume. It has been found experimentally that, to a high degree of accuracy, stresses in many fluids are related linearly to the rates of strain (derivatives of the velocity components). It can be shown, see e.g. [Lamb, 1945] or [Schlichting, 1979] that for Newtonian fluids the expressions are:

$$\sigma_{xx} = -p + 2\mu\frac{\partial u}{\partial x} - \frac{2}{3}\mu\nabla\cdot\vec{u}\,;$$
$$\sigma_{yy} = -p + 2\mu\frac{\partial v}{\partial y} - \frac{2}{3}\mu\nabla\cdot\vec{u}\,;$$
$$\sigma_{zz} = -p + 2\mu\frac{\partial w}{\partial z} - \frac{2}{3}\mu\nabla\cdot\vec{u}\,;$$
$$\tau_{xy} = \tau_{yx} = \mu\left(\frac{\partial v}{\partial x} + \frac{\partial u}{\partial y}\right); \quad \tau_{xz} = \tau_{zx} = \mu\left(\frac{\partial w}{\partial x} + \frac{\partial u}{\partial z}\right); \quad \tau_{yz} = \tau_{zy} = \mu\left(\frac{\partial w}{\partial y} + \frac{\partial v}{\partial z}\right) \tag{10.5}$$

where $\mu = \rho\cdot\nu$ is the dynamic viscosity of the fluid and p the pressure. Substituting the Eq. (10.5) into (10.4) yields the full momentum equations, which are called the Navier-Stokes equations. Nearly all analytical investigations involving viscous fluids are based on them. They are general in the sense that they are valid for compressible Newtonian fluids with varying viscosity.

When the density and the viscosity are constant – that is, when the fluid is incompressible and the temperature variations are small – the Navier-Stokes equations simplify to:

$$\rho\left(\frac{\partial u}{\partial t} + u\frac{\partial u}{\partial x} + v\frac{\partial u}{\partial y} + w\frac{\partial u}{\partial z}\right) = \rho\, f_x - \frac{\partial p}{\partial x} + \mu\left(\frac{\partial^2 u}{\partial x^2} + \frac{\partial^2 u}{\partial y^2} + \frac{\partial^2 u}{\partial z^2}\right) \quad ;$$
$$\rho\left(\frac{\partial v}{\partial t} + u\frac{\partial v}{\partial x} + v\frac{\partial v}{\partial y} + w\frac{\partial v}{\partial z}\right) = \rho\, f_y - \frac{\partial p}{\partial y} + \mu\left(\frac{\partial^2 v}{\partial x^2} + \frac{\partial^2 v}{\partial y^2} + \frac{\partial^2 v}{\partial z^2}\right) \quad ; \tag{10.6}$$
$$\rho\left(\frac{\partial w}{\partial t} + u\frac{\partial w}{\partial x} + v\frac{\partial w}{\partial y} + w\frac{\partial w}{\partial z}\right) = \rho\, f_z - \frac{\partial p}{\partial z} + \mu\left(\frac{\partial^2 w}{\partial x^2} + \frac{\partial^2 w}{\partial y^2} + \frac{\partial^2 w}{\partial z^2}\right)$$
$$\text{or in the vectorial notation} \qquad \frac{d\vec{u}}{dt} = f - \frac{1}{\rho}\nabla p + \nu\nabla^2\vec{u}$$

where $\nabla^2 = \nabla\cdot\nabla$ is the Laplacian operator given by $\nabla^2 = (\partial/\partial x^2 + \partial/\partial y^2 + \partial/\partial z^2)$.

Any fluid flow problem which involves the determination of the velocity components and the pressure distribution as a function of the spatial co-ordinates and the time requires simultaneously the solution of the continuity equation and the Navier-Stokes equations under the specific boundary and initial conditions. Although these set of equations are in most cases too complex to be solved analytically they may be solved by numerical means. Nevertheless, there exist some cases where the nature of the flow is such that they can be simplified considerably for an analytical solution.

A similar approach as for momentum and continuity equation derivation can be applied to deduce the energy equations. This derivation implies the first law of thermodynamics, which couples the thermal energy with the work done by the system and the total internal energy of the control volume. The complete derivation of the energy equation is described in the textbooks by [Keenan, 1941], [Van Vylen and Sonntag, 1979] or [Jischa, 1982]. The thermal energy equation finally reads to:

$$\rho\frac{du}{dt} = \nabla\cdot(\lambda\nabla T) + \sigma_{xx}\frac{\partial u}{\partial x} + \sigma_{yy}\frac{\partial v}{\partial y} + \sigma_{zz}\frac{\partial w}{\partial z} + \tau_{xy}\left(\frac{\partial v}{\partial x} + \frac{\partial u}{\partial y}\right) + \tau_{yz}\left(\frac{\partial w}{\partial y} + \frac{\partial v}{\partial z}\right) + \tau_{xz}\left(\frac{\partial u}{\partial z} + \frac{\partial w}{\partial x}\right) \tag{10.7}$$

in which λ is the thermal conductivity of the fluid, u the internal energy the and T the temperature. The internal energy is liked to the fluid enthalpy i by $I = \mathsf{u} + p/\rho$. The operator d/dt denotes the total derivative. If the relations for stress and strain acting upon a fluid element in a Newtonian fluid [Eq. (10.5)] are substituted into Eq. (10.7), it reduces to:

$$\rho \frac{d\mathsf{u}}{dt} = \nabla \cdot (\lambda \nabla T) - p \nabla \cdot \vec{u} + \mu \Phi \quad \text{with} \tag{10.8}$$

$$\Phi = 2\left[\left(\frac{\partial u}{\partial x}\right)^2 + \left(\frac{\partial v}{\partial y}\right)^2 + \left(\frac{\partial w}{\partial z}\right)^2\right] + \left(\frac{\partial v}{\partial x} + \frac{\partial u}{\partial y}\right)^2 + \left(\frac{\partial w}{\partial y} + \frac{\partial v}{\partial z}\right)^2 + \left(\frac{\partial u}{\partial z} + \frac{\partial w}{\partial x}\right)^2 - \frac{2}{3}\left(\nabla \cdot \vec{u}\right)^2$$

where u is the internal energy of the fluid per unit mass and Φ is called the dissipation function. The first term on the right hand side represents the net rate of heat conduction to the fluid particle per control volume, the second term is the rate of reversible work done on the control volume and the last term is the rate at which viscous forces do irreversible work in form of e.g. viscous dissipation or viscous heating per unit volume.

If one considers an incompressible fluid with $d\mathsf{u} = c_p \cdot dT$ the energy equation takes the form:

$$\rho c_p \frac{dT}{dt} = \nabla(\lambda \nabla T) + \mu \Phi \quad \text{with} \tag{10.9}$$

$$\Phi = 2\left[\left(\frac{\partial u}{\partial x}\right)^2 + \left(\frac{\partial v}{\partial y}\right)^2 + \left(\frac{\partial w}{\partial z}\right)^2\right] + \left(\frac{\partial v}{\partial x} + \frac{\partial u}{\partial y}\right)^2 + \left(\frac{\partial w}{\partial y} + \frac{\partial v}{\partial z}\right)^2 + \left(\frac{\partial u}{\partial z} + \frac{\partial w}{\partial x}\right)^2$$

Additionally, if the thermal conductivity λ is constant it reduces to:

$$\frac{dT}{dt} = \frac{\lambda}{\rho c_p} \nabla^2 T + \frac{\mu}{\rho c_p} \Phi \tag{10.10}$$

The continuity, Navier-Stokes and energy equations provide a comprehensive description of the thermal energy transfer in a flow field. These equations, however, present insurmountable mathematical difficulties due to the number of equations to be simultaneously satisfied and the presence of non-linear terms such as $u\partial u/\partial x$. Because of these non-linearities, the superposition principle is not applicable and complex flows may not be compounded from simple flow as e.g. possible for potential flows, see [Schlichting and Truckenbrodt, 1960]. Exact solutions were obtained for some simple cases, where the nonlinear terms are either small (approximate solutions) or identically zero. This class of solution appears in slow motion or creeping flows and is important for the theory of lubrication. In most practical heavy liquid metal applications the nonlinear terms are most often of greater magnitude than the other terms in the Navier-Stokes equations. The hydraulic Reynolds number defined in Eq. (10.2) is a dimensionless quantity which measures the ratio of the inertia effects to the viscous effects in a fluid. Creeping flows are therefore characterised by small Reynolds numbers, whereas in most practical flows the Reynolds number is far above unity. Finally, two important observations are worth mentioning. First, the velocity and temperature fields will be coupled if the fluid has a temperature dependent density and/or viscosity. Secondly the temperature field can become similar to the field under certain conditions. If $\nabla p = 0$, $\Phi = 0$ and $f = 0$ and if $Pr = 1$ then the solutions for the velocity and temperature fields are similar, provided that the boundary conditions are also similar. But as shown in Section 10.2 for any liquid metal flow the molecular Prandtl number is far below unity so that a similarity of both fields does practically not appear.

10.4 Laminar momentum exchange

This subsection is dedicated to describe the basic concepts to treat the laminar momentum exchange. The main aim is to obtain the local friction coefficient $c(x)$ of a flow in a geometry and the main ideas for the simplification of the Navier-Stokes equations in terms of an asymptotic approach. The results obtained in this chapter are necessary to elaborate the difference between the laminar and the turbulent flow and they form the basis for the understanding of the heat transfer phenomena appearing in both types of flows.

The laminar momentum exchange of a steady two-dimensional flow of an incompressible fluid with a constant kinematic viscosity ν is governed by the following equations:

$$\begin{aligned} &\frac{\partial u}{\partial x}+\frac{\partial v}{\partial y}=0 \quad , \\ u\frac{\partial u}{\partial x}+v\frac{\partial u}{\partial y}&=-\frac{1}{\rho}\frac{\partial p}{\partial x}+\nu\left(\frac{\partial^2 u}{\partial x^2}+\frac{\partial^2 u}{\partial y^2}\right) \quad ; \\ u\frac{\partial v}{\partial x}+v\frac{\partial v}{\partial y}&=-\frac{1}{\rho}\frac{\partial p}{\partial y}+\mu\left(\frac{\partial^2 v}{\partial x^2}+\frac{\partial^2 v}{\partial y^2}\right) \end{aligned} \tag{10.11}$$

This represents a system of partial non-linear differential equations of the elliptic type. A general solution does not exist and there are only a few exact solutions under rather restrictive boundary conditions like the channel or duct flow. Fortunately, most of the laminar momentum exchange processes can be simplified considerably. For large Reynolds numbers nearly all exchange processes take place in a thin layer, the so-called boundary layer. The boundary layer approximation is not restricted to flows over solid walls, also free jets or wake flows exhibit boundary layer character.

10.4.1 Channel or tube flow

Consider a steady planar fully developed flow in a duct as shown in Figure 10.4.1. Here fully developed means that the velocity component u in x-direction does not change. Because $\partial u/\partial x = 0$ also $\partial v/\partial y = 0$, which means that the v-component of the velocity is constant. Excluding suction or blowing immediately yields that $v = 0$. For Eqs. (10.11)b, c the convective terms on the left side diminish and from the force balance (10.11)c only the expression $\partial p/\partial y = 0$ remains. Thus, the pressure p depends only from the flow direction x and the force balance in flow direction reads to:

$$\frac{dp}{dx}=\mu\frac{d^2u}{dy^2}=\frac{d\tau}{dy} \tag{10.12}$$

and since u is only a function of y the partial derivative ∂ can be replaced by the simple derivative d. From the stress tensor only $\tau = \mu\partial u/\partial y$ remains. An integration immediately yields that the shear stress is linear and due to symmetry, which requires $\tau(y = H) = 0$ one obtains:

$$\tau_w=-\frac{dp}{dx}H \tag{10.13}$$

This correlates the wall shear stress with the pressure gradient. In dimensionless form it reads to:

$$\frac{\tau(y)}{\tau_w} = 1 - \frac{y}{H} \tag{10.14}$$

With $\tau = \mu \partial u/\partial y$ and a further integration the velocity distribution is obtained. Setting $u(y = H) = u_{max}$ yields:

$$u_{max} = \frac{\tau_w H}{2\mu} = -\frac{dp}{dx}\frac{H^2}{2\mu} = \frac{\Delta p H^2}{2\mu L} \tag{10.15}$$

where $\Delta p/L = -dp/dx$ is the pressure drop along the channel length L. Finally the dimensionless velocity distribution reads to:

$$\frac{u}{u_{max}} = \frac{y}{H}\left(2 - \frac{y}{H}\right) \tag{10.16}$$

which is the classical parabolic Hagen-Poiseuille profile.

Figure 10.4.1. Shear stress and velocity distribution of a fully developed channel flow for a planar duct and a circular pipe

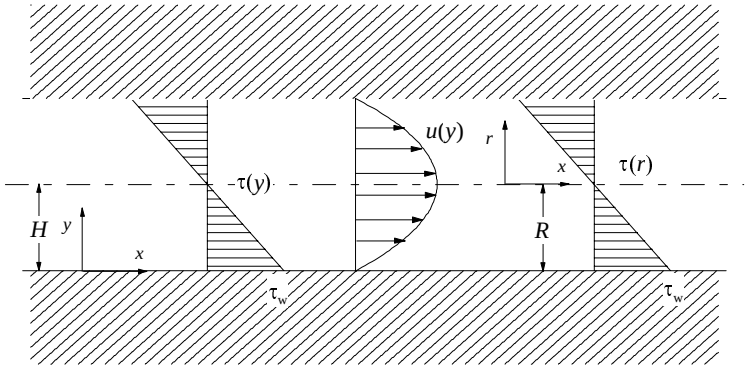

The same result is obtained for the fully developed laminar circular duct flow using the same procedure. Without describing the full details the following set is obtained for the configuration shown in Figure 10.4.1:

$$\frac{\tau(r)}{\tau_w} = \frac{r}{R}; \quad u(r) = \frac{\Delta p}{4\mu L}\left(R^2 - r^2\right); \tag{10.17}$$

$$u_{max} = \frac{\Delta p R^2}{4\mu L}; \frac{u}{u_{max}} = 1 - \left(\frac{r}{R}\right)^2$$

Here, R is the radius of the pipe and r the radial co-ordinate.

The factor ½ is explained by the fact that in a tube flow compared to a channel flow a ratio the cross-section on which the pressure acts is twice as large as the surface on which the viscous forces act to compensate the pressure. The flow rate V in a circular tube can be calculated to:

$$V = \int_{r=0}^{r=R} 2\pi r\, u(r)\, dr = \frac{\pi \Delta p R^4}{8 \mu L} \tag{10.18}$$

It is important to note the dependencies $V \sim \Delta p/L$ and $V \sim R^4$. For the same applied pressure gradient an increase of the diameter by 10% yields an increase of the flow rate of 46%. If one defines a mean velocity u_0 by applying $u_0 = V/A$ one obtains $u_0 = ½\, u_{max}$. For engineering purposes the pressure loss is one of the most interesting parameters. Taking $V = u_0 \pi R_2$ and using the diameter $D = 2R$, one gets for the pressure drop over a duct length of L:

$$\Delta p = \frac{\rho}{2} u_0^2 \, \frac{L}{D} \frac{64}{Re} \tag{10.19}$$

Defining a friction coefficient c_L in the way $\Delta p = \rho/2\, L/D\, u_0^2$ one obtains the friction law for a tube flow expressed by:

$$c_L = \frac{64}{Re} \tag{10.20}$$

Herein Re is the hydraulic Reynolds number defined as $Re = u_0 D/\nu$, which can be conceived as a force ratio of the inertial forces versus the viscous ones. This shows simply, how the pressure drop and the friction coefficient depend on the Reynolds number. The Reynolds number is in all momentum exchange processes the only appearing variable. Thus, for all laminar flows the Reynolds number correlations of any other liquid can be used and transferred to heavy liquid metals.

10.4.2 Boundary layer equations

The basis for the derivation of the boundary layer equations is the equation set (10.11)a-c. Figure 10.4.2 shows the used local co-ordinate system and the observed velocity distribution. The order of thickness of the boundary layer is *a priori* not known; the following assessment is aimed to give an estimate on this magnitude.

Figure 10.4.2. Co-ordinate system and observed velocity distribution

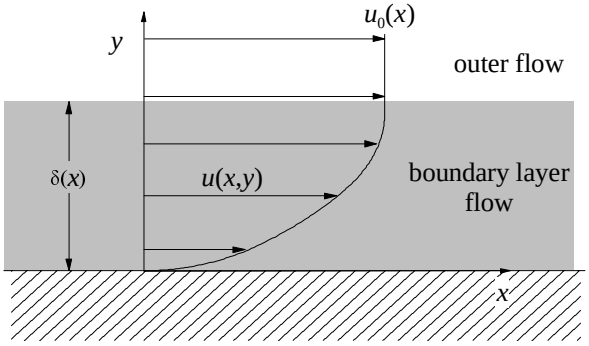

First we introduce the dimensionless variables in the following way:

$$x' = \frac{x}{L}; \quad y = \frac{y}{\delta(x)}; \quad u' = \frac{u}{u_0}; \quad p' = \frac{p}{\rho_0 u_0^2} \tag{10.21}$$

which are chosen in such a way that they are of order one in magnitude O(1). In a next step the length L and the mean velocity u_0 of the outer flow are taken as reference quantities. Further on there is:

$$v' = \frac{v}{u_0}; \quad \rho' = \frac{\rho}{\rho_0} = 1 \text{ (because } \rho = \text{const.)} \tag{10.22}$$

Introducing these variables into the continuity Eq. (10.11)a the following declaration can be made:

$$\frac{v}{u_0} \sim \frac{\delta}{L} \tag{10.23}$$

because u', x' and y' are of O(1). Introducing the variables into the Navier-Stokes Eq. (10.11)b in x-direction leads to the result that as determining parameter the Reynolds number appears, which characterises viscous flows. Returning to the assessment and postulating that the viscous terms are of the same order of magnitude as the inertial terms and the pressure force immediately yields that the thickness of the boundary layer scales as:

$$\frac{\delta}{L} \sim \frac{1}{\sqrt{Re}} \tag{10.24}$$

A similar insertion of the non-dimensional scaling into Eq. (10.11)c (in y-direction) exhibits the assertion that for $Re >> 1$ the derivative of the pressure in y-direction diminishes. This means that the pressure normal to the wall does not change within the boundary layer; it is rather given by the value from the inviscid outer potential flow. The pressure p in boundary layer theory is not an unknown quantity it is rather given as a boundary condition. All these order of magnitude estimates lead to the boundary layer equations, which were initially written by Ludwig Prandtl in 1904.

$$\begin{aligned} &\frac{\partial u}{\partial x} + \frac{\partial v}{\partial y} = 0 \quad , \\ &u\frac{\partial u}{\partial x} + v\frac{\partial u}{\partial y} = -\frac{1}{\rho}\frac{dp(x)}{dx} + \nu\frac{\partial^2 u}{\partial y^2} \end{aligned} \tag{10.25}$$

These are two equations to determine the unknowns u, $v = f(x,y)$. Because of Bernoulli's equation $p(x) + \rho/2 \cdot u_0^2(x) = \text{const.}$ the pressure and the velocity gradient of the inviscid outer flow are coupled. The boundary conditions of the equation system are:

$$\begin{aligned} &y = 0: \quad u = v = 0 \quad , \\ &y = \delta: \quad u = u_0(x) \end{aligned} \tag{10.26}$$

The system of the boundary layer equations is parabolic and represents an initial boundary problem. Due to the simplification of the viscous terms diffusion processes are only active in the y-direction. There is no upstream flux of information and all can be calculated straight forwards downstream. This is an enormous simplification compared to the elliptic Navier-Stokes equations, for which a simultaneous solution for all domains is required. There are some exact and approximate solutions of the boundary layer equations which can be found in [Schlichting, 1979] or [Jischa, 1982].

10.4.3 Summary and comments

The main aim to treat the laminar momentum equations is to determine the local $c_L(x)$ and/or the global friction coefficient c_W. Many textbooks show that these values can be given in a form $c_L(x) = f(Re_x^m)$ or $c_W = f(Re_L^n)$.

Herein, Re_x is the local Reynolds number and Re_L the Reynolds number built with the characteristic dimension of the body. For a duct or a tube flow $n = -1$ is obtained. The friction coefficient does not change in flow direction for a fully developed flow. This is different to a boundary layer flow along a plate, because there the boundary layer thickness grows along the flow direction x while the local friction coefficient decreases with x. In this case the local friction coefficient yields an exponent $m = -1/2$ and the total resulting friction coefficient exhibits a coefficient $n = -1/2$. Crucial in this context is that the only appearing dimensionless quantity is the Reynolds number, which can be conceived as the ratio of the inertial forces versus the viscous ones. For a fully developed flow the inertial force is replaced by the driving pressure gradient.

One can distinguish between different approaches to describe laminar flows:

- *Analytic solutions of the Navier-Stokes equations* can be only obtained for a few rather specific exceptions like the plane duct or the circular pipe flow.
- *Numeric solutions of the Navier-Stokes equations* are extremely time consuming. Here, a system of non-linear partial differential equations of the elliptic type must be solved. This is a boundary value problem and no consecutive methods like for parabolic partial differential equations can be applied. For some technically interesting cases like the developing flow into a tube or the flow near the leading edge of a plate, calculations were performed. In the engineering practice, however, these solutions are of minor importance. In the limiting case $Re \rightarrow \infty$ the Navier-Stokes equations mutate into the boundary layer equations. In many practically important cases the Reynolds number is large enough to apply the boundary layer equation. An exception in this context is the leading edge problem for which the prerequisite $d\delta/dx << 1$ and $\partial^2/\partial x^2 << \partial^2/\partial y^2$ is not fulfilled.
- *Exact solutions of the boundary layer equation* exist only for specific outer flows acting as boundary condition. The terminology exact means that this is not an analytic but an arbitrarily exact numeric solution of an ordinary differential equation. In case of the self-similar solutions the individual velocity profile does not alter its shape in flow direction and it can by an appropriate co-ordinate transformation reduced to the similar profile.

For an arbitrary outer flow the velocity profile changes its shape in flow direction; there exist no self-similar solutions and the boundary layer equation can only be solved numerically. This can be performed in two ways.

- *Numeric solutions of the boundary layer equations* exist for numerous cases. By means of difference methods the parabolic boundary layers equation can be numerically integrated as a initial boundary problem using a consecutive approach. Because of stability reasons implicit methods although they require more effort are preferred compared to simpler explicit schemes. The problems arising using the individual techniques are in detailed discussed in the book of Cebeci and Bradshaw (1977).
- *Integral schemes to solve the boundary layer equation*s are simple to treat and practically most often used. Often used are the schemes by Pohlhausen und v. Karman. The effort required for computing time as well as the memory consumption low. Also the solution of two coupled

non-linear ordinary differential equations is not problematic. These integral methods are still in use to calculate especially turbulent boundary layers. An exhaustive discussion on the different types of numeric approaches may be taken in the monograph by Walz [1966]. Despite the undeniable advantages of the integral methods one crucial disadvantage exists; the quality of the achieved results depends on the assumption of the chosen profile. The user must know a lot of properties of the solution in order to formulate an appropriate profile.

Empirical solutions must be used in all cases where complex geometries do not allow a direct numerical solution.

Finally, for completeness two problem circles should be shortly mentioned. This is the higher order boundary layer theory. This is a perturbation theory which is called the matched asymptotic expansions. It is a further development of Prandtl's boundary layer concept, where the boundary layer equation is the first order equation in the hierarchy. Effects of higher order like inclinations, etc., can be treated in this kind of concept. An overview on the different model ideas is given in the books by [Van Dyke, 1975] or [Cole, 1968]. The not treated rather complex issue are three-dimensional boundary layers, which appear in many technical applications. Here, the gracious reader should refer to the text books, e.g. [Schlichting, 1979] or [White, 1974].

10.5 Laminar energy exchange

In a moving fluid energy and momentum are exchanged if:

a) thermal energy is supplied to or removed from the fluid;

b) the kinetic energy of the flow is of the order of the inner energy so that by dissipation the temperature of the fluid is increased.

In Case (a) one distinguishes between forced and free convective flows. In forced convective flows an external forcing bean means of a supplied pressure gradient or a given outer flow is present, while in free or natural convection flows buoyancy forces caused by density differences (which are originating from temperature differences) are the driving source of the flow. Restricting ourselves to steady flows of single component Newtonian fluids one obtains the energy equation in the form described in Eq. (10.8) (see Section 10.3). The set of equations to be solved for the laminar energy exchange reads to:

$$\frac{\partial u}{\partial x}+\frac{\partial v}{\partial y}=0;\ \rho\left(u\frac{\partial u}{\partial x}+v\frac{\partial u}{\partial y}\right)=-\frac{\partial p}{\partial x}+\mu\left(\frac{\partial^2 u}{\partial x^2}+\frac{\partial^2 u}{\partial y^2}\right)+\rho g_x; \tag{10.27}$$

$$\rho\left(u\frac{\partial v}{\partial x}+v\frac{\partial v}{\partial y}\right)=-\frac{\partial p}{\partial y}+\mu\left(\frac{\partial^2 v}{\partial x^2}+\frac{\partial^2 v}{\partial y^2}\right)+\rho g_y;$$

$$\rho c_p\left(u\frac{\partial T}{\partial x}+v\frac{\partial T}{\partial y}\right)=\lambda\left(\frac{\partial^2 T}{\partial x^2}+\frac{\partial^2 T}{\partial y^2}\right)+u\frac{\partial p}{\partial x}+v\frac{\partial p}{\partial y}+\Phi$$

where the heat conductivity λ is assumed to be constant, g is the gravity vector in the form $g = (g_x, g_y)$ and Φ is the dissipation function defined in Eq. (10.9)b.

This section deals with the laminar flow and forced convection heat transfer characteristics of a variety of ducts interesting to heating and cooling devices in nuclear engineering. The results presented here are applicable to straight ducts with axially unchanging cross-sections. Also the duct

walls are considered smooth, non-porous, rigid, stationary and wetted. Furthermore, the duct walls are assumed to be uniformly thin, so that the temperature distribution within the solid walls has negligible influence on the convective heat transfer in the flowing fluid. Thus this section covers the steady, incompressible laminar flow of a constant property Newtonian fluid. All forms of body forces are neglected; moreover, the effects of natural convection, phase change, mass transfer or chemical reactions are omitted. A complete representation of the laminar heat transfer correlations and a detailed description of the methods can be found in the monographs by [Shah and London, 1978].

10.5.1 Types of laminar duct flow

Four types of laminar duct flows exist; namely, fully developed, hydrodynamically developing, thermally developing, and simultaneously developing. The latter means that the flow is at the same time hydrodynamically developing and thermally developing. A brief description of these flows is given here with an aid in Figure 10.5.1, which depicts a fluid with the uniform velocity u_0 and temperature T_0 entering a duct of an arbitrary cross-section at $x = 0$.

Figure 10.5.1. Types of laminar duct flow for constant wall temperature boundary condition

(a) Hydrodynamically developing flow followed by thermally developing (and hydrodynamically developed) flow
(b) Simultaneously developing flow in liquid metals (Pr << 1)
Solid lines denote the velocity distribution while the dotted grey lines represent the temperature profiles

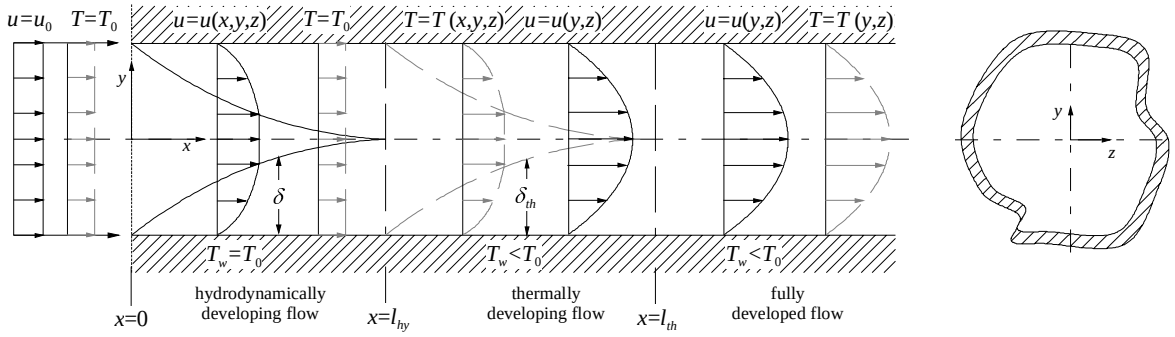

(a)

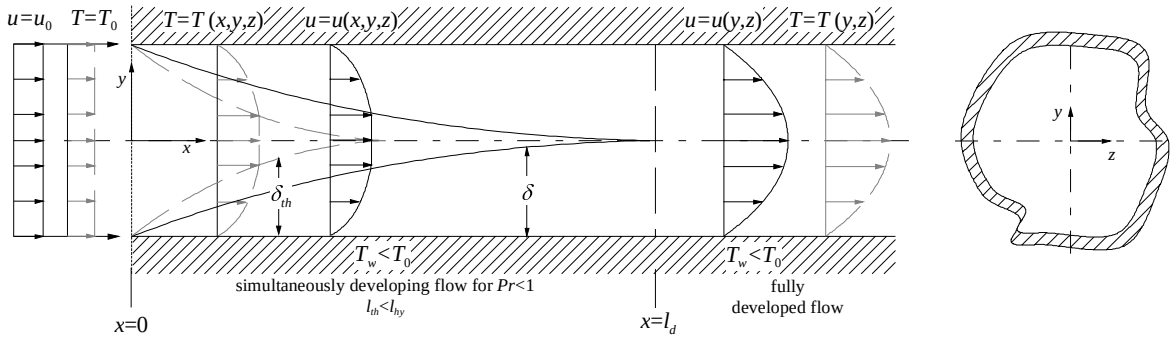

(b)

Referring to Figure 10.5.1, suppose that the temperature of the duct wall is kept at the entering fluid temperature T_0 and there is no generation or dissipation of heat within the fluid. In this case the fluid experiences no gain or loss of thermal energy. In such a case of an isothermal flow, the effect of viscosity spreads across the ducts cross-section commencing at $x = 0$. The hydrodynamic boundary layer develops according to Prandtl's boundary layer theory (see Subsection 10.4.2) and its thickness δ

grows proportional to $Re_x^{-1/2}$. The boundary layer separates the flow field in two domains; a viscous region near the wall and an essentially inviscid region around the ducts centreline. At $x = l_{hy}$ the viscous effects have completely spread across the wholes ducts cross-section. The domain $0 \le x \le l_{hy}$ is called the hydrodynamic entrance region and the flow in this domain is called the hydrodynamically developing flow. In the entrance region the velocity depends on all three spatial co-ordinates, while for $x > l_{hy}$ the velocity profile is independent of the axial co-ordinate x. After the flow becomes hydrodynamically developed consider that the duct wall temperature is dropped compared to the entering fluid $T_w < T_0$. In this case the thermal effects diffuse gradually from the duct wall commencing at $x=l_{hy}$. The extent of the thermal diffusion is denoted by the thickness of the thermal boundary layer δ_{th}, which grows along the axial co-ordinate x. A similarity analysis based on the boundary layer approximation approach immediately reveals that the thermal boundary layer grows as $\delta_{th}(x) \sim (Re \cdot Pr)^{-1/2}$. Moreover, applying the boundary layer approach the thermal boundary layer also divides the flow field in two regions; a heat affected region close to the wall and an unaffected domain in the ducts centre. A result of the dimensional analysis is also that the ration of the thermal boundary compared to the viscous one scales as:

$$\frac{\delta_{th}}{\delta} \sim \frac{1}{\sqrt{Pr}} \tag{10.28}$$

At $x = l_{th}$ the thermal effects have spread throughout the whole ducts cross-section and beyond this point the flow is called thermally developed. The region $l_{hy} \le x \le l_{th}$ is termed the thermal entrance region. Here the temperature varies with all three spatial co-ordinates. The simultaneously developing flow is displayed in the lower graph of Figure 10.5.1 for a liquid metal. In this case the viscous and the thermal effects diffuse simultaneously from the duct wall towards the ducts centre commencing at $x = 0$. The essential parameter here is the Prandtl number, which denotes the ratio of the kinematic viscosity to thermal diffusivity. The kinematic viscosity is the diffusion rate for momentum (velocity) in the same sense that the thermal diffusivity is the diffusion rate for heat (temperature). If $Pr = 1$, the viscous and thermal diffuse through the fluid at the same rate. This equality of diffusion rates does not guarantee that the viscous and thermal boundary layers in close duct flows will be of the same thickness at defined axial position x. The reason for this paradox lies in the fact that with $Pr = 1$, the applicable momentum and energy differential equations do not become analogous. As depicted in the Figure 10.5.1(b), within the region $0 \le x \le l_d$ viscous and thermal effects spread simultaneously towards the duct centre. Accordingly, this region is referred to as the combined entrance region. It is obvious that the length l_d depends on the Prandtl number. In this region both velocity and temperature depend on all three space co-ordinates. Only for $x > l_d$ when the flow is fully developed the temperature and velocity become axially invariant and depend only on y and z, i.e. $u = u(x,y)$ and $T = T(x,y)$.

10.5.2 Fluid flow and heat transfer parameters

The fluid flow characteristics of all duct flows is expressed in terms of certain hydraulic parameters. For the hydrodynamically developing flow, the dimensional axial distance x^+ is defined as:

$$x^+ = \frac{1}{Re}\frac{x}{d_h} \tag{10.29}$$

where d_h is the hydraulic diameter defined by $d_h = 4A/P$ with A the ducts cross-section and P the wetted perimeter. The hydrodynamic entrance length l_{hy} is defined as the axial distance required to attain 99% of the ultimate fully developed maximum velocity when the entering flow is uniform. The dimensionless hydrodynamic entrance length is expressed by $l_{hy}^+ = l_{hy}/(d_h \cdot Re)$.

The fluid bulk mean temperature, also referred to as the “mixing cup” or flow average temperature T_m is defined as:

$$T_m = \frac{1}{A\,u_0}\int_A u\,T\;dA \tag{10.30}$$

The circumferentially averaged but axially local heat transfer coefficient α_x is defined by:

$$q_{w,x} = \alpha_x \left(T_{w,m} - T_m\right) \tag{10.31}$$

where $T_{w,m}$ is the wall mean temperature and T_m is the fluid bulk mean temperature given by Eq. (10.30). The heat flux q_w and the temperature difference $(T_{w,m} - T_m)$ are by nature vector quantities. In the notation (10.31) the direction of heat transfer is from the wall to the fluid, and consistently the temperature drop is from the wall to the fluid. In contrast, if q_w represents the heat flux from the fluid to the wall the temperature difference entering Eq. (10.31) will be $(T_m - T_{w,m})$. The flow length averaged heat transfer coefficient α_m is the integrated value from $x = 0$ to x in the way:

$$\alpha_m = \frac{1}{x}\int_{x=0}^{x=x}\alpha_x\;dx \tag{10.32}$$

The ratio of the convective conductance α to the pure molecular conductance λ/d_h is defined as a Nusselt number *Nu*. The circumferentially averaged but axially local Nusselt number Nu_x is defined as:

$$Nu_x = \frac{\alpha_x\,d_h}{\lambda} = \frac{q_{w,x}\,d_h}{\lambda\left(T_{w,m} - T_m\right)} \tag{10.33}$$

Thus the Nusselt number is nothing else than the dimensionless temperature gradient at the wall. The Nusselt number can also be conceived as a ratio of two different lengths, namely the ratio of the characteristic length to the local thickness of the thermal boundary layer. The mean Nusselt number Nu_m based on α_m in the thermal entrance region reads to:

$$Nu_m = \frac{1}{x}\int_0^x Nu_x\;dx = \frac{\alpha_m\,d_h}{\lambda} = \frac{q_{w,m}\,d_h}{\lambda\left(\Delta T\right)_m} \tag{10.34}$$

The expression for $(\Delta T)_m$ could become complicated and depend upon the thermal boundary conditions. The dimensionless axial distance x^* is defined as:

$$x^* = \frac{1}{Pe}\frac{x}{d_h} = \frac{1}{RePr}\frac{x}{d_h} \tag{10.35}$$

The thermal entrance length l_{th} is defined as the axial distance required to achieve a value of the local Nusselt number Nu_x, which is 1.05 times the fully developed Nusselt number value. The dimensionless thermal entrance length is expressed as $l_{th}^* = l_{th}/(d_h \cdot Pe)$.

Also often the Stanton number *St* is used. It describes the ratio of the heat flux transferred from the wall to the enthalpy difference of the outer flow and is defined as:

$$St = \frac{\alpha}{\rho\,c_p\,u_0} = \frac{q_w}{\rho\,c_p\,u_0\,\Delta T} = \frac{Nu}{RePr} \tag{10.36}$$

10.5.3 Thermal boundary conditions

In order accurately interpret the highly sophisticated heat transfer results in the ensuing sections, a clear understanding of the thermal boundary conditions imposed on the duct walls is absolutely essential. A systematic exposition of the boundary conditions is provided by [Shah and London, 1978]. Here we focus on the technically most important ones.

a) Uniform wall temperature T_w with circumferentially and axially constant wall temperature, which is expressed by Eq. (10.37). It appears mostly in condensers or evaporators.

$$T_w = const. \tag{10.37}$$

b) Convective with axially constant wall temperature and finite thermal resistance normal to the wall. It is in principle the same as a) except that the wall thermal resistance is finite in these applications, which can yield to an upstream heating of the fluid. Especially in liquid metal heat transfer experiments this condition mostly appears, because they can not be directly heated due to their good electric conductivity. The formulation of this boundary condition reads to:

$$\begin{aligned} &T_{w0} = T_{w0}(y,z);\ T_w = T_w(x,y,z); \\ &\lambda\left(\frac{\partial T}{\partial n}\right)_w = \alpha_0 (T_{w0} - T_w); \\ &\frac{1}{\alpha_0} = \frac{t_w}{\lambda_w} + \frac{1}{\alpha_e} \end{aligned} \tag{10.38}$$

where T_{w0} is the temperature at the outside of the heater/cooler, T_w the fluid/wall interface temperature, α_0 the heat transfer coefficient at the fluid/wall interface, λ_w the heat conductivity of the wall, t_w its thickness, n the wall normal unity vector and α_e the heat transfer coefficient at the entrance, where the heat transfer starts.

c) Constant wall heat flux with circumferentially constant wall temperature and axially constant wall heat flux. This condition applies for electric resistance heating, nuclear heating and heat exchangers having nearly identical fluid capacity rates. However, this condition only applies if the wall materials are thermally highly conducting, i.e. $\lambda_w >> \lambda$ or the wall is considerably thinner than the characteristic duct dimensions. This condition is formulated by:

$$q_w = q_w(y,z);\ T_w = T_w(x) \tag{10.39}$$

d) Uniform axial and circumferential heat flux, which is nearly the same condition as for case c), but it refers to boundary conditions where the wall material has a low thermal conductivity and the wall thickness is uniform. It reads to:

$$q_w = const. \tag{10.40}$$

e) Convective with axially constant wall heat flux and a finite thermal resistance normal to the wall. Also this condition is nearly the same as case c) except for the finite thermal resistance normal to the wall. Moreover, there is assumed that there is negligible heat conduction along the ducts circumference. This condition is expressed by:

$$q_w = q_w(y,z);\ \lambda\left(\frac{\partial T}{\partial n}\right)_w = \alpha_0 (T_{w0} - T_w) \tag{10.41}$$

f) Finally, the conductive boundary condition with axially constant wall heat flux and finite heat conduction along the walls circumference, which is an extension of the case e). This boundary condition is described by:

$$q_w = q_w(y,z);\ \frac{q_w}{\lambda} - \left(\frac{\partial T}{\partial n}\right)_w + \frac{\lambda_w t_w}{\lambda}\left(\frac{\partial^2 T}{\partial s^2}\right) = 0 \tag{10.42}$$

where s is the circumferential co-ordinate.

This list of boundary conditions applies both for the laminar and the turbulent heat transfer phenomena and it demonstrates the necessity for a detailed description of the experimental set-up. Only a complete description of the thermo-physical properties of the materials used, the heater type applied and the exact geometric dimensions allows to judge on the thermal boundary condition to be applied for the analysis of the experiment. Apart from the choice of the correct boundary conditions it says nothing about the quality of the performance of the experiment. Even a laminar experiment may be superimposed by buoyancy effects which considerably changes the experimental results.

10.5.4 Laminar heat transfer in circular ducts

The circular duct is the most widely used geometry in fluid flow and heat transfer devices. Accordingly, it has been analysed in detail for various boundary conditions. Also available in literature is a lot of information on the effects of viscous dissipation, fluid axial conduction, thermal energy sources and axial momentum diffusion. Some of the results will be shown within this subsection.

10.5.4.1 Fully developed flow

The velocity profile and the leading correlations for a fully developed laminar flow in a circular duct are elaborated already in Subsection 10.4.2. In this context we refer to these equations and show the results for the different thermal boundary conditions.

a) Uniform wall temperature (condition a)

The temperature distribution in circular ducts for non-dissipative flows in the absence of flow work, thermal energy sources and fluid axial conduction is given exactly. The expression for the fluid bulk mean temperature is given by the following asymptotic formula applicable for $x^* > 0.0335$, see [Bhatti, 1985]:

$$\frac{T_w - T_m}{T_w - T_e} = 0.819048\exp(-2\lambda_0^2 x^*) \quad \text{with} \quad \lambda_0 = 2.70436442 \tag{10.43}$$

It should be noted that although the local temperature T is both a function of the radial and the axial co-ordinates the fluid mean bulk temperature T_m depends on the axial co-ordinate only (the dimensionless temperature $(T_w - T)/(T_w - T_m)$ is only a function of the radius. The Nusselt number of the fully developed flow can be calculated to:

$$Nu = \frac{\lambda_0^2}{2} =^* 3.6568 \tag{10.44}$$

For fully developed flows and the thermal condition a) is the result is independent of the Prandtl number of the fluid. However, if the Peclet number *Pe* is smaller than 10, the influence of the axial fluid conduction is not negligible anymore. In this parameter regime the asymptotic expressions presented by [Michelsen and Villadsen, 1974] are recommended:

$$Nu = \begin{cases} 4.180654 - 0.18346 \cdot Pe & \text{for } Pe < 1.5 \\ 3.656794 + 4.4870 / Pe^2 & \text{for } Pe > 5.0 \end{cases} \tag{10.45}$$

b) Uniform wall heat flux (q_w = const. condition d)

The temperature distribution in circular ducts for non-dissipative flows in the absence of flow work, thermal energy sources and fluid axial conduction can be written analytically in the following form:

$$\frac{T_w - T}{T_w - T_m} = 6\left[1 - \left(\frac{r}{R}\right)^2\right]\left[\frac{3 - (r/R)^2}{11}\right] \quad ; \quad \lambda\left(\frac{T_w - T_m}{q_w\, d_h}\right) = \frac{11}{48} = \frac{1}{Nu} = \frac{\lambda}{\alpha\, d_h} \tag{10.46}$$

The Nusselt number obtained for constant wall heat flux is for a fully developed laminar flow about 20% larger than that for constant wall heat flux. The qualitative shape of the fluid bulk mean temperature distribution the wall heat flux and the wall temperature profile as a function of the axial co-ordinate *x* is qualitatively depicted in Figure 10.5.2.

Figure 10.5.2. Qualitative shape of the fluid bulk mean temperature, the wall temperature and the wall heat flux for the case of a constant wall heat flux q_w = const. (condition d) left graph and a constant wall temperature T_w = const (condition a) right graph

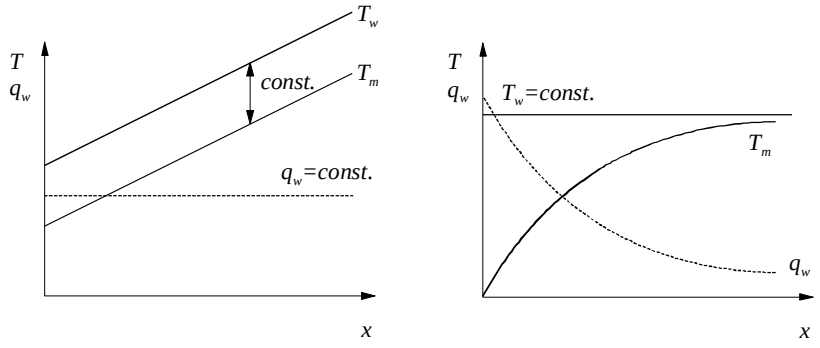

c) Convectively heated or cooled duct wall (condition b)

For this boundary condition the temperature is assumed to be constant axially but the duct has a finite thermal resistance normal to the wall. The thermal resistance can be embedded in an external convective heat transfer coefficient α_e, which is included in the dimensionless Biot number *Bi* defined as $Bi = \alpha_e\, d_h/\lambda$. The Biot number can also include the effect of the wall thermal resistance. In this case $Bi = 1/R_w$, where $R_w = (\lambda\, t_w)/(\lambda_w\, d_h) + \lambda/(\alpha_e\, d_h)$. The limiting cases are the constant wall temperature condition corresponding to $Bi \to \infty$ and the constant heat flux condition implying $Bi = 0$. Hence the Biot number can be conceived as a ratio of the thermal resistance of the wall compared to that of the fluid. For a constant α_e [Hickman, 1974] developed an asymptotic solution for the Nusselt number in the form (10.47). The overall mean Nusselt number $Nu_{o,m}$ then reads to:

$$Nu = \frac{\frac{48}{11} + Bi}{1 + \frac{59}{220} Bi} \quad ; \quad \frac{1}{Nu_{o,m}} = \frac{1}{Nu} + \frac{1}{Bi} \quad \text{with } Nu_{o,m} = \frac{\alpha_0 d_h}{\lambda} = \frac{q_w d_h}{\lambda (T - T_m)} \tag{10.47}$$

$Nu_{o,m}$ is quite insensitive to circumferential variation of Bi according to [Sparrow, *et al*.,1978].

10.5.4.2 Hydrodynamically developing flow

The problem of hydrodynamic flow development has been theoretically investigated by numerous scientists. Depending on the Reynolds numbers various solutions can be categorised as:

a) solutions involving the boundary layer equations valid for Reynolds number $Re > 400$;

b) solutions involving the Navier-Stokes equations for $Re < 400$;

c) creeping flow solution for $Re \rightarrow 0$, which hardly exist in liquid metal flows.

a) Solutions involving the boundary layer simplification

The various solutions using this approach are reviewed and classified in detail by the book of [Shah and London, 1978]. Among them the numerical solution of [Hornbeck, 1964] is technically most used. According to these results the dimensionless hydraulic developing length l_{hy}^+ and the dimensionless pressure gradient Δp^* can be calculated using:

$$l_{hy}^+ = 0.0565 \; ; \quad \Delta p^* = 13.74\sqrt{x^+} + \frac{1.25 + 64x^+ - 13.74\sqrt{x^+}}{1 + 2.1 \cdot 10^{-4} \left(x^+\right)^{-2}} \tag{10.48}$$

b) Solutions involving the Navier-Stokes equations

Close to the duct inlet the axial momentum diffusion and the radial pressure variation are of importance. The proper accounting of these effects introduces the Reynolds number as a parameter in the solution and also requires a careful specification of the inlet flow velocity profile. Using modern computational fluid dynamic code packages this problem can be arbitrarily exact solved for different inlet velocity distributions. Assuming a constant velocity far of the inlet the analysis by [Chen, 1973] can be used as most accurate for the hydraulic developing length. It reads to:

$$l_{hy}^+ = 0.056 + \frac{0.6}{Re(1 + 0.035Re)} \tag{10.49}$$

10.5.4.3 Thermally developing flow

Within this subsection a hydrodynamically fully developed flow is assumed for the velocity distribution in the circular duct. The temperature profile is allowed to develop under the individual thermal boundary conditions.

a) Constant wall temperature (T_w = const.)

Neglecting viscous dissipation, fluid axial conduction and thermal energy sources the solution of the problem is called in the literature the Graetz problem [Graetz, 1885], who solved this configuration

analytically. Based on the Graetz and extended Leveque solutions, the local Nusselt number Nu_x can be obtained from the following formulas depending on the axial co-ordinate x^*:

$$Nu_x = \begin{cases} 1.077\left(x^*\right)^{-\frac{1}{3}} - 0.7 & \text{for } x^* \le 0.1 \\ 3.657 + 6.874\left(10^3\, x^*\right)^{-0.488} \exp\left(-57.2 x^*\right) & \text{for } x^* \ge 0.1 \end{cases} \tag{10.50}$$

[Hausen, 1943] presented the following correlation for the mean Nusselt number Nu_m valid in the entire range of x^*:

$$Nu_m = 3.66 + \frac{0.0668}{x^{*1/3}\left(0.04 + x^{*2/3}\right)} \tag{10.51}$$

The error is in the range of 2% compared to a full numerical solution. The effect of fluid axial conduction is negligible for $Pe > 50$, according to [Hennecke, 1968]. However, the thermal developing length l_{th}^* increases considerably from 0.033 for $Pe = \infty$ to 0.5 for $Pe = 1$. The dimensionless temperature distribution T^* as a function of r/R and x^* is depicted in Figure 10.5.3(a) and the mean local Nusselt number Nu_x and the mean Nusselt number Nu_m is shown in Figure 10.5.4(a).

b) Constant wall heat flux (q_w = const.)

Similar to the Graetz problem with T_w = constant solution, the thermal entrance length for the thermally developing flow with q_w = const. is of large practical interest. The solution obtained for this problem can be analytically expressed in terms of a series as demonstrated by [Siegel, *et al*., 1958] or [Hsu, 1965]. Based on the Graetz type and Leveque solutions also the mean local Nusselt number Nu_x and the mean Nusselt number Nu_m can be expressed by approximation formulas, which where derived by [Bird, *et al*., 1960].

$$Nu_x = \begin{cases} 1.302\left(x^*\right)^{-1/3} - 1.0 & \text{for } x^* \le 5\cdot 10^{-5} \\ 1.302\left(x^*\right)^{-1/3} - 0.5 & \text{for } 5\cdot 10^{-5} \le x^* \le 1.5\cdot 10^{-3} \\ 4.364 + 8.68\left(10^3\, x^*\right)^{-0.56} \exp\left(-41 x^*\right) & \text{for } x^* \ge 1.5\cdot 10^{-3} \end{cases} \tag{10.52}$$

$$Nu_m = \begin{cases} 1.953\left(x^*\right)^{-1/3} & \text{for } x^* \le 0.03 \\ 4.364 + 0.0722 / x^* & \text{for } x^* \ge 0.03 \end{cases} \tag{10.53}$$

The error made by the approximation is about ±2% compared to the exact solution. From the analysis of [Hennecke, 1968] the effect of fluid axial conduction is negligible for $Pe > 10$ if $x^* > 0.005$, which is less than for constant wall temperature. The thermal entrance or developing length l_{th}^* is found to be 0.0430527, see [Grigull and Tratz, 1965].

c) Convectively heated or cooled duct wall (condition b in Section 10.5.2)

The convective boundary condition can also be solved by means of a series expansion incorporating the Biot number, see [Hsu, 1968]. The local Nusselt numbers as a function of the dimensionless distance x^* for different Biot numbers are shown in Figure 10.5.4(b). The curves corresponding to $Bi = 0$ (q_w = const.) and $Bi \to \infty$ (T_w = const.) are the same as in Figure 10.5.4(a).

Figure 10.5.3. Dimensionless temperature distribution in the thermal entrance region of a circular duct and a thermally developing laminar flow as a function of the dimensionless length x^* for the thermal condition T_w = constant (a) and the condition q_w = constant (b) from [Grigull and Tratz, 1965]

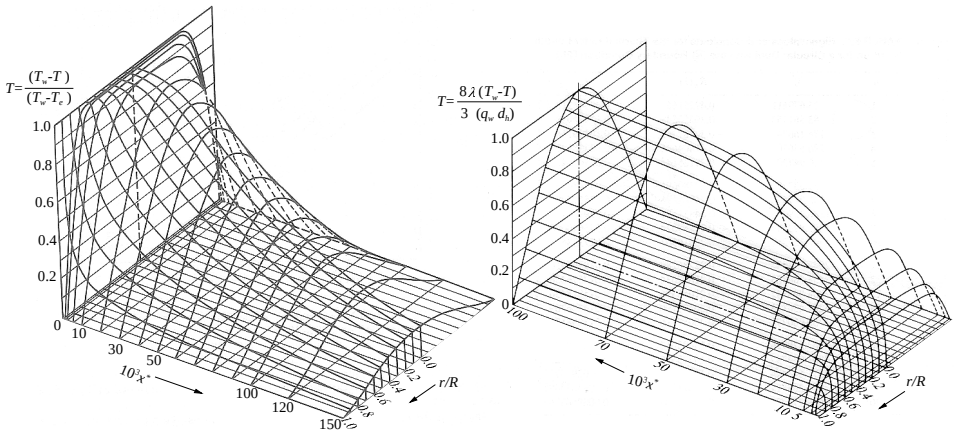

(a) (b)

Figure 10.5.4. Nusselt number as a function of the dimensionless entrance length x^* for a hydraulically developed and thermally developing laminar flow in a circular tube

a) Local and mean Nusselt numbers Nu_x and Nu_m for T_w = constant and q_w = constant
b) Local Nusselt number Nu_x for mixed convective thermal boundary conditions expressed by the Biot number

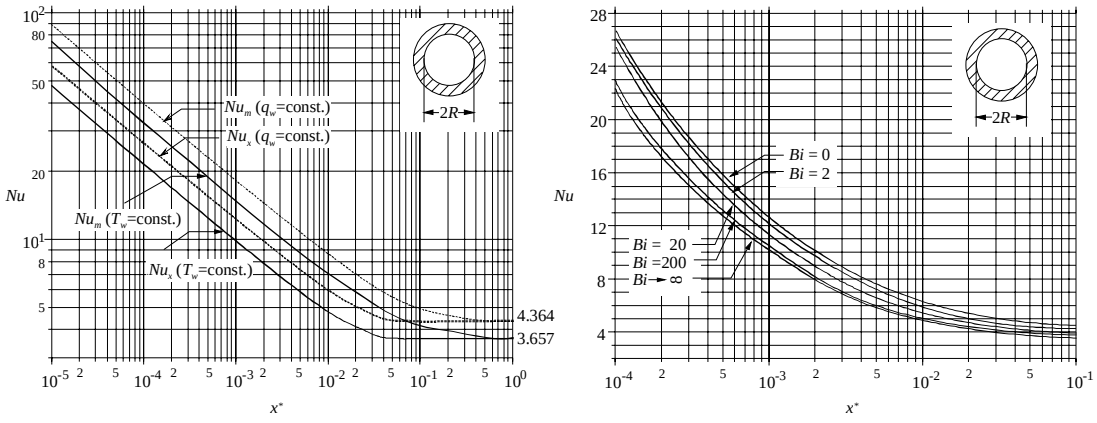

(a) (b)

10.5.4.4 Simultaneously developing flow

All results presented so far have been based on the rather idealised assumption of an already hydraulically fully developed flow. This assumption is in most cases far away from the practical use in liquid metals, because in flows with the Prandtl number being far below unity, the hydraulic entrance length is considerably longer than the thermal one (see discussion in Section 10.5.1). The idealisation of a fully developed velocity profile at the duct inlet may lead to a significant error in the predicted performance. In such cases, the results pertaining to simultaneously developing velocity and temperature profiles should be applied. An inherent result of the both flow types developing is that the solution depends immediately on the Prandtl number. Subsequent we discuss the results for a circular duct for different thermal boundary conditions.

a) Uniform wall temperature (T_w = const.)

For $Pr \to \infty$ the flow is hydraulically already developed before the temperature profile starts developing. This represents the limiting case discussed in Subsection 10.5.3.3. According the Nussel numbers curves coincide. In case of a good conducting fluid, assume idealised that $Pr = 0$ the temperature profile develops much faster than the velocity profile. So in this limiting case, while the temperature profile develops the velocity distribution remains nearly unchanged. The non-modified velocity profile with its small boundary layer has a large flow rate close to the wall, which immediately yields considerably larger heat transfer from the wall expressed by the Nusselt number. The solution for the limiting cases were already obtained by [Graetz, 1883] and rediscovered by [Leveque, 1928]. For the ideal case of $Pr = 0$ and $Pr \to \infty$ the solutions can be expressed by analytic means, while for the other Prandtl number series expansions incorporating Bessel functions and numerical approximations are necessary. The mean and the local Nusselt numbers Nu_x and Nu_m as a function of the dimensionless entrance length x^* for different Prandtl numbers are displayed in Figures 10.5.5(a) and (b).

Figure 10.5.5. Local and mean Nusselt numbers Nu_x (a) and Nu_m (b) as a function of the dimensionless entrance length x^* for a simultaneously developing flow in a circular tube with the thermal boundary condition T_w = constant and for different fluids expressed by the Prandtl number

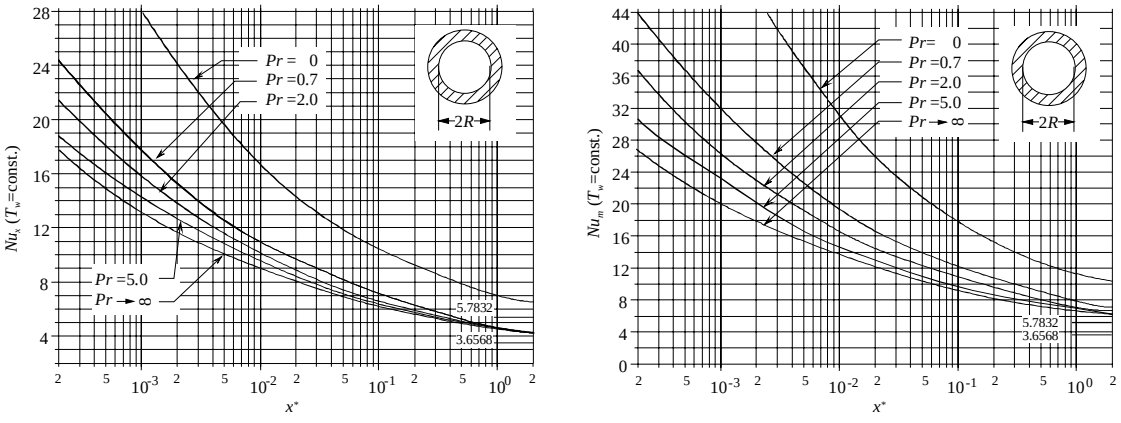

Note that for $Pr = 0$ the local and the mean Nusselt number approach the value of 5.7832, whereas the remainder of the curves approach the value of 3.6568. The thermal entrance lengths for the simultaneously developing are according to [Bhatti, 1985] found to be:

$$l_{th}^* = \begin{cases} 0.028 & \text{for } Pr = 0 \\ 0.037 & \text{for } Pr = 0.7 \\ 0.033 & \text{for } Pr \to \infty \end{cases} \tag{10.54}$$

b) Uniform wall heat flux (q_w = const.)

A similar approach like for the previous thermal boundary condition can be used for the case with a uniform wall heat flux. It is interesting to note, that the curve for the local Nusselt number in case of $Pr = 0$ tends for large x^* to the asymptotic value of 8, which is about 40% more than for the uniform wall temperature condition. The dependence of the local Nusselt number as a function of the entrance length is shown in Figure 10.5.6. Not only the heat transfer is larger in for the uniform wall heat flux

but also the thermal entrance length increases. In case of well molecular conducting fluids it is by 50% larger than for the uniform wall temperature. The analysis performed by [Bhatti, 1985b] yields the following values:

$$l_{th}^{*} = \begin{cases} 0.042 & \text{for } Pr = 0 \\ 0.053 & \text{for } Pr = 0.7 \\ 0.043 & \text{for } Pr \to \infty \end{cases} \tag{10.55}$$

Figure 10.5.6. Local Nusselt numbers Nu_x as a function of the dimensionless entrance length x^* for a simultaneously developing flow in a circular tube with the thermal boundary condition q_w = constant and for different fluids

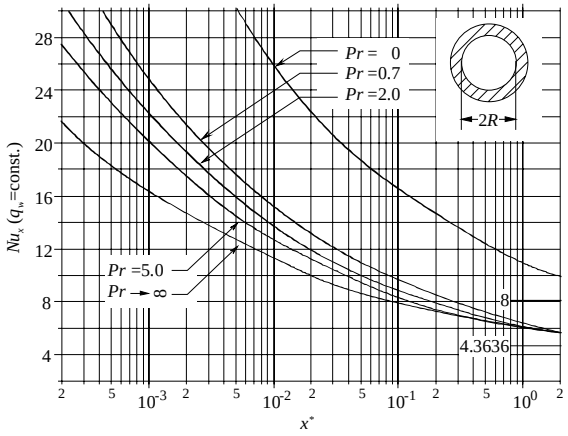

10.5.5 Summary on the laminar heat transfer

Within this section the laminar heat transfer has been considered for different thermal boundary conditions. The description has been focused to describe the main effects of developing length, heat local and global transfer performance under different thermal boundary conditions. The effect of the fluid properties in the non-dimensional sense were found to play a crucial role for developing flows. This section was intended to define the terminology of the individual transport properties, which will be kept the same throughout this chapter on thermal-hydraulics.

The central task of this laminar heat transfer section was to determine the wall heat flux transferred at the fluid wall interface in dependence on the specific geometries (here mainly the circular duct) and on the fluid properties. More details on the heat transfer in other geometries may be taken from [Shah and London, 1985]. The wall heat flux is given by $q_w = -\lambda(\partial T/\partial n)_w$ and it depends only on the molecular heat conductivity of the individual fluid and the temperature gradient at the wall.

Although the laminar heat transfer is a pure molecular transport process the flow field plays an essential role. For the convective transport of internal energy or enthalpy the flow is responsible and influences the temperature gradient in a significant manner. It is obvious that the heat transfer can be enhanced by increasing the flow velocity. The faster energy is convectively transported the more energy can be removed from the wall. For incompressible fluids the flow field is determined by only one characteristic number. In forced convective problems this is the Reynolds number ,while in buoyant convection the Grashof number appears. In both characteristic numbers the molecular viscosity ν appear, which is responsible for the momentum exchange. For the heat exchange in a

flowing liquid the ratio of the molecular viscosity ν to the molecular heat conductance $\kappa = \lambda/(\rho\, c_p)$, the so-called Prandtl number, is of crucial importance. In contrast to the Reynolds or the Grashof number the Prandtl number is a pure material constant and it depends only on the fluid properties.

One normalises the wall heat flux with an appropriate temperature difference and this is named the heat transfer coefficient $\alpha = q_w/\Delta T$. The heat transfer coefficient can be represented non-dimensional in different manners. The Stanton number is the ratio of the wall heat flux to the enthalpy difference density and does not contain the heat conductivity. More often used is the Nusselt number, in which the heat transfer coefficient multiplied with a characteristic dimension is related to the molecular heat conductivity. In case of pure forced convection the results can be compressed in the way:

$$\frac{Nu_x}{\sqrt{Re_x}} = f\left(Pr^n\right) \text{ with } 0 < n < 1 \tag{10.56}$$

The expression $Nu_x/\sqrt{Re_x}$ increases with rising Prandtl number. This does not mean that the heat transfer or the heat transfer coefficient also increases with increasing Prandtl number, because the Nusselt number itself contains the molecular heat conductivity.

For a fully developed flow (both thermally and hydrodynamically) the heat transfer is given only by a constant Nusselt number. The constants depend uniquely on the chosen thermal boundary condition. The Prandtl number influences only the heat transfer in the thermal entrance (or developing) region.

In order to determine the heat transfer correlation there exist in principle the following possibilities:

- Analytic solutions including the whole set of conservation equations. Mostly, this is only applicable for drastic simplifications like the fully developed duct flow or the Couette-flow.
- Numeric solution of the conservation equations. This requires a lot of effort in computing time and memory capacity, since the equations are of elliptic type. However, the progress of the computers in calculation power makes many problems even now tractable.
- Exact solutions of the boundary layer equations. The similar solutions are of major importance for the determination of heat transfer correlations, since they are available in tables, diagrams or in form of series approximations.
- Numeric solutions of the boundary layer equations require mathematical effort, but are with commercially available computational fluid dynamics codes easier accessible than in the past.
- Approximate solutions using integral methods. They are less accurate than numeric solutions but they are still in practical use. The numeric effort is low and complex and expensive codes are not necessary.
- Analogies between heat and momentum transfer are only applicable for $Pr = 1$ fluids and are results of exact solutions.
- Empirical correlations. They must be used if complex geometries do not allow another solution.

10.6 Turbulent momentum exchange

Turbulent flows are of immense technological importance for all liquid metal applications as they occur normally under usual operation conditions. The main advantage of turbulent flows over laminar flows is that they are capable of providing vastly enhanced heat and mass transfer rates. However this is at the expense of increased friction factors accompanying the turbulent flows.

The fluid flow and heat transfer characteristics of all ducts are described in terms of certain hydrodynamic and thermal parameters. Many of them have been explained in the sections of the laminar momentum and energy exchange. In order to describe turbulent flows additional parameters that are peculiar to turbulent duct flows will be defined.

10.6.1 Description of turbulence

In the year 1883 Osborne Reynolds showed with his famous colour stripe water experiment that a laminar tube flow above a certain flow rate turns into a turbulent flow. This critical threshold or border for the transition is given by a critical Reynolds number. He found in the experiments that the transition occurs at $Re_{crit} \approx 2.300$ and supposed that the laminar-turbulent transition is a stability problem. For the development of turbulence mainly two questions are of importance:

- How develops turbulence from a laminar flow? This is essentially the stability problem of the laminar turbulent transition, which has been initially solved by Tollmien 1929 by means of a perturbation analysis. A detailed description of the methodology, the assumptions used and the interpretation of the obtained results for this type of analysis is far beyond this chapter. Here, a extensive amount of literature exists. As examples the books of [Schlichting, 1979], [Lin, 1961], [Betchov and Criminale, 1967] and [White, 1974] are recommended for the interested reader.
- How emerges turbulence in an already turbulent flow? Why remains a turbulent flow turbulent? This is mainly a question of the production of turbulence.

Turbulent flows are always unsteady, three-dimensional and stochastic. From experiments it is known that the laminar turbulent transition is accompanied by:

- an increase of the pressure drop;
- an increase of the boundary layer thickness.

This is caused by turbulent diffusion. Due to the intense macroscopic oscillation motion the turbulent velocity profile becomes “fuller” and the turbulent boundary layer gets thicker than in the laminar case. All variables in the turbulent flow depend on the spatial co-ordinates *x*, *y* and *z* and the time *t*. Restricting the considerations to incompressible single component flows the unknowns of the isothermal flow are *u*, *v*, *w* and *p* which are all functions of the three space co-ordinates and the time. Consider a in the mean steady flow, which means that it is statistically steady, then the flow variables can be decomposed in a time averaged mean value plus the fluctuations around the mean value. For the velocity this so-called Reynolds decomposition reads to:

$$u_i(x_i,t) = \overline{u_i(x_i)} + u_i'(t,x_i) \tag{10.57}$$

where we have used the tensorial notation in the form $u_i = (u, v, w)$. The time averaged mean is given by:

$$\overline{u_i(x_i)} = \frac{1}{\Delta t}\int_t^{t+\Delta t} u_i(x_i,t)\,dt \tag{10.58}$$

where the time interval Δt, over which is integrated, must be sufficiently large but not too large to retain the capability to study long term unsteady changes of the flow. By definition the time average of the fluctuations diminishes, but the mean value of their squares is far from being zero. The turbulence intensity or *RMS* value is given by:

$$\phi = \sqrt{\overline{u_i'^2}} = \sqrt{u'^2 + v'^2 + w'^2} \tag{10.59}$$

The relative intensity of the velocity fluctuations is defined:

$$Tu = \frac{\sqrt{\overline{u_i'^2}}}{\left|\overline{u_i}\right|} \tag{10.60}$$

is called the turbulence level. According to [Jischa, 1982] the turbulence level is about 1% downstream a sieve, approximately 10% close to a wall and more than 10% in a free jet. Generally, the turbulent flow types can be divided in three classes:

- *Isotropic turbulence*: The statistic properties in the whole flow field are the same and are independent of the direction ($\overline{u'^2} = \overline{v'^2} = \overline{w'^2}$). They are invariant against any translation and rotation of the co-ordinate system.
- *Homogeneous turbulence*: All statistic properties depend only on the direction and not on the location. They are translation invariant.
- *Anisotropic or shear turbulence*: This is of practical interest in technical applications, since it appears in boundary layer flows, free jets, duct flows, etc.

10.6.2 Reynolds equations for turbulent flows and derivation of transport equations

The unsteady Navier-Stokes equations are generally considered to be valid for turbulent flows in the continuum regime. However, the complexity and random nature of the turbulent motion prevents an exact solution of these equations. Most of the present day prediction methods for turbulent flows are based on the time averaged Navier-Stokes equations. These equations are referred to as the Reynolds equations. Time averaging the equation of motion gives rise to new terms which can be interpreted as apparent stress gradients or heat flux quantities associated with the turbulent motion. These new quantities must be related to the mean flow variables through turbulence models. This transfer process introduces further assumptions and approximations. Thus, this attack on the turbulent flow problem through solving the Reynolds equations of motion does not follow entirely from fist principles, since additional assumptions must be made to "close" the system of equations. In the subsequent listing of the Reynolds equations, one in the mean steady flow of an incompressible Newtonian fluid is considered.

- Reynolds form of the continuity equation:

$$\frac{\partial \overline{u_i}}{\partial x_i} = 0 = \frac{\partial \overline{u}}{\partial x} + \frac{\partial \overline{v}}{\partial y} + \frac{\partial \overline{w}}{\partial z} \tag{10.61}$$

- Reynolds form of the momentum equation:

$$\rho \overline{u_j} \frac{\partial \overline{u_i}}{\partial x_j} = -\frac{\partial \overline{p}}{\partial x_i} + \frac{\partial}{\partial x_j}\left(\mu \frac{\partial \overline{u_i}}{\partial x_j} - \rho \overline{u_i' u_j'}\right) \tag{10.62}$$

Here appears the apparent or virtual Reynolds stress tensor $\tau_{tur} = -\rho\ \overline{u_i' u_j'}$ which differs from the molecular one which is given by $\tau_{ij} = \mu\left(\partial \overline{u_j} / \partial x_i + \partial \overline{u_i} / \partial x_j\right)$. It is important to note that the additional Reynolds stresses are only registered in relation to the temporal mean motion. The equation of motion

for the instantaneous quantities does not contain any additional turbulence term. The transition from the instantaneous equations of motion to the Reynolds equation of motion makes the turbulence problem obvious. The "price" of the temporal averaging is the introduction of the unknown Reynolds stress tensor, which originates from the non-linear convective terms in the Navier-Stokes equations. The major task in solving the turbulence problem is to correlate the Reynolds stress tensor with the temporal mean velocity field by means of appropriate turbulence models. The methodology to solve the unknown Reynolds stress tensor is performed using balancing equations. Like any other transport quantity it must obey a common form. These types of balancing equations often called transport equations are the basis for nearly all new closure assumptions.

The starting point for the formulation of the transport equations is the derivation of the Navier-Stokes equation for the instantaneous quantities. Following a strict mathematical derivation process according to [Rotta, 1972] the transport equations for the Reynolds stress tensor is obtained:

$$\underbrace{\overline{v_k}\frac{\partial}{\partial x_k}\left(\overline{v_i' v_j'}\right)}_{C} + \underbrace{\overline{v_i' v_k'}\frac{\partial \overline{v_j'}}{\partial x_k} + \overline{v_j' v_k'}\frac{\partial \overline{v_i'}}{\partial x_k}}_{P} + \underbrace{2\nu\frac{\partial \overline{v_i'}}{\partial x_k}\frac{\partial \overline{v_j'}}{\partial x_k}}_{DS} - \underbrace{\overline{\frac{p'}{\rho}\left(\frac{\partial v_i'}{\partial x_j} + \frac{\partial v_j'}{\partial x_i}\right)}}_{PSC} + \underbrace{\frac{\partial}{\partial x_k}\left[\overline{v_i' v_j' v_k'} - \nu\frac{\partial}{\partial x_k}\left(\overline{v_i' v_j'}\right) + \overline{\frac{p'}{\rho}\left(\delta_{kj} v_i' + \delta_{ki} v_j'\right)}\right]}_{D} = 0 \tag{10.63}$$

Herein *C* is the convective change and *P* the turbulence production, which is the product of the Reynolds stress tensor with the velocity gradients of the time averaged mean velocity. *DS* represents the turbulent dissipation, which is essentially a negative production, *PSC* is pressure shear correlation, which contributes similar like the diffusion *D* to the reorganisation of the flow. The production term is the most essential one, since it describes that only in flows with a velocity gradient (shear flows) turbulence can be maintained. The velocity gradient of the time averaged velocity is the generator of turbulence. The necessary energy is taken from the mean flow. The tensor equation exists of nine components. An important case of the transport equation is obtained by the formal contraction $i = j$, for which the transport equation of the turbulent kinetic energy k is obtained. If one defines k as $k = 1/2\ \overline{v_j'^2} = 1/2\left(\overline{u'^2} + \overline{v'^2} + \overline{w'^2}\right)$ the transport equation for the turbulent energy reads to:

$$\underbrace{\overline{v_k}\frac{\partial k}{\partial x_k}}_{C} + \underbrace{\overline{v_j' v_k'}\frac{\partial \overline{v_j'}}{\partial x_k}}_{P} + \varepsilon + \underbrace{\frac{\partial}{\partial x_k}\left[\overline{\left(k + \frac{p'}{\rho}\right)v_k'} - \nu\frac{\partial k}{\partial x_k} - \nu\frac{\partial}{\partial x_j}\left(\overline{v_j' v_k'}\right)\right]}_{D} = 0 \tag{10.64}$$

in which ε is the dissipation. The turbulence energy is not averaged and the turbulent dissipation ε is given by:

$$\varepsilon = \nu\overline{\frac{\partial v_j'}{\partial x_k}\left(\frac{\partial v_j'}{\partial x_k} + \frac{\partial v_k'}{\partial x_j}\right)} \tag{10.65}$$

The transport equations play an essential role in the development of modern turbulent flow calculation methods. Although the Reynolds stress tensor can be described by the transport equations, these equations does not solve the closure problem, since they contain unknown correlation functions. For the correlation functions new transport equations can be formulated, which themselves contain new unknown correlations. The order of the obtained tensors increases with each step by the factor one.

To summarise, the closure problem can not be solved directly. There exist always more unknowns the available equations. The only closure possibility is the use of semi-empirical closure assumptions, which in the simplest form can be applied directly to the Reynolds equations like the Prandtl mixing length model.

10.6.3 A flashlight on turbulence modelling

Several attempts have been made to solve the turbulence closure problem by the introduction of a succession of turbulence models. The simplest one of them is Prandtl's mixing length model, see [Prandtl, 1928]. This model and its variations on the hand of [Taylor, 1915], [v. Karman, 1931] and [Van Driest, 1956] have proven reasonably adequate for plain two-dimensional flows.

For the general case of three-dimensional flows higher order turbulence models are required. They utilise one or more partial differential equations derived from the modified Navier-Stokes equations for quantities like the turbulent kinetic energy k, the kinetic energy dissipation ε, and the components of the turbulent stress tensor τ_{ij}.

The turbulence model employing the single partial differential equation for the turbulent kinetic energy in conjunction with the algebraic expression for the turbulence length scale (e.g. Prandtl mixing length l) is referred to as the one equation model or k-l-model.

Another model, employing the partial differential equations for the kinetic energy and its dissipation is called the two-equation k-ε model, which has bee initially proposed by [Harlow and Nakayama, 1968] and modified by [Jones and Launder, 1972] and [Launder and Spalding, 1974]. It is technically most often used and spread nearly throughout all commercially available codes. Many applications of the k-ε model have made use of wall functions to treat the near wall region. Alternatively, additional terms have been added to the k and ε to extend their applicability to the viscous sublayer by [Jones and Launder, 1972] or [Chien, 1982]. In this connection the viscous sublayer is often referred to as the region of low turbulence Reynolds number ($k^{1/2}l/\nu$). The inner model is crucial for complex turbulent flows as for example those containing flow separation or severe property variations. The uncertainty of such inner-region modelling for complex flows appears to limit the range of the applicability of the k-ε model. The k-ε models that have been modified so that they are applicable in the viscous sublayer [Jones and Launder, 1972 or Rodi, 1980] are known as low Reynolds number k-ε models. Details of such models are beyond the aim of this article. Modifications to the k-ε model to include the effect of buoyancy and streamline curvature on the turbulence structure have also been proposed. Numerous other two-equation models have been suggested, the most frequently used being the Ng-Spalding [Ng-Spalding, 1972] model, and the [Wilcox and Traci, 1976] model. All of these models employ a modelled form of the turbulence kinetic energy equation, but the modelling for the gradient diffusion term is different. The most striking difference, however, is in the choice of dependent variable for the second model transport equation from which the length scale is determined. Often two-equation models coexist; a famous example is the so-called shear stress turbulence model (SST). The SST model combines the advantages of the k-ε model with the ones of the k-ω model, where ω is the vorticity. It takes advantage of the fact that for using in the near wall region the k-ω model an analytical solution for the viscous sublayer is known for small y^+ values, see e.g. [Wilcox, 1986]. The matching of the k-ω model close to all walls to the k-ε model in the rest of the fluid domain is performed by means of blending functions.

The complicated multi-equation models involve solutions of the partial differential equations for all components of the turbulent stress tensor and are referred to as stress equation models. A brief description of the turbulence models together with pertinent references is amongst the tremendous

literature available in this field given in the articles and books by [Reynolds, 1976] and [Arpaci and Larsen, 1984]. Here only the main ideas of these Reynolds stress models (RSM) are outlined. RSM models are those models that do not assume that the turbulent shearing stress is proportional to the rate of strain. That is for a 2-D incompressible flow:

$$-\rho\overline{u'v'} \neq \mu_t \left(\frac{\partial u}{\partial y} + \frac{\partial v}{\partial x} \right) \tag{10.66}$$

in which μ_t is the turbulent viscosity being $\mu_t \sim k^2/\varepsilon$. The most widely used Reynolds stress models are those of [Hanjalic and Launder, 1972], [Launder et al., 1975] and [Donaldson, 1972]. The RSM require at least three additional partial differential equations (PDE) compared to the *k*-ε model and the RSM must still utilise approximations and assumptions in modelling terms which presently are difficult to measure experimentally. A simplification of the Reynolds stress modelling known as an algebraic stress or flux model has a large popularity in isothermal flows. This approach is discussed in detail in [Rodi, 1981]. In the algebraic stress modelling it is generally assumed that the transport of the Reynolds stresses is proportional to the transport of the turbulent kinetic energy. For boundary layer flows without buoyancy effects, the algebraic stress model results in:

$$\overline{u'v'} = C_\mu \frac{k^2}{\varepsilon} \frac{\partial u}{\partial y} \tag{10.67}$$

which is identical to the results obtained from the *k*-ε model. However, in the algebraic stress model, C_μ becomes a function of the ratio of the production to dissipation of the turbulent kinetic energy rather than a constant.

10.6.4 Boundary layer approximations

Many technical flows have boundary layer character. The laminar boundary layer equations as derived in Section 10.4.2 can not be transferred to the turbulent case because the oscillation velocities v_k' are rapid in space and time and so their derivatives are not negligible compared to the other terms, although their absolute magnitude is an order of magnitude smaller than the mean values. Thus the boundary layer approximation must be directly derived within the Reynolds equations and the transport equations. The procedure is similar to that for the laminar flow and the details may be taken from textbooks like [Burmeister, 1983] or [Anderson, *et al*., 1984]. For a two-dimensional flow the boundary layer equations read to:

$$\frac{\partial \bar{u}}{\partial x} + \frac{\partial \bar{v}}{\partial y} = 0 \quad ,\rho\left(\bar{u}\frac{\partial \bar{u}}{\partial x} + \bar{v}\frac{\partial \bar{u}}{\partial y} \right) = -\frac{dp_\delta}{dx} + \frac{\partial}{\partial y}\left(\mu\frac{\partial \bar{u}}{\partial y} - \rho\overline{u'v'} \right) \tag{10.68}$$

in which p_δ is the pressure at the border of boundary layer to the bulk flow. A similar procedure can be performed for the transport equations and one obtains according to [Jischa, 1982] the transport equation for the shear stress and the turbulent kinetic energy equation in the form (10.69) for a 2-D flow.

$$\underbrace{\bar{u}\frac{\partial\left(\overline{u'v'}\right)}{\partial x}+\bar{v}\frac{\partial\left(\overline{u'v'}\right)}{\partial y}}_{C}+\underbrace{\overline{v'^2}\frac{\partial\bar{u}}{\partial y}}_{P}+\underbrace{2\nu\left[\overline{\frac{\partial u'}{\partial x}\frac{\partial v'}{\partial x}}+\overline{\frac{\partial u'}{\partial y}\frac{\partial v'}{\partial y}}+\overline{\frac{\partial u'}{\partial z}\frac{\partial v'}{\partial z}}\right]}_{DS}-\underbrace{\overline{\frac{p'}{\rho}\left(\frac{\partial u'}{\partial y}+\frac{\partial v'}{\partial x}\right)}}_{PSC}+\underbrace{\frac{\partial}{\partial y}\left[\overline{u'v'^2}-\nu\frac{\partial}{\partial y}\left(\overline{u'v'}\right)+\overline{\frac{p'u'}{\rho}}\right]}_{D}=0 \tag{10.69}$$

$$\underbrace{\bar{u}\frac{\partial k}{\partial x}+\bar{v}\frac{\partial k}{\partial y}}_{C}+\underbrace{\overline{u'v'}\frac{\partial\bar{u}}{\partial y}}_{P}+\varepsilon+\underbrace{\frac{\partial}{\partial y}\left[\overline{\left(k+\frac{p'}{\rho}\right)v'}-\nu\frac{\partial k}{\partial y}-\nu\frac{\partial\overline{v'^2}}{\partial y}\right]}_{D}=0$$

The most terms in both transport equations can be measured experimentally, except for the local pressure oscillations. Fortunately the pressure oscillations do not appear in the equation for the turbulent kinetic energy.

Most flows are confined by walls and by approaching the wall the velocity oscillations hence the Reynolds shear stress approaches zero.

$$\lim_{y\to 0}\mu\frac{\partial\bar{u}}{\partial y}=\tau_w \tag{10.70}$$

If we assume a fully developed 2-D turbulent flow near a wall all statistic properties depend only on the co-ordinate *y*. Since the derivate of the velocity in axial direction vanishes, the continuity equation immediately yields that the mean velocity in *y*-direction is also zero. In this specific case convective terms and the pressure are zero in the Reynolds equation and it remains:

$$0=\frac{\partial}{\partial y}\left(\mu\frac{\partial\bar{u}}{\partial y}-\rho\overline{u'v'}\right) \tag{10.71}$$

With the boundary condition at the wall one gets:

$$\frac{\tau_w}{\rho}=\nu\frac{\partial\bar{u}}{\partial y}-\overline{u'v'} \tag{10.72}$$

Obviously only the parameters ν, τ_w/ρ appear and one defines shear stress velocity u_τ as:

$$u_\tau=\sqrt{\frac{\tau_w}{\rho}}\quad=u_0\sqrt{\frac{f}{2}} \tag{10.73}$$

where f is the friction coefficient $f = 2\tau_w/(\rho\, u_0^2)$. Defining the dimensionless co-ordinates u^+ and y^+ in the way:

$$u^+=\bar{u}\Big/u_\tau\quad\text{and}\quad y^+=yu_\tau\Big/\nu \tag{10.74}$$

the velocity distribution close to the wall can be given in an universal manner $u^+ = f(y^+)$. The solution of f in the immediate vicinity of the wall is immediately obtained because the velocity fluctuations close to the wall are zero and at the wall the non-slip condition holds, so that $u^+ = y^+$. This is the so-called viscous sub-layer, in which the molecular shear stress is significantly larger than the Reynolds stress. With increasing distance from the wall the Reynolds stress grows considerably and simultaneously the molecular part becomes negligible. This yields to a logarithmic expression for the dimensionless velocity in the form:

$$u^+ = \frac{1}{C_1} \ln y^+ + C_2 \tag{10.75}$$

which was initially determined by Prandtl 1932. Between the viscous sublayer and the fully turbulent boundary layer a transition layer appears, for which different but mostly logarithmic functions can be used. An overview on the different definitions between viscous sublayers and fully developed boundary layer may be taken from [Shah and London, 1978].

For the transition of the anisotropic turbulent boundary layer towards the isotropic core flow the logarithmic laws loose their applicability. Within this region the so-called wake laws are introduced. There exist numerous articles for the velocity profile description in pipe flows, in which many differ only by the constants chosen for the wake profile. A comprehensive picture on the dimensionless velocity distribution in liquid metal flows can be found in the PhD thesis by [Fuchs, 1973]. Newer results can be taken from [Zagarola, 1996, 1997], [Barenblatt and Chorin, 1998] [Guo and Julien, 2003].

10.6.5 Summary

The numerical prediction of turbulent boundary layer flows is mainly possible on the basis of semi-empirical closure assumptions. They are applied directly in the Reynolds equations or in the transport equations. The applicability of closure methods of the first order is rather limited and thus mainly closure assumptions of higher order are applied, which numerically can be applied with rather small effort.

Fortunately for the formulation of semi-empirical assumptions a lot of experimental data exist and so the turbulent momentum transfer can be satisfactory described for the forced convective liquid metal flow in simple geometries with a high degree of accuracy. Regarding the turbulent momentum transport in fully developed forced convective flows the only influencing parameter is the Reynolds number and thus pressure drop correlations, friction factors as well as production and dissipation rates can be taken from standard engineering handbooks for the individual geometry considered in the application. This is completely different to the turbulent energy exchange, since there next to the velocity data temperatures have to be determined. One should be careful to define a heavy liquid metal experiment with a small heat transfer rate to be a solely forced convective flow if only Reynolds number is quite large. This holds especially for horizontal arrangements of the experiments. Mercury experiments performed by [Gardner, 1969] or [Lefhalm, *et al*., 2004] have shown that even at Reynolds numbers $Re > 10^5$ buoyancy forces can become important and modifies the local flow quantities.

10.7 Turbulent energy exchange

Regarding the turbulent energy the similar procedures as for the turbulent momentum exchange can be applied. Unfortunately less experimental data are available for the turbulent energy exchange in liquid metals than for the turbulent momentum exchange where also data from other fluids can be applied. Thus, a lot of correlations appear which were derived only from one experiment sometimes with speculations on their boundary conditions. So often no uncertainty estimates can be given.

The energy equation of a steady flow of an incompressible fluid in the temperature notation writes to:

$$\rho c_p \left(v_k \frac{\partial T}{\partial x_k} \right) = \lambda \frac{\partial^2 T}{\partial x_k^2} \quad \text{or} \quad \rho c_p \left(u \frac{\partial T}{\partial x} + \frac{\partial T}{\partial y} + \frac{\partial T}{\partial z} \right) = \lambda \left(\frac{\partial^2 T}{\partial x^2} + \frac{\partial^2 T}{\partial y^2} + \frac{\partial^2 T}{\partial z^2} \right) \tag{10.76}$$

10.7.1 Reynolds equations for the turbulent energy exchange

When the turbulent stream involves heat transfer its instantaneous temperature T_i can be decomposed according to Reynolds in a fluctuating component and a time averaged value. The time averaged component must not be confused with the bulk mean temperature T_m. The former is a local quantity at a discrete point, whereas the latter is a flow average quantity across the whole ducts cross-section. The Reynolds approach leads to the following equation:

$$\rho c_p \left(\overline{v_k} \frac{\partial \overline{T}}{\partial x_k} \right) = \lambda \frac{\partial^2 \overline{T}}{\partial x_k^2} - \underbrace{\rho c_p \frac{\partial}{\partial x_k} \left(\overline{v_k' T'} \right)}_{RH} \tag{10.77}$$

in which *RH* is the apparent or virtual heat flux often referred to as the Reynolds heat flux. The Reynolds heat flux exists only due the temporal averaging of the equations. It describes a macroscopic exchange originating from the oscillating components. In contrast to the Reynolds shear stress tensor the Reynolds heat fluxes are vectorial quantities, because the transported property contains a scalar in comparison to the vectorial momentum. Also for the heat flux transport equations can be derived. In contrary to the momentum transport the turbulent energy exchange is referred to as a passive transport process.

Similar to the momentum exchange also boundary layer approximations can be applied to the energy equation. For a 2-D in the mean steady flow of an incompressible fluid they read to:

$$\rho c_p \left(\overline{u} \frac{\partial \overline{T}}{\partial x} + \overline{v} \frac{\partial \overline{T}}{\partial y} \right) = - \frac{\partial}{\partial y} \left(- \lambda \frac{\partial \overline{T}}{\partial y} + \rho c_p \overline{v' T'} \right) \tag{10.78}$$

10.7.2 Analogies between fluid flow and heat transfer parameters

In analogy with Newton's law of friction for the laminar shear stress τ a law of the friction for the apparent turbulent stress τ_{tur} was introduced by [Boussinesq, 1877]:

$$\tau = -\mu \frac{\partial \overline{u}}{\partial y} \quad \text{and} \quad \tau_{tur} = -\mu_t \frac{\partial \overline{u}}{\partial y} \tag{10.79}$$

where μ_t is an apparent viscosity also referred to as a virtual or eddy viscosity. Note that the eddy viscosity is not a property of the fluid like the dynamic viscosity μ, but depends on the time average flow velocity. In analogy with the molecular momentum diffusivity ν, eddy diffusivity for momentum ε_M is often required to characterise turbulent flow. ν and ε_M are defined as:

$$\nu = \frac{\mu}{\rho} \quad \text{and} \quad \varepsilon_M = \frac{\mu_t}{\rho} \tag{10.80}$$

In analogy with Fourier's law of heat conduction for laminar flow, a law of heat conduction for turbulent flow is introduced. These laws are:

$$q = -\lambda \frac{\partial \overline{T}}{\partial y} \quad \text{and} \quad q_{tur} = \lambda_{tur} \frac{\partial \overline{T}}{\partial y} \tag{10.81}$$

where λ_{tur} is an apparent (virtual or eddy) conductivity, which is also not a fluid property, but depends on the time average flow velocity as well as on the time-average bulk mean temperature. In analogy with the thermal diffusivity κ, an eddy diffusivity for heat transfer, ε_H is defined.

$$\kappa = \frac{\lambda}{\rho c_p} \quad \text{and} \quad \varepsilon_H = \frac{\lambda_{tur}}{\rho c_p} \tag{10.82}$$

Furthermore, in analogy with the molecular Prandtl number *Pr*, a turbulent Prandtl Pr_t number is introduced:

$$Pr = \frac{\nu}{\kappa} \quad \text{and} \quad Pr_t = \frac{\varepsilon_M}{\varepsilon_H} \tag{10.83}$$

Experiments on the turbulent Prandtl number in circular tubes exhibit that the turbulent Prandtl number depends on the Reynolds number *Re*, the molecular Prandtl number *Pr* and the distance from the wall expressed by (*y/R*). Such a relation in the form:

$$Pr_t = f\left(Re, Pr, y/R\right) = \frac{\overline{u'v'}}{\overline{v'T'}} \frac{\overline{\partial T}}{\overline{\partial y}} \frac{\overline{\partial u}}{\overline{\partial y}} \tag{10.84}$$

is expected. [Eckert and Drake, 1972] collected measurements of the turbulent Prandtl number for various fluids including heavy liquid metals. They wrote, “The experimental difficulties are obviously so large, that no satisfying coherence between the individual data sets can be established for the liquid metals.” [Fuchs, 1973] describes the problems in more detail. The main error sources are:

- determination of the temperature and velocity gradients from a measured temperature and velocity distribution;
- determination of the correlation $\overline{v'T'}$, as well as which is in liquid metals hardly possible due to the lack of adequate measurement techniques.

Consider a fully developed turbulent flow in a circular duct. Within such a problem the resulting wall shear stress τ and the resulting heat flux *q* can be described using the turbulent exchange quantities in the following way:

$$\tau = \left(\mu + \rho \varepsilon_M\right) \frac{d\bar{u}}{dy} \quad \text{or} \quad \frac{\tau}{\rho} = \left(\nu + \varepsilon_M\right) \frac{d\bar{u}}{dy} \quad \text{and}$$
$$q = -\left(\lambda + \rho c_p \varepsilon_H\right) \frac{d\bar{T}}{dy} \quad \text{or} \quad \frac{q}{\rho c_p} = -\left(\kappa + \varepsilon_H\right) \frac{d\bar{T}}{dy} \tag{10.85}$$

The Reynolds analogy

In fully turbulent flows $\nu << \varepsilon_M$ and $\kappa << \varepsilon_H$ except for the immediate vicinity of the wall. If one assumes that the turbulent energy transport has a constant ratio as the turbulent momentum transport, in the extreme case $\varepsilon_H = \varepsilon_M$ this yields immediately $Pr_t = 1$. This major assumption is called the Reynolds analogy and yields immediately for $Pr_t = 1$:

$$c_p d\overline{T} = -\frac{q}{\tau} d\overline{u} \tag{10.86}$$

This can be easily integrated, assuming at the wall non-slip for the mean velocity and the wall temperature T_w for $\overline{T}(y=0)$ and for the outer flow the position is used at which the mean velocity and the mean temperature is attained, i.e. $\overline{u} = u_0$ and $\overline{T} = T_m$. Both quantities are defined:

$$c_p \int_{T_w}^{T_m} d\overline{T} = -\frac{q}{\tau} \int_{0}^{u_0} d\overline{u} \quad \text{or} \quad c_p (T_w - T_m) = \frac{q_w}{\tau_w} u_0 \tag{10.87}$$

Assuming the Reynolds analogy in the tube this immediately yields for the friction factor c_λ and for the Stanton number *St* the following result:

$$c_\lambda = 8 \frac{\tau_w}{\rho u_0^2} \quad \text{and} \quad St = \frac{Nu}{Re\,Pr} = \frac{c_\lambda}{8} \tag{10.88}$$

The Reynolds analogy yields good results for molecular Prandtl numbers larger than $Pr > 0.71$. It is also embedded in a lot of commercial code systems using the *k*-ε model. It definitely fails describing the heat transport in liquid metals because the initial boundary condition of $\varepsilon_H \sim \varepsilon_M$ and constant is not fulfilled for this type of fluids. Thus, any approach of a constant Prandtl number assumption that means using the Reynolds analogy will lead to miscellaneous results. This problem is known since [Martinelli, 1947] and has during the last two decades been reviewed critically by several authors like [Grötzbach and Wörner, 1992], [Kays, 1994], [Carteciano and Grötzbach, 2003] or [Arien, 2004].

The Prandtl analogy

Within this approach the flow field is separated into two domains a viscous sublayer and a fully turbulent bulk flow. In the viscous sublayer the molecular viscosity is larger than the eddy viscosity and the molecular conductivity dominates over the eddy diffusivity, i.e. $\nu >> \varepsilon_M$ and $\kappa >> \varepsilon_H$. This yields:

$$\frac{\tau}{\rho} = \nu \frac{d\overline{u}}{dy} \quad , \quad \frac{q}{\rho c_p} = -\kappa \frac{d\overline{T}}{dy} \quad \text{and} \quad c_p d\overline{T} = -Pr \frac{q}{\tau} d\overline{u} \tag{10.89}$$

The relations can be integrated from the wall to the border of the laminar sublayer, for which $\overline{u} = u_1$ and $\overline{T} = T_1$ is assumed. For the fully turbulent bulk the model takes use of the Reynolds analogy with the assumptions $\nu << \varepsilon_M$ and $\kappa << \varepsilon_H$ and using them the Eqs. (10.85) can be integrated from the border of the sublayer towards the bulk, which yields the result:

$$c_p (T_w - T_m) = \frac{q}{\tau} u_0 \left[1 + \frac{u_1}{u_0} (Pr - 1) \right] \tag{10.90}$$

The velocity at the border of the viscous sublayer in direction of the bulk is known since there $u^+ = y^+$ holds. Setting $y^+ = 5$ the relation (10.91) known as Prandtl analogy is obtained, which reads for the Stanton number to:

$$St = \frac{Nu}{Re\,Pr} = \frac{c_\lambda / 8}{1 + 5\sqrt{c_\lambda / 8}(Pr - 1)} \tag{10.91a}$$

For $Pr = 1$ the Prandtl analogy is similar to the Reynolds analogy. The impact of the molecular Prandtl number is reflected by taking it into account in the viscous sublayer. The factor 5 is arbitrary. But, due to the increase of the turbulent Prandtl number with decreasing molecular Prandtl number, as observed in numerous experiments, the Prandtl analogy is only very restricted applicable to liquid metal flows. The largest hint is the assumption that except for the viscous sublayer the turbulent Prandtl number is set to unity, although the thermal boundary layer is considerably larger than the viscous one.

V. Karman analogy

Following the ideas of Prandtl, v. Karman divided the flow field instead of two into three layers, the viscous sublayer ($y^+ < 5$) a transition layer ($5 < y^+ < 30$) and the turbulent wake ($y^+ > 30$). In the intermediate transition layer he assumed an identity of the molecular and the turbulent quantities, i.e. $\nu = \varepsilon_M$ and $\kappa = \varepsilon_H$, and obtained for the Stanton number the following relation. The exact derivation may be taken from the book of [Gebhardt, 1971]:

$$St = \frac{Nu}{Re\,Pr} = \frac{c_\lambda / 8}{1 + 5\sqrt{c_\lambda / 8}\left(Pr - 1 + \ln\left[\left(5Pr + 1\right)/ 6\right]\right)} \tag{10.91b}$$

Again for $Pr = 1$ the Reynolds analogy is obtained.

Further analogies

[Martinelli, 1947] extended the three layer model of v. Karman in the way that he considered both the molecular heat conductivity and the eddy diffusivity in the full turbulent range. Using this approach his analogy is applicable also to liquid metals. The considerations of Martinelli [Martinelli, 1947] and especially its restrictions are extensively discussed in the books of [Rohsenow and Choi, 1961] as well as in [Knudsen and Katz, 1958]. The results obtained consist of a number of tables. [Rohsenow and Choi, 1961] even extended Martinelli's ideas by implementing a relation of $Pr_t = f(Pr)$. However, a comparison of the results with the experiment show only satisfactory results for Peclet number larger than $Pe > 700$. Moreover, the turbulent Prandt number remains space independent, which does not hold for liquid metals as the following paragraph denotes.

10.7.3 Experimental observations of the turbulent heat transport

The equation (10.84) in particular makes clear that to evaluate the turbulent Prandtl number at any point it is necessary to measure four quantities: the turbulent shear stress, the turbulent heat flux, the velocity gradient and the temperature gradient. This is the reason why direct measurements of turbulent Prandtl numbers in duct flows are relatively scare and hardly available in boundary layers.

Despite the large experimental difficulties it is clear that the turbulent Prandtl number is larger than unity in case of the liquid metals, because liquid metals possess a large molecular conductivity compared to their molecular viscosity. A turbulence parcel will transfer in liquid metals easier energy than momentum to the adjacent fluid. Thus, the turbulent Prandtl number should increase with decreasing molecular Prandtl number. There is an influence of the wall distance (y/R) on the turbulent Prandtl number in fully developed flows. In the majority of the experimental investigations Pr_t seems to decrease with increasing distance from the wall, see [Azer and Chao, 1960] or [Davies, 1969]. For the fully developed turbulent flow in circular tubes the local turbulent Prandtl number Pr_t was evaluated in detail by [Fuchs, 1973] in sodium with a molecular Prandt number $Pr = 0.007$ as a function of y/R. The experimental results are depicted in Figure 10.7.1(a). This general tendency is supported by the measurements of [Sleicher, *et al*., 1973] or [Brown, *et al*., 1957].

Besides the dependence of the turbulent Prandtl number on the radial co-ordinate the dependence of the measured mean turbulent Prandtl number Pr_{tm} on the molecular Prandtl number seems to be even larger, as depicted in Figure 10.7.1(b). The experimental data on the mean turbulent Prandtl number define show a quite large scatter for the liquid metals, which can be partially be explained by the reasons mentioned in [Fuchs, 1973]. Another aspect may be also the fact of the determination of the mean turbulent Prandtl number Pr_{tm}. For an exact formulation it should be gained from the Lyon-Integral [Lyon, 1951] in the form:

$$\int_0^1 \frac{\left(\int_0^{r/R} \frac{u}{u_0} r' dr'\right)^2}{r\left(\frac{\varepsilon_M}{\nu}\frac{Pr}{Pr_t}+1\right)} dr = \frac{1}{\frac{\varepsilon_M}{\nu}\frac{Pr}{Pr_t}+1} \int_0^1 \frac{\left(\int_0^{r/R} \frac{u}{u_0} r' dr'\right)^2}{r} dr \tag{10.92}$$

and assuming a constant molecular Prandtl number in the cross-section of interest one gets:

$$Pr\,\overline{\frac{\varepsilon_M}{\nu}\frac{1}{Pr_t}} = \frac{Nu}{Nu_{min}} - 1 \tag{10.93}$$

where $Nu_{\min}$ is the Nusselt number in case of pure heat conduction. Some authors tried based on different assumptions to derive formulas for the mean turbulent Prandtl number. This aspect will be discussed in the context of the different closure models in the next section.

Figure 10.7.1. (a) Measured turbulent Prandtl number Pr_t as a function of the dimensionless distance (y/R) in a fully developed turbulent circular duct flow with a constant wall heat flux (q_w = const.) from [Fuchs, 1973]. b.) Measured mean turbulent Prandtl number Pr_{tm} for different molecular Prandtl numbers Pr for a fully developed turbulent circular duct flow with a constant wall heat flux (q_w = const.) for two different Reynolds numbers $Re = 2 \cdot 10^4$ (open symbols) and $Re = 10^5$.

The experimental data are from [Fuchs, 1973] for □ Na, [Buhr, et al., 1968] for O NaK and Δ Hg, [Subbotin, et al. 1962] ▽ Na, ◊ PbBi, [Sleicher, 1958] ✲ air, [Allen and Eckert, 1964] + water

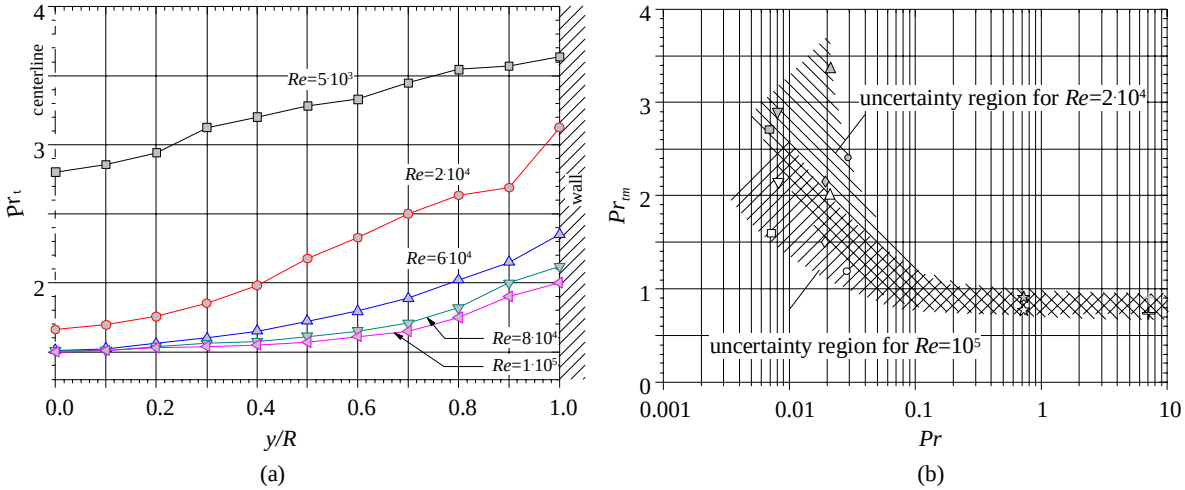

From the experimental observations the following statements on the mean turbulent Prandtl number Pr_{tm} can be made:

- For $Pr \geq 1$ (air water, oil, etc.) the turbulent Prandtl number seems to be constant and independent of the Reynolds number and molecular Prandtl number.
- The influence of the Prandtl number and the Reynolds number increases both with decreasing Prandtl number and decreasing Reynolds number.
- The turbulent Prandtl number increases with decreasing Prandtl number and decreasing Reynolds number.

10.7.4 Closure methods for the turbulent heat flux

The knowledge of the turbulent Prandtl number is a central problem of all theoretical considerations concerning the turbulent heat transfer in two-dimensional boundary layers or in duct flows. A large number of models have been published in the past which address the prediction of the turbulent Prandtl number Pr_t for such situations. There is a very strong influence of the molecular Prandtl number on the value of Pr_t for fluids with very low Prandtl numbers (liquid metals). Additionally, here is an influence of the wall distance on the value of the turbulent Prandtl number which tends to increase Pr_t close to the wall. This increase in Pr_t near the wall is especially important for high Prandtl number fluids because of the very thin thermal boundary layer. Outside this thin layer near the wall the turbulent Prandtl number seems to be constant for $Pr > 1$. Because of the strong dependence of Pr_t on molecular Prandtl number for low Prandtl number fluids (liquid metals) effort has been taken in the past to develop prediction models for Pr_t, which are able to take the dependence of Pr_t on the molecular Prandtl number as well as the dependence of Pr_t on the wall distance into account. In principle all the proposals can be divided into mainly four classes (of course containing numerous amount of subclasses):

a) semi-empirical or empirical closure methods of zero and first order;

b) turbulent Prandtl number from analytic solutions;

c) modelling of the turbulent heat flux by means of transport equations at different levels;

d) direct numerical simulation of the whole set of the time-dependent Navier-Stokes equations.

The length of this chapter extends a little compared to the previous ones. But the currently excessive use of numerical simulation tools to design critical components of liquid metal cooled devices in many technical fields requires a principle understanding of what is modelled in the individual closure assumptions for the turbulent heat fluxes. The type of this modelling plays a decisive role in the analysis of the results. It is clear, that not all the details of the modelling can be described within this context. However, the main ideas, the assumptions and the approaches yielding to the specific results for the different types of closure methods are flash-lighted. Moreover, the limiting parameter range for their validity is given as far as known to the author. Hopefully, a list of the most relevant literature is cited in this context. At the end of each section a “sometimes” rather personal assessment is given on the individual class of closure type.

a) Semi-empirical closure methods of zero and first order

Reviews of the existing work of these types of closure methods can be found in the overview article by [Reyno1ds, 1975] or in [Kays, 1994]. Within these types of models a whole branch of assumptions is hided.

The simplest ones are purely empirical correlations, in which the turbulent Prandtl number is mainly fitted to experimental data from various experiments, as e.g. by [Notter, 1969]. Some workers, though aware of attempts to predict the dependence of the eddy diffusivity ratio an molecular diffusivities and position within the flow, have rejected these analytical results, in view of the contradictions among the several models, between models and experiments, and even between different experiments. In this view [Kunz and Yerazunis, 1969] adopted for the for the turbulent Prandtl number of turbulent liquid metal flows in a circular duct:

$$Pr_t = \left(\frac{2}{3}\right)\exp\left[0.9\left(\frac{\varepsilon_M}{\nu}\right)^{0.64}\right] \tag{10.94}$$

With this they accept deviations of ±0.5 from the experiments they consider and further, it does not contain a dependence of the radial co-ordinate. Again, in the view of the scatter of their measurements, [Quarmby and Quirk, 1972, 1974] felt that it was impossible to isolate the dependence of the turbulent Prandtl number on the molecular Prandtl number and the duct Reynolds number. Nevertheless, they found an important variation across the pipe and formulated for their individual experiment the relation:

$$Pr_t = \left(1 + 400^{-y/R}\right)^{-1} \tag{10.95}$$

This yields a turbulent Prandtl number near the wall of $Pr_t = 0.5$, which is considerably to low for liquid metal flows [see Figure 10.7.1(a)], while close to the ducts centre a value of $Pr_t \approx 1$ is obtained, which is acceptable for $Re > 5{\cdot}10^4$. These purely empirical results offer neither practical nor fundamental advantages. And as matter of fact the effort spent on these methods ended around the late seventies.

A more theoretical approach offered the individual mixing length models already mentioned in the context of the analogies between heat and mass transfer. These analyses seek to account for the exchange of momentum and heat transfer between the instantaneous surroundings and a lump of fluid which moves across gradients of velocities and temperature. At the end of its journey the lump (mostly considered to be a sphere) is assumed to mix instantaneously with the surrounding fluid; the transfer rate is calculated using the terminal properties of the moving element. Clearly, these types of models are inconsistent in that no account is taken of that fraction of the transferred (heat or momentum) flux which is conveyed only part way along the mixing length. This implies more or less a proportional relation between turbulent heat and turbulent momentum flux known from the Reynolds analogy. Several types of mixing length models were proposed ranging from the beginning fifties up to the end of the sixties. The most famous are the Jenkins type mixing models after [Jenkins, 1951] with several modifications, which are listed in Table 10.7.1 and basically yield the turbulent Prandtl number as a function of the molecular Prandtl number and ε_M/ν. They do only marginally contain a local dependence of Pr_t on y/R..

Table 10.7.1. Different Jenkins type mixing length models and their range of validity for the turbulent Prandtl number Pr_t

Author	Functional form	Empirical constants	Validity
Jenkins, 1951	$f(Pr, \varepsilon_M/\nu)$	0	All Pr
Sleicher and Tribus, 1957	$f(Pr, \varepsilon_M/\nu)$	$f(\varepsilon_M/\nu)$	All Pr
Roshenow and Cohen, 1960	$f(Pr)$	1	$Pr << 1$
Tien, 1961	$f(Pr, \varepsilon_M/\nu)$	1	All Pr
Senechal, 1968	$f(y^2\nu'/(l\,\kappa))$	1	$Pr < 1$

The other class of mixing length models is formed by the Deissler type models after [Deissler, 1952], which is focussed on mainly small Prandtl number fluids as the liquid metals. They take into account only the heat transfer from the moving element and relate the length scale of an imaginary fluid sphere in the temperature gradient field to the mixing length. On this scale only molecular diffusion is assumed. These types of models are listed in Table 10.7.2 with their range of validity. A problem here is similar as in the Jenkins models that the velocity field is coupled directly to the temperature field, although knowing from the experiments that the statistical features of both are different.

Table 10.7.2. Different Deissler type mixing length models and their range of validity for the determination of the turbulent Prandtl number Pr_t

Author	Functional form	Empirical constants	Validity
Deissler, 1952	$f(Pe)$	1	$Pr << 1$
Lykoudis and Touloukian, 1958	$f(Pr)$	1	$Pr << 1$
Aoki, 1963	$f(Pr\ Re^{2.25})$	1	$Pr << 1$
Mizushina and Sasano, 1963	$f(Pr, \varepsilon_M/\nu)$	3	$Pr < 1$
Mizushina, *et al*., 1969	$f(Pr, \varepsilon_M/\nu, a/l)$	3	$Pr < 1$
Wassel and Catton, 1973	$f(Pr, \varepsilon_M/\nu)$	3	All Pr

The more advanced mixing length models adopt a more sophisticated picture of the turbulent activity. Thus the defining feature of this category is not the use of an immutable mixing length but the introduction of a discrete element which gains or looses heat and momentum as it moves through the bulk of the fluid. Nevertheless, also this analysis is constrained by the assumption of a basic analogy between momentum and heat transfer, at least in its statistical behaviour. In the article by [Reynolds, 1975] the individual aspects of these type of models are discussed as well as their advantages and disadvantages in use. They seem to fit quite well for the turbulent Prandtl number in duct and plate flow but do not generally account for the temporal behaviour of the temperature and flow field. These more advanced models are listed in Table 10.7.3.

Table 10.7.3. Different varied mixing length models and their range of validity for the determination of the turbulent Prandtl number Pr_t

Author	Functional form	Empirical constants	Validity
Azer and Chao, 1960	$f(Pe, Pr, y/R)$	1+	$Pr << 1$
Buleev, 1962	$f(Pr, Re,$ geometry$)$	5	All Pr
Dwyer, 1963	$f(Pr, \varepsilon_M/\nu)$	2	$Pr << 1$
Tyldesley and Silver, 1968	$f(Pr)$	1	All Pr
Tyldesley, 1969	$f(Pr, ?)$	2	All Pr
Ramm and Johannsen, 1973	$f(Pr, Re,$ geometry$)$	5+	All Pr

These semi-empirical types of closure methods contains also another group of models which is based on the analysis of the Reynolds equations without the direct formulation of transport equations. Additionally, [Kays and Crawford, 1993] developed a prediction model for Pr, which can be used for all molecular Prandtl numbers. The model contains two empirical constants which must be determined from available experimental data. [Cebeci, 1973] adopted van Driest's idea of near-wall damping of the mixing length to propose a turbulent Prandtl number concept. This model was extended by [Chen and Chiou, 1981] for liquid metal flow in pipes by incorporating the enthalpy thickness δ_T, in Pr_t. Although the predictions of Chen and Chiou agree well with measured Nusselt numbers for liquid metal flows, their model has the disadvantage that an additional nonlinearity is introduced into the

energy equation by using the enthalpy thickness δ_T, in Pr_t. This restricts the possibility of analytical solutions of the energy equation for hydrodynamically fully-developed flows. Furthermore, the von Kármán constant is changed in the mixing length expression for their calculation. This might lead to misleading results for larger molecular Prandtl numbers.

Summary on semi-empirical or empirical closure methods of zero and first order

All semi-empirical closures for the turbulent heat flux independent of their order do not give detailed insight in the turbulent exchange mechanisms between the velocity fluctuations and the temperature oscillations. For engineering purposes some of them can be applied to assess the heat exchange, but one should be careful on the model, its validity and the empirical constants chosen, because they often apply only for one fluid in a rather limited parameter field. By nature the Reynolds analogy can give only reliable results for large Reynolds numbers, in which the thermal boundary layer remains small and the turbulent Prandtl number tends to unity. As soon as one arrives to lower Reynolds numbers, this analogy leads to inaccurate results. This should be taken into account also for numerical simulations using the *k*-ε model without an additional turbulent heat flux modelling. As benchmark studies have shown, see [Arien, 2004] this can lead to severe discrepancies.

b) Turbulent Prandtl number from analytic solutions

[Yakhot, *et al*., 1987] present an analytic solution based on what they call the "renormalisation group analysis method" and this is result is apparently devoid of any empirical input. The relative simple equation reads to:

$$\left[\frac{\left(Pr_{eff}^{-1}-1.1793\right)}{\left(Pr^{-1}-1.1793\right)}\right]^{0.65}\left[\frac{\left(Pr_{eff}^{-1}+2.1793\right)}{\left(Pr^{-1}+2.1793\right)}\right]^{0.35}=\frac{1}{\left(1+\varepsilon_M/\nu\right)}\quad\text{with}\quad Pr_{eff}=\frac{\left(1+\varepsilon_M/\nu\right)}{\left(\frac{\varepsilon_M/\nu}{Pr_t}+\frac{1}{Pr}\right)} \tag{10.96}$$

It is not clear whether this result is expected to be valid over the entire boundary layer or only in the region where the logarithmic law holds. It is remarkable that the results obtained with that relationship matches the nearly all experimental observations quite well. And it seems even to work for higher molecular Prandtl number. [Kays, 1994] fitted the relation (10.96) by an asymptotic curve in the form:

$$Pr_t=\frac{0.7}{Pe_t}+0.85\quad\text{with}\quad Pe_t=\left(\varepsilon_M/\nu\right)Pr \tag{10.97}$$

where Pe_t is the turbulent Peclet number. It looks similar like a suggestion performed by [Reynolds, 1975] but in that case Pr_t is an average throughout the whole boundary layer.

[Lin, *et al*., 2000] modified the renormalisation group analysis performed by [Yakhot, *et al*., 1987]. Within the model a quasi-normal approximation (see [Chou and Chin, 1940]) is assumed for the statistical correlation between the velocity and temperature fields. Due to the statistical approach the different time scales of the temperature fluctuations and the velocity fluctuations remain in the model and are coupled together by the wave number *k*. A differential argument leads to derivation of the turbulent Prandtl number Pr_t as a function of the turbulent Peclet Pe_t number, which in turn depends on the turbulent eddy viscosity ε_M. The functional relationship between Pr_t and Pe_t is comparable to that of [Yakhot, *et al*., 1987] but it contains in contrast to the Yakhot, *et al*. solution the spectral properties of both oscillating fields. But, the resulting formula for the effective turbulent Prandtl number Pr_{eff} is very close to Eq. (10.96). It reads to:

$$\left[\frac{\left(Pr_{eff}^{-1}-1\right)}{\left(Pr^{-1}-1\right)}\right]^{2/3}\left[\frac{\left(Pr_{eff}^{-1}+2\right)}{\left(Pr^{-1}+2\right)}\right]^{1/3}=\frac{1}{\left(1+\varepsilon_M/\nu\right)}\quad\text{with}\quad Pr_{eff}=\frac{\left(1+\varepsilon_M/\nu\right)}{\left(\frac{\varepsilon_M/\nu}{Pr_t}+\frac{1}{Pr}\right)} \tag{10.98}$$

The apparent resemblance between the formulas (10.96) and (10.98) is quite remarkable not only because of the similarity in mathematical structure, but because the results are basically derived entirely from different approaches to renormalisation group analysis of turbulence. Pr_t can be represented in terms of Pe_t for any given molecular Prandtl number Pr. A comparison with the direct numerical simulation results (in which the whole set of time dependent Navier-Stokes equation is solved) of [Kasagi, *et al*., 1992] and [Kim and Moin, 1987] shows excellent agreement for a Prandtl number of $Pr = 0.1$. Also a comparison of the results with the experimental data taken from [Bremhost and Krebs, Sheriff and O'Kane, and Fuchs, 1973] all measured in liquid sodium at the centreline of thermal turbulent pipe flow shows excellent agreement, see Figure 10.7.2(a). Next, they noticed that the Peclet number Pe_t is a thermal analogy of the Reynolds number. The reason why Pr_t always tends to 1 as Pe_t becomes sufficiently large would be that at this time the thermal flow turbulence is completely convection dominated and the temperature field T responds immediately to any change of the velocity field v.

Figure 10.7.2. a.) The turbulent Prandtl number Pr_t versus the turbulent Peclet number Pe_t plotted based on Eq. (10.98) for liquid sodium ($Pr = 0.007$) in comparison with experimental data measured by [Bremhost and Krebs, 1992, □], [Sheriff and O'Kane, 1980, Δ] and [Fuchs, 1973, O]. b.) The scaling law of the thermal energy spectrum $E_{Htur}(k)$ versus the normalised wave number k/k_0 for $Pr << 1$ after [Lin, *et al*., 2000] in comparison with experiments by [Boston and Burling, 1972].

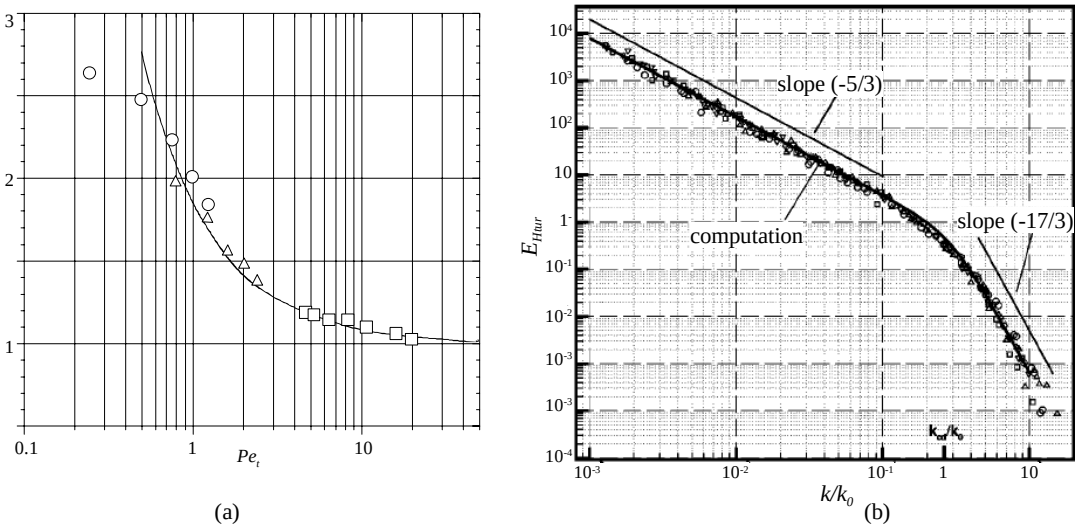

[Batchelor, 1958a, b] was the first to propose scaling laws for the thermal energy spectrum for $Pr << 1$ and $Pr >> 1$, respectively, leaving a proportional constant C_B undetermined. Subsequently, many authors have tried to estimate or measure the value of C_B under various flow conditions. In theory, [Kraichnan, 1971] had the estimate $C_B = 0.208$, and [Gibson and Schwarz, 1963a] had the estimate $C_B = 0.9$, while [Yakhot, *et al*., 1987] obtained $C_B = 1.16$ according to their ε-based renormalisation group analysis. [Kerr, 1990] obtained numerically the value $C_B = 0.6$. In experiment, [Gibson and Schwarz, 1963b] had $C_B = 0.35$, [Grant, *et al*., 1968] obtained $C_B = 0.31$, and [Boston and Burling, 1972] got $C_B = 0.81$.

Due to the retaining of the spectral information in the model by [Lin, *et al*., 2000] the scaling laws for the thermal energy spectrum (E_{Htur}) versus the wave-number k can be obtained. Such a thermal energy spectrum as a function of the normalised wave-number is depicted in Figure 10.7.2(b). It is visible that in the inertial-convective range the thermal energy spectrum follows a power law of -5/3 and in the inertial-conductive range of a slope of -17/3 is obtained. Especially, the latter is different to large Prandtl number fluids, where in the inertial conductive domain a slope of -1 is observed, see experiments by [Grant, *et al*., 1968]. Thus, an essential result of the renormalisation group analysis is that the Batchelor constant is not a universal constant, but depends on the shape of the actual thermal energy spectrum.

The usual Smagorinsky model is used for the large-eddy simulation of the Navier-Stokes equation. One can construct a parallel model for turbulent transport of the passive scalar, which yields that constant C_P depends on $Pr_t^{-1/2}$ and on the wave number k.

In order to model the turbulent thermal transport process at a wall boundary the surface renewal concept initially introduced by [Danckwerts, 1951] can also be used. This was recently modified by [Tricoli, 1999]. The basic assumption considers the surface to be covered by a mosaic of laminar flowing patches of fluid, where transport occurs only by molecular diffusion These fluid patches are supposed to be periodically replaced by new ones “surface renewal model” or to form viscous layers that periodically grow and collapse “growth-breakdown model”. These are unsteady state 1-D models. It has also been proposed that the fluid patches are arranged in a regular repetitive pattern of steady state boundary layers developing for a given length. These simple models are able to explain a number of qualitative features observed in turbulent transport. The model derived by [Tricoli, 1999] appeal to postulated mechanistic pictures of turbulence and the concepts and the quantities involved have no fundamental relationship with the correlated turbulent fluctuations, the sole quantities that actually determine turbulent transport. He constructed a theory able to predict turbulent heat transport from fundamental information, namely the thermal diffusivity and the normal turbulence intensity in the fluid bulk. This theory applies to heat transfer in turbulent incompressible flow for $Pr << 1$. His approach is based on the primary ingredients of turbulent transport, i.e. the turbulence fluctuation and the molecular momentum or heat diffusivity and does not contain empirical expressions for such quantities “eddy diffusivity models” or postulates a physical picture of the transport mechanism at the wall surface “surface renewal”. The predictions show an excellent agreement with available experimental data and empirical correlations for the turbulent heat transport in liquid metal flows in pipes. The most remarkable results of this approach refer to a relationship of the Nusselt numbers in a fully developed turbulent circular duct flow with different thermal boundary conditions. This relation valid for $Pe > 10^3$ reads to:

$$Nu_{(T=const)} = \frac{\pi^2}{12} Nu_{(q_w=const)} \tag{10.99}$$

Summary on turbulent Prandtl number derivations from analytic solutions

The analytic class of solutions for the turbulent Prandtl number may be difficult to handle in the context of a numerical treatment of a commercial code package. But it gives important results to the near wall behaviour of the heat flux and thus contributes considerably to the treatment of the thermal wall functions. Another aspect is that, especially within the renormalisation group analysis, the temporal behaviour of the temperature field is still a part of the final result. This allows verifying the validity of direct numerical simulations (DNS), which are in principle exact but may use a too coarse grid. Only the analytic solutions are able to provide near wall data of the kinetic and thermal energy spectrum, because current measurement technologies are still in a stage where they hardly can resolve the viscous and thermal boundary layers simultaneously and the analytic solutions are able to provide assessments

in complex geometries, which are currently not accessible with a direct numerical simulation. Unfortunately, for engineering applications to assess a mean turbulent heat transport form a wall this type of analysis is time consuming and requires a lot of effort.

c) Modelling of the turbulent heat flux by means of transport equations at different levels

The modelling of the turbulent heat fluxes by means of the transport equations contains in some sense also to the semi-empirical methods, because the development of each transport equation generates a set of constants *a priori* not known. These constants can be either experimentally determined or calculated by exact solutions (analytic ones or a direct numerical simulation). The modelling of the turbulent heat flux transport equations follows the same systematic scheme as shown in the section of the turbulent momentum exchange.

A first proposal to model the turbulent heat fluxes using transport equations was made by [Jischa and Rieke, 1979]. The final form of their transport equation for boundary layer type flows reads for the heat flux in wall normal direction to:

$$\underbrace{u\frac{\partial}{\partial x}\left(\overline{v'T'}\right)+v\frac{\partial}{\partial y}\left(\overline{v'T'}\right)}_{Convection}+\underbrace{\overline{v'^2}\frac{\partial \bar{T}}{\partial y}-\frac{\overline{u'v'}}{\rho c_p}\frac{d\bar{p}}{dx}}_{Pr\ oduction}\underbrace{-\frac{1}{c_p}\overline{v'\varepsilon}+\frac{\nu(Pr+1)}{Pr}\overline{\frac{\partial v'}{\partial x_j}\frac{\partial T'}{\partial x_j}}}_{Dissipation}\underbrace{-\overline{\frac{p'}{\rho}\frac{\partial T'}{\partial y}}+.....}_{\text{Redistribution}}+\underbrace{\frac{\partial}{\partial y}\left[\overline{v'^2T'}+.....\right]}_{Diffusion}=0 \qquad (10.100)$$

Generally, all types of turbulent transport equations exhibit the same structure consisting of convective terms, turbulence production, dissipation, redistribution and finally diffusion. Every of the newly modelled transport equations contain correlation or time averaged products not known. The challenging task after formulating these flux transports, dissipation or destruction terms is to model the unknown correlations or gradients in an appropriate manner. This can be conducted in form of a gradient approach like the Boussinesq approach for the shear stress, where $\overline{u'v'} \sim \partial\bar{u}/\partial y$ was set, or even an additional transport equation if a simple gradient approach can not match all the transport processes taking place in the individual problem.

In the work by [Jischa and Rieke, 1979 and 1982] the turbulent fluctuations $\overline{v^{2'}}$ are assumed to be proportional to the turbulent kinetic energy *k* and for the dissipation of the turbulent kinetic energy the Prandtl mixing length approach has been used. The latter is problematic with respect to liquid metals since the molecular heat conduction is not negligible. Finally, the dissipation of the gradients of the velocity and temperature fluctuations were set to be proportional to the turbulent heat fluxes in the form $(\nu/Pr)\overline{\partial v'\partial T'} = C_D(\nu/Pr)\overline{v'T'}/L^2$, where C_D is a constant and L^2 the square of a characteristic length. All these assumptions yield finally to a simplified transport equation, in which the turbulent heat flux is a function of the temperature gradient. Although this model is rather crude, since the turbulent heat flux model is only taking into account a forced convective transport, it exhibits the dependence of the turbulent Prandtl on the distance from the wall and on the Reynolds number. As a disadvantage it should be clearly noted that the thermal eddy diffusivity ε_H is still linked to the momentum diffusivity ε_M assuming a similar statistical behaviour of the turbulence and that it is valid only for high Peclet numbers in purely forced convective flows. Thus, any kind of mixed or even buoyant flow can not be treated.

In the past decade a considerable effort has been spend on the development of a more detailed modelling of the turbulent heat fluxes, the turbulent temperature variance $\overline{T'^2}$ and its dissipation or destruction ε_T. A first order four-equation type model has been developed by [Nagano, *et al.*, 1988, 1994 and 1995], which was able to represent the physics in more detail, but required of course data for

the unknown constants appearing in the new transport equations and information on the statistical behaviour of the fluctuations near the boundaries especially the walls. Especially, close to the wall or in mixed and even more in buoyant convective flows the turbulence field is strongly anisotropic, which does not allow to match the turbulent shear stresses $\overline{v'^2}$ with the turbulent kinetic energy k, see [Durbin, 1993a]. The details of the more advanced shear stress modelling close to the walls may be taken from [Durbin, 1993a and b], [Manceau, *et al*., 2000], [Oi, *et al*., 2002] or [Speziale and So, 1998].

Also the modelling of the turbulent heat flux evolution equations is still problematic and the reported results are only slightly better than obtained with lower order closures which based on the eddy diffusivity formulation, see [Nagano and Kim, 1988]. Thus in many forced convective problems the two-equation approaches accounting for the temperature variance $\overline{T'^2}$ and its destruction $\varepsilon_{T'^2}$ are current state of the art, see [Grötzbach, *et al*. 2004] and [Karcz and Badur, 2005]. A lot of attention must be paid to the destruction rate of temperature variance transport equation and this especially close to the wall. Different approaches are generally employed to predict the generation of $\varepsilon_{T'^2}$. The details on the different approaches may be taken from [Sommer, *et al*., 1992], [Abe, *et al*. 1995], [Shikazono and Kasagi, 1996], [Deng, *et al*., 2001] or in a comprehensive study by [Nagano, 2002].

Next to wall near flows also any buoyancy influenced flow exhibits a strong anisotropy. In such types of flow even a second order description of the turbulent transport of heat should be applied [see Grötzbach, *et al*., 2004], which means the use of independent transport equations for the three components of the turbulent heat flux vector. These kinds of turbulence models called "Turbulent model for buoyant flow mixing" (TMBF) proposed by [Carteciano, *et al*., 1997], [Carteciano and Grötzbach, 2003] belong to this class of models.

Summary on modelling of the turbulent heat flux by means of transport equations at different levels

Any computational fluid dynamic calculation, which is conducted to assess the liquid metal heat transfer in turbulent flows must be performed by a skilled user, which is aware of the specific features appearing in liquid metal flows. In purely forced convective flows, which may even not appear for hydraulic Reynolds number beyond $Re > 10^5$ (see [Gardner, 1968] or [Lefhalm, 2004]) a k-ε model may exhibit sensible results if the thermal wall function formulation chosen is correct and applies for the problem considered. In strongly anisotropic flows liquid metal flows associated with heat transfer the k-ε model using a constant turbulent Prandtl number of $Pr_t = 0.9$ (Reynolds analogy) yields unphysical results. In this context higher order closure approaches are necessary in which the turbulent heat fluxes are modelled in such a sense that the transport equations contain the statistical features of the thermal field. By performing such an approach unknown triple correlations and constants are generated. The spatial distribution of the correlations may be directly evaluated in benchmark experiments, which is due to the limited capability of the currently available measurement techniques difficult. More often the correlations and constant are determined by the comparison of the modelling data with the exact solution obtained by means of direct numerical simulation.

d) Direct numerical simulation (DNS)

The direct numerical solution of the time dependent Navier-Stokes equations represents in principle an exact solution of the problem. Although the progress in memory storage capacity and computing speed increased considerably in the past decade the application of a DNS is still limited to rather heat transfer problems in simple geometries. Nevertheless, the progress made in the computer technology allows now to perform DNS-calculations which are not only slightly turbulent as the first ones by [Kim and Moin 1989], where it was difficult due to the low Reynolds number to detect the logarithmic region of the velocity profile. The DNS performed in the recent years where focused to

study the effect of the Prandtl number both in case of isotropic turbulence [Kasagi, *et al*., 1993], in near wall flows ([Kawamura, *et al*., 1998, 1999] or [Piller, *et al*. 2002]) and in buoyancy governed flows [Otic, *et al*., 2005] (here only a few publications of exemplary nature are cited). An immediate result of these computations is the spatial and temporal dependence of the statistical properties of the thermal and the momentum field on the different boundary conditions, which is especially experimentally not accessible. Thus, the DNS is currently the only available tool to qualify and verify the completeness and quality of computer codes based on a transport equation modelling. It reveals their modelling deficits and offers the possibility to model more adapted higher order closures. In this sense DNS can be conceived as a complementary tool for a more advanced turbulence modelling for technical and engineering applications, from which the DNS is still far away.

10.7.5 Heat transfer correlations for engineering applications

All the heat transfer correlations referred to in this subsection are valid for the single-phase heat transfer of a turbulent liquid metal flow in a specified geometry. They are gained by experiments performed since the late forties up to the present. For many of the described and shown heat transfer correlations the whole set of boundary conditions were not available, so that a final judgement on the quality of the obtained data can not be drawn. Especially, data on the homogeneity of the produced wall heat flux, the temperature uncertainty, the inlet-conditions for the flow field and the methodology to determine if the flow or the temperature field is fully developed or not. Another aspect in this context is the question, how the Nusselt number is determined. In many publications it is unclear if this has been performed using a global or a local method.

The survey of the heat transfer correlations does not cover the uncertainties of the turbulent velocity profiles, since for most of the liquid metal experiments conducted in the past, except for a few rather specific ones, a full set is not available.

Taking into account the numerous heat transfer correlations being on the “market” this subsection tries to outline, how large the uncertainty margin for the individual correlation is and where the deviation to the other arise from. But, before turning into the technical description of the forced convective heat transfer processes some critical remarks to the terminology forced convection should be mentioned.

Despite the considerable effort made in the computational fluid dynamics, for engineering purposes, heat transfer correlations play still a significant role. It may be to assess, how much heat can be transferred in a particular set-up or they may be used in the context of a system analysis. Many technical configurations consist of several devices and each of them acts as a heat sink (heat exchanger) or a heat source (by viscous dissipation as a valve or a mechanical pump, by direct electric heating like an electro-magnetic pump, or the fluid flow around a the reactor thermal source). Current computational simulations are by far not capable to represent the whole set three-dimensionally. Hence, the component interaction is mainly performed by one-dimensional models taking into account the heat transfer correlations and the friction factor in the flow components in order to predict the temporal system performance in dependence of normal and abnormal operation cases.

10.7.5.1 Free convection distortion in liquid metal heat transfer

Free convection becomes important at low Reynolds numbers in liquid metals and usually influences the heat transfer by distorting the according temperature and velocity profiles from the expected symmetrical behaviour. This effect is even more emphasised for heavy liquid metals. Free

convection distortion have been already observed by [Schrock, 1964] in sodium-potassium (NaK) for Reynolds number up to $1.6 \cdot 10^4$, by [Lefhalm, *et al*., 2003 and 2004] in lead-bismuth up to $Re = 1.1 \cdot 10^5$ and [Gardner, 1969] in mercury for $Re = 3 \cdot 10^5$ in horizontal tubes, while in vertical circular tubes [Kowalski, 1974] detected free convection distortion up to Reynolds numbers of $Re = 9 \cdot 10^4$. All the experimental data exhibit that the velocity profile rapidly distorts as the heat flux is increased. At high heat flux a limiting profile shape with the centreline velocity well below the mean velocity u_0. As a matter of this fact the experimentally determined Nusselt number in even in a "fully developed pipe flow" depends on several parameters, such as whether the pipe flow is upwards or downwards, the pipe is horizontal or vertical, the direction of the heat flux (cooled or heated) and the value of the Rayleigh number. Figure 10.7.3(a) displays the measured Nusselt number variations in dependence of the angle of the perimeter for a horizontal turbulent mercury pipe flow having free convection distortion. In an order of magnitude estimation performed by [Buhr, 1967] he introduced a parameter, say *Z*, which can be conceived as a ratio of the buoyancy forces versus the inertia forces. This parameter is defined as:

$$Z = \frac{Ra}{Re}\frac{d_h}{L} \quad \text{with } Ra = Gr \cdot Pr, Gr = \frac{d_h^3 \beta g \Delta T}{\nu^2} \text{ and } \Delta T = \frac{dT}{dx} d_h \tag{10.101}$$

Herein, *Re* is the hydraulic Reynolds number, d_h the hydraulic diameter, *Ra* the Rayleigh number, *Gr* the Grashof number, β the expansion coefficient, *g* the gravity constant, ν the kinematic viscosity and Δ*T* the axial temperature difference. He analysed a series of vertical and horizontal heat transfer experiments in pipe flow and found that if $Z > 2 \cdot 10^{-4}$ free convection affects the forced convective measured Nusselt number *Nu*. Also he is mentioning that the fluid properties especially for larger temperature differences should be evaluated at the bulk mean temperature $T_m = (T_{in} + T_{out})/2$.

Figure 10.7.3. a.) Measured local Nusselt number at several angles of the perimeter in a turbulent mercury in a horizontal pipe with convection distortion effects from [Gardner, 1969]. b.) Dependence of the Nusselt number on the *Z*-parameter, in a vertically upward directed turbulent mercury pipe flow exhibiting free convection effects.

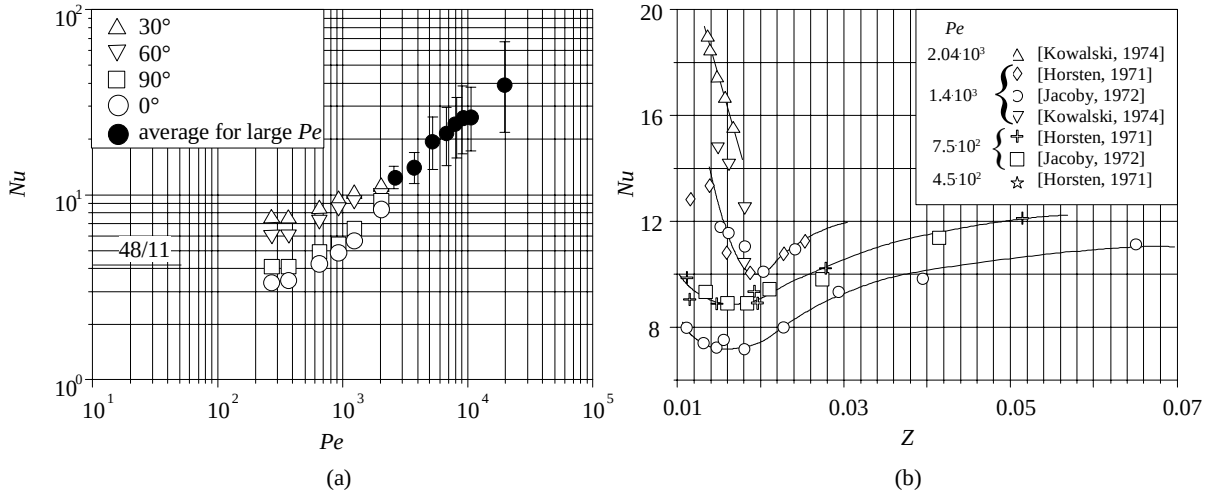

When the flow is dominated by forced convection, the following qualitative picture of the effects of free convection on the forced convection heat transfer is observed. Buoyancy forces enhance the turbulent heat transfer to liquid metals for downwards oriented flow while it retards it for upwards directed flow. Buoyancy forces influence the convective heat transfer indirectly through their effect on shear stress distribution in the liquid metal. In vertically downward flow, the buoyancy forces operate

against the mean flow direction and increase the isothermal shear stress near the heated surface. In contrast to the upwards flow the shear stress is reduced by the buoyancy. The increase in shear stress in the downwards flowing case leads to an increase of the turbulence production and hence will enhance the heat transfer. The opposite holds for the upward flow. If the temperature gradients are large the buoyancy effects become more and more important and the enhancement of heat transfer occurs in both upward and downward flow as observed by [Jackson, 1983]. The effects of buoyancy on heat transfer to liquid metals are for the relatively "light" alkali metals less than for ordinary fluids because of the reduced importance of turbulent eddy conduction at low Peclet numbers. For heavy liquid metals, however, due to their low viscosity they are of crucial importance.

This qualitative picture is supported by Figure 10.7.3(b), which exhibits that the Nusslet number is a function of the parameter Z – initially decreasing, then growing as Z increases. Z is essentially proportional to the applied heat flux. As the buoyancy forces become comparable to the inertia forces of the flow the Nusselt number reaches a minimum, begins to increase, and finally appears to reach a limiting value. It can be seen that the effects of free convection distortion can affect the measured value of the Nusselt number and could, therefore, explain some of the well-known scatter in the Nusselt number data for the liquid metal heat transfer. Needless to say, the effects of free convection distortion must be considered when dealing with liquid metal heat transfer systems, especially for heavy liquid metal systems.

10.7.5.2 Turbulent heat transfer in circular ducts

The turbulent heat transfer in circular ducts is one of the most often investigated configuration of the liquid metal heat transfer. Similar as in the laminar energy exchange one can distinguish between the three cases:

a) fully developed flow (either hydraulically and thermally);

b) hydraulically developing;

c) thermally developing.

a) Fully developed turbulent flow

For liquids with Prandtl number around unity both the temperature and the velocity distribution can be calculated approximately in terms of a series expansion. But, for liquids with $Pr << 1$ (as well as for $Pr >> 1$) no closed form formulas for the temperature distribution are available either for the condition of a constant wall temperature (T_w = const.) or a constant wall heat flux (q_w = const.). A ridiculously large number of correlations, both theoretical and empirical have been developed for the heat transfer in a smooth circular duct. [Shah and Johnson, 1981] put many of them together in tabular form, which is extended by the correlations known to the authors in the context of this handbook. The correlations for constant wall temperature (T_w = const.) are displayed in Table 10.7.4 while for the condition of a constant wall heat flux (q_w = const.) they are shown in Table 10.7.5.

Case: T_w = constant

Referring to the least error in the scatter of all experimental data the correlation proposed by [Notter and Sleicher, 1972] seems to fit best to all data for the case of a constant wall temperature. The computational work and dimensional analysis in the late seventies performed by [Leslie, 1977] and numerical calculations by [El-Hadidy, *et al.*, 1982] yield that there are no different exponents regarding the Reynolds and the Prandtl number. Their main result is that for T_w = const. the Nusselt

number is proportional to $Nu \sim Pe^{0.8}$, which holds for $Pe > 2 \cdot 10^2$ and pure convective flow. For a long time it was difficult to calculate the heat transfer in a circular tube by means of a direct numerical simulation, because of the singularity at the ducts centreline. However, a transformation of the problem made it accessible for a DNS and [Yu, *et al*., 2001] showed a universal solution in principle valid for all Prandtl numbers. They tried to match their findings with the different wall heat fluxes and to derive a unique correlation. The following set of equations is recommended as the best choice for $Pr_t > Pr$, but is subject to possible significant improvement, because still some simplifications had to be applied to the DNS.

$$u_0^+ = 3.2 \cdot \frac{227}{r^+} + \left(\frac{50}{r^+}\right)^2 + \frac{1}{0.436} ln\left[r^+\right] \quad ; \tag{10.102 (a-d)}$$

$$\frac{Nu - Nu(Pr=0)}{Nu(Pr=Pr_t) - Nu(Pr=0)} = \frac{1}{1 + \left(\frac{Pr}{Pr_t}\right)^{\frac{1}{8}} \left(\frac{Pr_t}{Pr} - 1\right) \frac{\left(Nu(Pr=Pr_t, y\to\infty) - \frac{2}{3} Nu(Pr=Pr_t)\right) Nu(Pr=Pr_t)}{(Nu(Pr=Pr_t) - Nu(Pr=0)) Nu(Pr=Pr_t, y\to\infty)}}$$

$$\text{with} \quad Nu(Pr=0) = \frac{8}{1 + \frac{1.540}{(u_0^+)^{1/3}}} \quad \text{and} \quad Nu(Pr=Pr_t) = \frac{\mathrm{Re}(f/2)}{1 + \frac{145}{(u_0^+)^{5/2}}}$$

where r^+ is the dimensionless tube co-ordinate ($r^+ = r\nu(\tau_w \cdot \rho)^{½}$), and u_0^+ the dimensionless velocity normalised by ($u^+_0 = u_0\nu(\tau_w \cdot \rho)^{½}$), Pr the molecular and Pr_t the turbulent Prandtl number, Re the Reynolds number and f the (Fanning-) friction factor ($f = 2\tau_w/(\rho\, u_0^2)$). According to their estimates on the error compared to the [Notter and Sleicher, 1972] correlation is reduced by more than 50%.

Although some simplifications and assumptions were introduced (for details see e.g. [Churchill, 2000 or Churchill, *et al*., 2000]) they found a good representation for all of the computed values of Nu without the introduction of any explicit empiricism compared to other DNS calculations. In either event, a correlation for turbulent Prandtl number Pr_t like the subsequent named ones (10.103)(a,b) is necessary to obtain numerical values of Nu using a pocket computer. Also empirical expressions (from the DNS) such as the two equations (10.102)(c,d) are needed for $Nu = Nu(Pr = 0)$ and $Nu = Nu(Pr = Pr_t)$ for values of r^+ intermediate to or above those for which the computations were carried out by [Yu, *et al*., 2001].

$$Pr_t = \left(1 + \frac{10}{35 + \left[\frac{\left(\overline{u'v'}\right)^+}{1 - \left(\overline{u'v'}\right)^+}\right]}\right)^{-1} \frac{1 + \Phi}{\left(0.025 Pr \left[\frac{\left(\overline{u'v'}\right)^+}{1 - \left(\overline{u'v'}\right)^+}\right] + \Phi\right)} \tag{10.103 (a,b)}$$

$$\text{with} \quad \Phi = 90 Pr^{3/2} \left[\frac{\left(\overline{u'v'}\right)^+}{1 - \left(\overline{u'v'}\right)^+}\right] \quad \text{and} \quad \left(\overline{u'v'}\right)^+ = -\frac{\rho}{\tau}\left(\overline{u'v'}\right) \text{ or}$$

$$Pr_t = 0.85 + \frac{0.015}{Pr}$$

The later expression already appeared in the article by [Jischa and Rieke, 1979].

It is interesting to note in this context that the ratio of the wall Nusselt numbers for the constant wall temperature and the case of constant wall heat flux found in the DNS studies is nearly exact the same as the analytical result derived by [Tricoli, 1999], see Eq. (10.99). That means that the Nusselt numbers for a constant wall temperature are in any case lower than for a constant wall heat flux at least by this ratio for a fully thermally and hydrodynamically developed turbulent pipe flow.

Table 10.7.4. Fully developed turbulent flow Nusselt numbers in a smooth circular duct for $Pr < 0.1$ with a constant wall temperature (T_w = const.) from experiments

Investigator	Correlation	Remark
[Gilliland, *et al*., 1951]	$Nu = 3.3 + 0.02\,Pe^{0.8}$	$0 \le Pr \le 0.1$ and $10^4 \le Re \le 5{\cdot}10^6$, rather speculative description of the boundary conditions.
[Sleicher and Tribus, 1957]	$Nu = 4.8 + 0.015\,Re^{0.91}Pr^{1.21}$	$0 \le Pr \le 0.1$ and $10^4 \le Re \le 5{\cdot}10^6$, the predictions are within a bandwidth of -33% and +19.5% of [Notter & Sleicher, 1972].
[Hartnett and Irvine, 1957]	$Nu = Nu_{slug} + 0.015\,Pe^{0.8}$ with $Nu_{slug} = 5.78$ assuming a slug velocity profile	$0 \le Pr \le 0.1$ and $10^4 \le Re \le 5{\cdot}10^6$, the predictions are 40% below the [Notter & Sleicher, 1972] correlation
[Azer and Chao, 1961]	$Nu = 5 + 0.05\,Re^{0.77}Pr^{1.02}$	$0 \le Pr \le 0.1$ and $10^4 \le Re \le 5{\cdot}10^5$, the predictions are within +14.2% and -18.6% of the [Notter & Sleicher, 1972] correlation.
[Notter and Sleicher, 1972]	$Nu = 4.8 + 0.0156\,Re^{0.85}Pr^{0.93}$	$0.004 \le Pr \le 0.1$ and $10^4 \le Re \le 10^6$, the predictions are based on a numerical analysis and the minimum error of the cloud of experimental data.
[Chen and Chiou, 1981]	$Nu = 4.5 + 0.0156\,Re^{0.85}Pr^{0.86}$	$0 \le Pr \le 0.1$ and $10^4 \le Re \le 5{\cdot}10^6$, the predictions are within a bandwidth of +36% and -2% of [Notter & Sleicher, 1972].

Case: q_w = constant

The fully developed Nusselt numbers computed from the [Notter and Sleicher, 1972] correlations covers a wide range of the Reynolds numbers and molecular Prandtl numbers with the smallest error to all experimental data currently available. [Heng, *et al*., 1998] conducted a numerical study for the constant heated fully developed circular tube case based on the models proposed by [Churchill, 1997a and b]. The integrals to be solved are rather complex and can not be used in the context of an engineering approach. However, the results obtained by [Heng, *et al*., 1998] almost coincide with the DNS of [Yu, *et al*., 2001]. The maximum deviation found occurs for small r^+, where [Heng, *et al*., 1998] underpredict the Nusselt number by 1.8%. Since the experimental data basis for the uniform wall heating is considerably larger than for the uniform wall temperature, the empirical correlation derived by [Notter and Sleicher, 1972] is recommended to fit best all experimental data available. The deviation to the DNS data and other numerical results is for its valid Reynolds number range within the range of +5% over-prediction of the mean *Nu*.

All preceding heat transfer results pertain to uniform heat flux or uniform wall temperature around the tubes perimeter. The technically important problem of circumferentially varying but axially constant wall heat flux was solved by [Reynolds, 1963], [Sparrow and Lin, 1963] and [Gartner, *et al*., 1974]. To the best knowledge of the author the only available experimental data are available by [Black and Sparrow, 1967], unfortunately not for liquid metals. Nevertheless, the analysis by [Gartner,

et al., 1974] is performed also low Prandtl number fluids. Assuming a cosine heat flux variation at a given cross-section of the duct, the local Nusselt number around the perimeter can be calculated by:

$$q_w(\varphi) = \bar{q}\cdot(1 + b\cos\varphi) \quad \text{yields } Nu(\varphi) = \frac{1 + b\cos\varphi}{1/\,Nu + (2G/b)\cos\varphi} \tag{10.104}$$

where Nu is the value of the uniform wall heat flux, $\bar{q}$ the mean heat flux, b a specified constant and G the circumferential heat flux function calculated by [Gartner,1974]. G is unity for laminar flows for all Prandtl numbers. The tabulated values can be taken from Table 10.7.6.

Table 10.7.5. Fully developed turbulent flow Nusselt numbers in a smooth circular duct for $Pr < 0.1$ with a constant wall heat flux (q_w = const.) from experiments

Investigator	Correlation	Remark
[Lyon, 1949, 1951] [Subbotin, *et al*., 1962]	$Nu = 5 + 0.025\,Pe^{0.8}$	$0 \le Pr \le 0.1$ and $10^4 \le Re \le 5\cdot10^6$, the predictions are within +33% and -6.5% of [Notter & Sleicher, 1972].
[Lubarski and Kaufman, 1955]	$Nu = 0.625\,Pe^{0.4}$	$0 \le Pr \le 0.1$ and $10^4 \le Re \le 10^5$, significant underprediction of [Notter& Sleicher, 1972] by -43%.
[Sleicher and Tribus, 1957]	$Nu = 6.3 + 0.016\,Re^{0.91}Pr^{1.21}$	$0 \le Pr \le 0.1$ and $10^4 \le Re \le 5\cdot10^6$, the predictions are within a bandwidth of -32% and +26% of [Notter & Sleicher, 1972].
[Hartnett and Irvine, 1957]	$Nu = Nu_{slug} + 0.015\,Pe^{0.8}$ with $Nu_{slug} = 8$ assuming a slug velocity profile	$0 \le Pr \le 0.1$ and $10^4 \le Re \le 5\cdot10^6$, the predictions are 44% below the [Notter & Sleicher, 1972] correlation
[Dwyer, 1963]	$Nu = 7 + 0.025\left[RePr - \frac{1.82Re}{(\varepsilon_M/\nu)_{max}^{0.14}} \right]^{0.8}$ where $(\varepsilon_M/\nu)_{max} = 0.037Re\sqrt{f}$	$0 \le Pr \le 0.1$ and $10^4 \le Re \le 5\cdot10^6$, the predictions are within +31% and -6.5% of the [Notter & Sleicher, 1972] correlation.
[Skupinski, *et al*., 1965]	$Nu = 4.82 + 0.0185Pe^{0.827}$	$0 \le Pr \le 0.1$ and $10^4 \le Re \le 5\cdot10^6$, the predictions are within +22% and -18% of the [Notter & Sleicher, 1972] correlation.
[Notter and Sleicher, 1972]	$Nu = 6.3 + 0.0167\,Re^{0.85}Pr^{0.93}$	$0.004 \le Pr \le 0.1$ and $10^4 \le Re \le 10^6$, the predictions are based on a numerical analysis and the minimum error of the cloud of experimental data
[Chen and Chiou, 1981]	$Nu = 5.6 + 0.0165\,Re^{0.85}Pr^{0.86}$	$0 \le Pr \le 0.1$ and $10^4 \le Re \le 5\cdot10^6$, the predictions are within a bandwidth of +34% and -7% of [Notter & Sleicher, 1972]
[Lee,1983]	$Nu = 3.01\,Re^{0.0833}$	$0.001 \le Pr \le 0.02$ and $5\cdot10^3 \le Re \le 10^5$, where its predictions are within +25% and -44% of [Notter & Sleicher, 1972].

Table 10.7.6. Calculated circumferential heat flux function *G* for the use in conjunction with Eq. (10.104) for a fully developed turbulent pipe flow with varying thermal boundary conditions as a function of the Reynolds and Prandtl number from [Gartner, *et al*., 1974]

G					
Pr	***Re* = 10^4**	***Re* = $3 \cdot 10^4$**	***Re* = 10^5**	***Re* = $3 \cdot 10^5$**	***Re* = 10^6**
0	1	1	1	1	1
0.001	0.9989	0.9937	0.9561	0.8059	0.4853
0.003	0.9929	0.9613	0.8005	0.5042	0.2300
0.01	0.9499	0.7915	0.4567	0.2185	0.0867
0.03	0.7794	0.4705	0.2055	0.0888	0.0336

b) Hydrodynamically developing turbulent flow

Several attempts have been made to solve the problem of turbulent flow development in a smooth circular duct starting with a uniform velocity profile at the ducts inlet. The closed form analytical solution of [Zhi-quing, 1982] is particularly suitable for engineering applications. According to this analysis the velocity distributions in the hydrodynamic entrance region is given by:

$$\frac{u}{u_{max}} = \begin{cases} (y/\delta)^{1/7} \text{ for } 0 \le y \le \delta \\ 1 \text{ for } \delta \le y \le R \end{cases} \quad ; \quad \frac{u_0}{u_{max}} = 1 - \frac{1}{4}\left(\frac{\delta}{R}\right) + \frac{1}{15}\left(\frac{\delta}{R}\right)^2 \tag{10.105}$$

where the hydrodynamic boundary layer thickness δ, which varies with the axial co-ordinate *x* in accordance with the relation:

$$\frac{x/d_h}{Re^{1/4}} = 1.4039\left(\frac{\delta}{R}\right)^{\frac{5}{4}}\left[1 + 0.1577\left(\frac{\delta}{R}\right) - 0.1793\left(\frac{\delta}{R}\right)^2 - 0.0168\left(\frac{\delta}{R}\right)^3 + 0.0064\left(\frac{\delta}{R}\right)^4\right] \tag{10.106 (a)}$$

Although new DNS studies calculate the entrance length problem nearly exact for engineering purposes the following relation by [Zhi-quing, 1982] matches for a smooth circular duct the hydraulic developing length l_{hy}/d_h quite well. The accuracy is around ±10%. According to their proposal the developing length, defined as the axial distance at which the hydrodynamic boundary layer growing from the duct wall reaches the ducts centreline, reads to:

$$\frac{l_{hy}}{d_h} = 1.3590 \cdot Re^{1/4} \tag{10.106 (b)}$$

c) Thermally developing turbulent flow

The problem of a hydraulically developed and a thermally developing flow has been analytically, numerically and experimentally considered by many authors.

Case: T_w = constant

For the case of a constant wall temperature this problem is often referred to as the turbulent Graetz problem. The first, who treated this problem considering liquid metals analytically where [Sleicher and Tribus, 1956]. [Notter and Sleicher, 1972] provided analytical solutions for numerous

Prandtl numbers in the range from $0 < Pr < 10^4$. All solutions presented are of infinite series type like in the laminar case. But, in contrast to the laminar flow the individual eigenvalues and constants are functions of the Reynolds and the Prandtl number.

Related to the analytical solutions the thermal entrance length l_{th} can be calculated according to the solution of [Notter and Sleicher, 1972]. The deviation to newer numerical calculations performed by [Weigand, 1996] is of marginally nature (<2%) except for Reynolds numbers less than 10^4, where axial conduction becomes important. In this context the thermal entrance length is defined as the axial distance at which the local Nusselt number Nu_x reaches 1.05 times the Nusselt number of the fully developed flow problem, i.e. $Nu_x = 1.05 \cdot Nu$. The calculated thermal entrance length as a function of the Reynolds number is displayed in Figure 10.7.4.a for various Prandtl numbers according to [Notter and Sleicher, 1972].

Certain correlations for the Nusselt numbers in the thermal entrance region of a smooth circular duct were developed by several authors. However, many of them were applicable to only to a limited range of the Reynolds number and the Prandtl number. A comprehensive study relevant for liquid metals was only performed by [Chen and Chiou, 1981]. They propose the following correlations for the local and the mean Nusselt numbers valid for x/d_h and $Pe > 5 \cdot 10^2$:

$$\frac{Nu_x}{Nu_\infty} = 1 + \frac{2.4}{x/d_h} - \frac{1}{(x/d_h)^2} \quad \text{and} \quad \frac{Nu_m}{Nu_\infty} = 1 + \frac{7}{x/d_h} + \frac{2.8}{(x/d_h)} \ln\left[\frac{x/d_h}{10}\right] \tag{10.107}$$

where Nu_∞ is the Nusselt number of the fully developed flow. They recommend in this context the Notter-Sleicher-correlation with:

$$Nu_\infty = 4.5 + 0.0156 Re^{0.85} Pr^{0.86} \tag{10.108}$$

Case: q_w = constant

A similar approach was performed by [Becker, 1956] and was modified by [Genin, *et al*., 1978]. While the latter supported their analytical studies by several experiments they found that the local Nusselt number in the thermally developing flow can be calculated according to:

$$Nu_x = Nu_\infty + 0.006\left(\frac{x/d_h}{Pe}\right)^{-1.2} \quad \text{with} \quad Nu_\infty = 5.6 + 0.0165 Re^{0.85} Pr^{0.86} \tag{10.109 (a)}$$

In a parametric study they show that their correlation is valid for $1.9 \cdot 10^2 < Pe < 1.8 \cdot 10^3$ with an accuracy of ±9%. The thermal entrance length corresponding to $Nu_x = 1.05\, Nu_\infty$ was found to be best represented by their experimental data with the correlation:

$$\frac{l_{th}}{d_h} = \frac{Pe}{1 + 0.002 Pe} \tag{10.109 (b)}$$

[Lee, 1983] confirmed their studies and, moreover, he studied the effect of axial conduction on the solution for constant wall heat flux. Similar to the previous authors he found, that the thermal developing length for a constant wall heat flux are larger than those for a constant wall temperature. The normalised thermal developing length l_{th}/d_h as a function of the Reynolds number for a constant wall heat flux is depicted in Figure 10.7.4(b).

Figure 10.7.4. Normalised thermal developing length l_{th}/d_h as a function of the Reynolds number in a hydraulically fully developed flow of a smooth circular tube for different Prandtl numbers from [Notter and Sleicher, 1972]

a) T_w = constant, b) q_w = constant

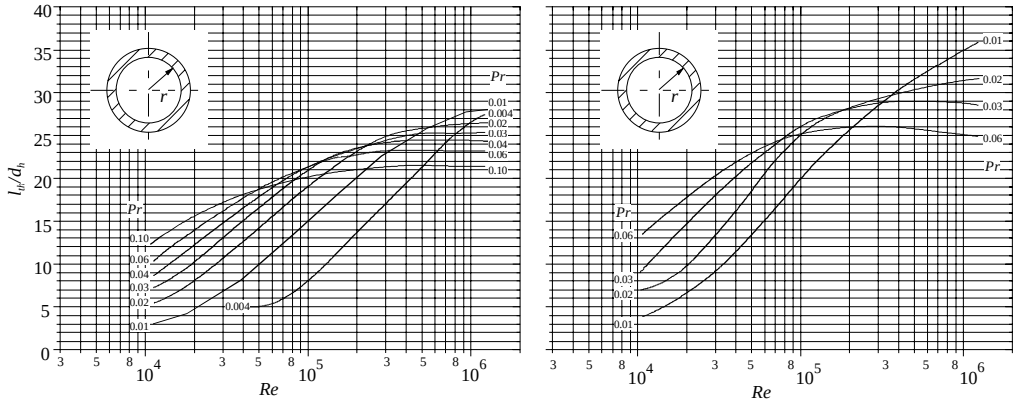

d) Simultaneously developing turbulent flow

The simultaneously turbulent flow in a smooth duct is affected appreciably by the type of duct entrance configuration. [Boelter, *et al*., 1948] and [Mills, 1962] conducted an extensive experimental study for various inlet configurations into a smooth circular duct. While the first employed a constant wall temperature the latter performed a series for a constant wall heat flux. As a result of all these measurements it turned out that the measured local Nusselt numbers are substantially larger than that of thermally developing flow (at hydraulically developed flow), underscoring the decisive role played by the duct entrance configuration. Especially, the square inlet region for $x/d_h < 2$ exhibits a strange Nusselt number distribution with a steep increase and then a rapid drop for $x/d_h > 2$, which is apparently caused by the flow contraction followed by the re-expansion in the vicinity of the duct inlet. While for liquids with $Pr \geq 0.72$ Sparrow and co-workers ([Sparrow, *et al*., 1980], [Sparrow and O'Brien, 1980], [Sparrow and Gurdal, 1981], [Sparrow, *et al*., 1981], [Sparrow and Chaboki, 1984], [Lau, *et al*., 1981], [Sparrow and Bosmans, 1983], [Wesley and Sparrow, 1976] and [Molki and Sparrow, 1983]) performed extensive semi-analytical and experimental studies the data basis and the experimental verification for liquid metals is rather sparse. [Chen and Chiou, 1981] presented correlations for the simultaneously developing flow of liquid metals in a smooth circular duct with uniform velocity profile at the inlet. The correlations for the local Nusselt number Nu_x valid for $2 \leq x/d_h \leq 35$, $Pe > 5 \cdot 10^2$ and $Pr \leq 0.03$ are given by:

$$\frac{Nu_x}{Nu_\infty} = 0.88 + \frac{2.4}{x/d_h} - \frac{1.25}{(x/d_h)^2} - A \quad , \qquad (10.110)$$

$$\frac{Nu_x}{Nu_\infty} = 1 + \frac{5}{x/d_h} + \frac{1.86}{(x/d_h)} ln\left(\frac{x/d_h}{10}\right) - B$$

where for a constant wall temperature (T_w = const.) the constants A and B read to:

$$A = \frac{40 - x/d_h}{190} \quad , \quad B = 0.09 \qquad (10.111)$$

while for constant wall heat flux (q_w = const.) A and B vanish to zero.

10.7.5.3 Turbulent heat transfer in a flat duct

The flat duct heat transfer problem has been studied quite extensively by many authors in the past as this type of duct constitutes the limiting geometry for the family of rectangular and concentric annular ducts. In this context a duct is considered to be flat if its height ($2a$) to width ($2b$) ratio is smaller than 0.1, i.e. $a/b \leq 0.1$.

a) Fully developed flow

[Kays and Leung, 1963] presented comprehensive turbulent heat transfer results for arbitrarily prescribed heat fluxes at the two duct walls. Based on their analysis, the fully developed Nusselt number for the constant wall heat flux case can be represented from:

$$Nu_{(q_w=const)} = \frac{Nu}{1-\gamma\varphi} \tag{10.112}$$

where γ is the ratio of the prescribed heat fluxes at the two duct walls, i.e. for $\gamma = 0$ one wall is heated and the other adiabatic, for $\gamma = 1$ both are heated with the same heat flux and $\gamma = -1$ one is heated and the other cooled with the same rate. The Nusselt number Nu and the influence coefficient φ entering Eq. (10.112) can be taken from Table 10.7.7 for the case of $\gamma = 0$.

Table 10.7.7. Nusselt numbers and influence coefficients for fully developed turbulent flow in a smooth flat duct with uniform heat flux at one wall and the other adiabatic ($\gamma = 0$) from [Kays and Leung, 1963]

Pr	$Re = 10^4$		$Re = 3\cdot10^4$		$Re = 10^5$		$Re = 3\cdot10^5$		$Re = 10^6$	
	Nu	φ	*Nu*	φ	*Nu*	φ	*Nu*	φ	*Nu*	φ
0	5.7	0.428	5.78	0.445	5.80	0.456	5.80	0.460	5.80	0.468
0.001	5.7	0.428	5.78	0.445	5.80	0.456	5.88	0.460	6.23	0.460
0.003	5.7	0.428	5.80	0.445	5.90	0.450	6.32	0.450	8.62	0.422
0.01	5.8	0.428	5.92	0.445	6.70	0.440	9.80	0.407	21.5	0.333
0.03	6.1	0.428	6.90	0.428	11.00	0.390	23.00	0.330	61.2	0.255

In order to verify whether the Nu predictions can be derived from the circular duct correlations, the predictions of the Eq. (10.112) are compared to the Notter-Sleicher-correlation in Table 10.7.5. Comparing the calculated data and building the ratio $Nu_{flat\ duct}/Nu_{pipe}$ this ratio varies from +1.57 to -1.055 in the Reynolds number range $10^4 < Re < 10^6$. Similar to the results for the circular duct, it is found that the Nusselt numbers in a flat duct for a constant wall temperature are lower than for a constant wall heat flux. Certain empirical correlations are developed to calculate the fully developed heat transfer in a smooth flat duct for different boundary conditions. For $\gamma = 0$ (one wall is heated and the other adiabatic) three correlations are available, one presented by [Buleev, 1959], [Dwyer, 1965] and [Duchatelle and Vautrey, 1964]. They read to:

$$Nu_{(q_w=const)} = 5.1 + 0.02Pe^{0.8} \quad , \tag{10.113}$$

$$Nu_{(q_w=const)} = 5.6 + 0.01905Pe^{0.775} \quad ,$$

$$Nu_{(q_w=const)} = 5.85 + 0.000341Pe^{1.29}$$

All these correlations are claimed to be valid for $0 \le Pr \le 0.004$ and $10^4 \le Re \le 10^5$. The latter expression derived by [Duchatelle and Vautrey, 1965] matches the analytic result obtained by [Kays and Leung, 1963] with an accuracy of +24% to -11% best for $\gamma = 0$ and is thus recommend for use. Many newer DNS calculations (see [Kasagi and Otsubo, 1993] or [Kawamura, 1995]) show that the Nusselt number varies only marginally with increasing Peclet number up to $Pe \sim 3 \cdot 10^2$. The only experiment matching this finding within an accuracy of ±6% is the Duchatelle and Vautrey experiment.

[Dwyer, 1965] presented the following empirical correlation for both walls heated ($\gamma = 1$):

$$Nu_{(q_w=const)} = 9.49 + 0.0596 Pe^{0.688} \qquad (10.114\text{ a})$$

DNS results from [Lyons, *et al*., 1993] and [Kim and Moin, 1989] considering a similar problem, however, show that the Dwyer correlation yields to too optimistic Nusselt numbers (about 20% larger than the DNS values). A detailed analysis performed by [Kawamura, *et al*., 1998] shows that the correlation derived by [Sleicher and Rouse, 1975] matches the experimental results for $\gamma = 1$ best.

For the case of a constant wall temperature with $\gamma = 0$ (one wall is heated and the other adiabatic) only one relevant experiment is available, which was performed by [Seban, 1950]. It yields to the following correlation:

$$Nu_{(T_w=const)} = 5.8 + 0.02 Pe^{0.8} \qquad (10.114\text{ b})$$

A critical review on the quality of this relation can not be given since DNS data for this specific case could not be found in literature. But the lower Nusselt number for the case of constant wall temperatures compared to constant wall heat flux looks quite sensible.

b) Thermally developing flow

The thermally developing turbulent flow in a flat duct with uniform and equal wall temperatures has been solved analytically by [Sakakibara and Endo, 1976] and by [Shibani and Özisik, 1977]. The solution can be expressed by a series expansion similar like for the laminar flow.

[Hatton and Quarmby, 1963] studied the problem with one part of the plates being at a constant temperature and the opposite being insulated. The type of solution corresponds to the ones mentioned above and is of series expansion type. [Hatton, *et al*., 1964] and [Sakakibara, 1982] presented semi-analytical solutions for the case with constant wall heat flux. [Faggiani and Gori, 1980] studied analytically the effect of axial fluid conduction on thermally developing flows in a Reynolds number range of $7.06 \cdot 10^3 \le Re \le 7.4 \cdot 10^4$ for Prandtl numbers $0.001 \le Pr \le 0.1$. They concluded that the influence of axial fluid conduction is to significantly reduce the Nusselt numbers in the thermal entrance region. This effect however occurs mainly at weakly turbulent flow ($Re \le 10^4$) and for small $x/d_h < 5$. Unfortunately, in none of the analytical and semi-analytical solutions the order of magnitude for the thermal developing length l_{th} is mentioned or a Nusselt number correlation for the thermal entrance region is developed in dependence on the Reynolds number and the Prandtl number. Moreover, to the knowledge of the authors no experimental verification or a direct numerical simulation calculation exists, which could give an estimate on the quality of the derived solutions.

c) Simultaneously developing flow

Also the information on the simultaneously developing turbulent flow between parallel plates is relatively sparse. Here, however, an experiment conducted by [Duchatelle and Vautrey, 1964], in which

the local Nusselt numbers have been measured exists. In their set-up one wall was insulated and to the opposite one a constant wall heat flux was supplied. Figure 10.7.5 shows that the ratio of the local Nussel number Nu_x to the fully developed flow Nusselt number Nu attains unity at $Pe/(x/d_h) = 25$.

Figure 10.7.5. Normalised local Nusselt number for simultaneously developing turbulent flow in a smooth flat duct for *Pr* = 0.02 with one wall heated and the other insulated from [Duchatelle and Vautrey,1964]

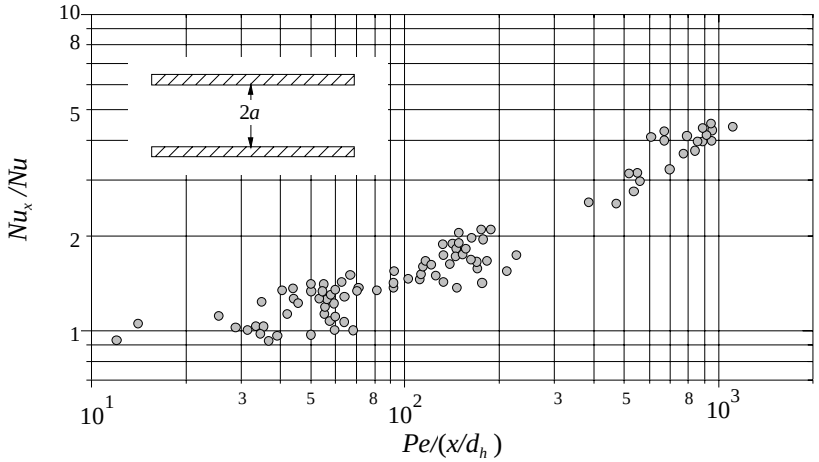

Thus the thermal entrance length l_{th} for the simultaneously developing flow can be estimated to $l_{th}/d_h = Pe/25$. For the thermally developing but hydrodynamically developed flow these authors estimate a significantly smaller thermal entrance length, i.e. $l_{th}/d_h = Pe/80$.

10.7.5.4 Turbulent heat transfer in a rectangular duct

It is generally difficult to give engineering correlations for the heat transfer in rectangular ducts, since the attainable Nusselt numbers depend not only on the heat flux transferred to the fluid but also to the thermal boundary conditions for the wall, the symmetry, the shape of the corners with the associated secondary flow, the pre-conditioning of the flow and many other aspects. Thus, the correlations presented in this context can only be used as an assessment of the potential heat transfer capability in a rectangular duct. The correlations shown are far away to perform a detailed design of a heat transfer unit because of a lack of detailed experimental data or verification by a direct numerical simulation. The database for both of the latter named classes is rather sparse for liquid metals. For an estimate on the heat transfer capability of a specific geometrical set-up a CFD simulation is recommended. It can give a more detailed insight in the heat transfer mechanisms than the use of the subsequent correlations, even if rather rough models like the simple k-ε model (with all the deficits mentioned in Subsection 10.7.4) are used in the simulation.

A simple correlation is available for estimating fully developed Nusselt numbers in turbulent flow of liquid metals in rectangular ducts either for a constant wall heat flux and a constant wall temperature. The correlation was derived by [Hartnett and Irvine, 1957] for a uniform velocity distribution (slug flow) and a pure molecular conduction heat transfer mechanism. This correlation is given by:

$$Nu = \frac{2}{3} Nu_{slug} + 0.015 Pe^{0.8} \quad \text{with} \begin{cases} Nu_{slug} = 5.78 & \text{for } T_w = \text{const.} \\ Nu_{slug} = 8.00 & \text{for } q_w = \text{const.} \end{cases} \tag{10.115}$$

In case of thermally developing or simultaneously developing flows no analytical and hardly experimental data are available. There are some correlations on the "market", which look quite inconsistent to the results obtained for the circular tube and the subsequently described concentric annulus problem.

10.7.5.5 Turbulent heat transfer in a concentric annulus

The flow in a concentric annulus like a rod in a circular tube is one of the most studied turbulent thermal heat transfer problems. Especially in context with nuclear systems, where typically circular fuel rods are placed with a specific arrangement, the concentric annulus is often considered as a solution of the single problem. There exist numerous possibilities of thermal boundary conditions for this problem and not all of them are covered by a correlation. Below a consistent representation to the circular duct flow is tried and we concentrate our focus only to concentric annuli.

a) Fully developed flow

[Rensen, 1981] measured the fully developed Nusselt numbers in a concentric annulus, with the inner wall subjected to a uniform heat flux and the outer to be thermally insulated. The radius ratio r^*, which is defined as $r^* = r_i/r_o$, where r_i is the radius of the inner annulus and r_o that of the outer one was in his experiment $r^* = 0.5409$. From the experiment conducted for sodium ($Pr \approx 0.005$) in a Reynolds number regime from $6 \cdot 10^3 < Re < 6 \cdot 10^4$ he obtained a Nusselt number correlation in the form:

$$Nu = 5.75 + 0.022\,Pe^{0.8} \tag{10.116}$$

[Hartnett and Irvine, 1957] presented an analytic solution for liquid metals with small Prandtl numbers [see Eq. (10.115)], which requires the knowledge of the slug Nusselt numbers for the conditions of constant wall heat flux and constant wall temperature. The slug Nusselt numbers Nu_{slug} for these two cases are depicted in Figure 10.7.6(a). For the case where one wall is subjected to a uniform heat flux and the other is insulated, which is in literature often referred to as the fundamental solution of the second kind, the slug Nusselt numbers are shown in Figure 10.7.6(b).

Figure 10.7.6. Slug flow Nusselt numbers for smooth concentric annular ducts with (a) constant wall temperature and constant wall heat flux and (b) inner or outer wall heated and the other wall being adiabatic from [Hartnett and Irvine, 1957]

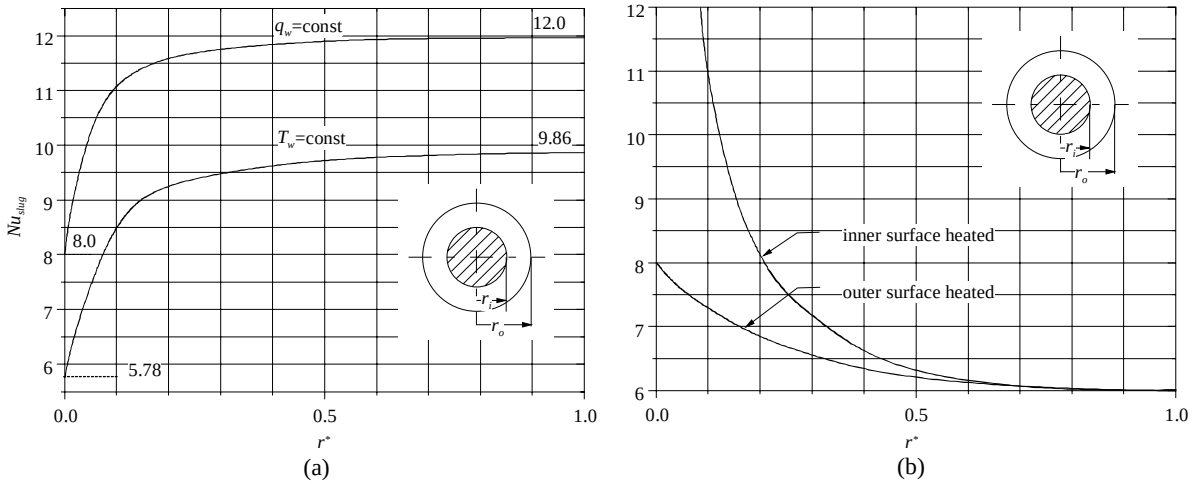

The prediction of Eq. (10.115) for $r^* = 0.5409$ in conjunction with Figure 10.7.6(b) for the case of the inner wall heated and the outer wall insulated are 32% lower than those of Eq. (10.116). Related to this specific experiment Eq. (10.116) is limited to be valid for $28 \le Pe \le 354$.

[Dwyer, 1966] developed semi-empirical correlations for liquid metal flows with $Pr < 0.03$ in concentric annuli with one wall subjected to a uniform heat flux and the other wall insulated. For the case of the outer wall heated the equations read to:

$$Nu = A_0 + B_0 \cdot (\beta Pe)^n \quad \text{with} \tag{10.117}$$

$$A_0 = 5.26 + \frac{0.05}{r^*} \quad , B_0 = 0.01848 + \frac{0.003154}{r^*} - \frac{0.0001333}{r^{*2}} \quad ,$$

$$n = 0.78 - \frac{0.01333}{r^*} + \frac{0.000833}{r^{*2}} ,$$

$$\beta = 1 - \frac{1.82}{Pr(\varepsilon_M / \nu)_{max}^{1.4}} \quad \text{with}$$

$$\left(\frac{\varepsilon_M}{\nu} \right)_{max} = \frac{1}{2} \left(\frac{\varepsilon_M}{\nu} \right)_{max,core}$$

An expression for $(\varepsilon_M/\nu)_{max,core}$ applicable to a circular duct ($r^* = 0$) was developed by [Bhatti and Shah, 1987] which is $(\varepsilon_M/\nu)_{max,core} = 0.037\ Re\ f^{0.5}$, with f the Fanning friction factor. The agreement with the experimental data from [Petrovichev, 1959] is excellent. The data of [Baker and Sesonske, 1962] exhibit about 15% higher Nusselt numbers, however, an analysis of the data immediately exhibits that their flow was not fully developed. In the experiment by [Nimmo and Dwyer, 1966] the validity of the equations was extended to $Pe \sim 3 \cdot 10^3$.

For the case of the inner wall heated the [Dwyer, 1966] correlation read to:

$$Nu = A_0 + B_0 \cdot (\beta Pe)^n \quad \text{with} \tag{10.118}$$

$$A_0 = 4.63 + \frac{0.686}{r^*} \quad , B_0 = 0.02154 - \frac{0.000043}{r^*} \quad , n = 0.752 + \frac{0.01657}{r^*} - \frac{0.000883}{r^{*2}}$$

The equations in Eq. (10.118) demonstrated their validity in the Prandtl number range $0.005 \le Pr \le 0.03$ for Peclet numbers $3 \cdot 10^2 \le Pe \le 10^5$. The accuracy in this range is about 10-15%.

The predictions of Eq. (10.117) for $r^* = 1$ are within +20% and -13% of the prediction of Eq. (10.113c) derived by [Duchatelle and Vautrey, 1965]. For Peclet numbers below $Pe = 1.2 \cdot 10^3$ the uncertainty level falls below 6%.

b) Thermally developing flow

[Quarmby and Anand, 1970] provided an eigenvalue solution for the concentric annuli problem for different r^* and Prandtl numbers covering the Reynolds number range $2 \cdot 10^4 \le Re \le 2.4 \cdot 10^5$. This solution looks quite well for large Prandtl numbers but underestimated the data of [Rensen, 1981]

A detailed measurement of the thermal entrance length l_{th}/d_h was only performed in the experimental studies by [Rensen, 1981]. In his set-up with the inner wall heated (q_w = const.) and the outer adiabatic he found for sodium ($Pr = 0.0054$) a strong dependence of the thermal entrance length on the Reynolds number, which is tabulated in Table 10.7.8. Here, a fully developed flow is established if the criterion $Nu_x < 1.05 Nu$ is matched.

Table 10.7.8. Thermal entrance length l_{th}/d_h for thermally developing flow in a smooth concentric annulus with $r^* = 0.5409$ for sodium ($Pr = 0.0054$) with the inner wall heated and the outer adiabatic after [Rensen, 1981]

Re	l_{th}/d_h
$2 \cdot 10^3$ (laminar)	80.0
$6 \cdot 10^3$ (laminar-turb. transition)	2.1
$8 \cdot 10^3$	2.7
$1 \cdot 10^4$	3.2
$2 \cdot 10^4$	6.0
$5 \cdot 10^4$	13
$6 \cdot 10^4$	13.5

c) Simultaneously developing flow

There appears to be little information available on simultaneously developing flow in concentric annuli. An integral analysis presented by [Roberts and Barrow, 1967] who also conducted an extensive experimental series found that the results are not very much different to those obtained for thermally developing flows with a hydrodynamically developed velocity profile.

10.7.5.6 Turbulent heat transfer over rod bundles

Since the sixties the adequate cooling performance of the fuel elements using liquid metals was a major issue for the feasibility of fast breeder reactors. Many experimental investigations were performed to study the heat transfer in turbulent flow through rod bundles. They can be classified locally into three regions, the United States, the European Union and the former USSR. Without complaining completeness, numerous experimental heat transfer correlations have been developed, which are valid in a wide range of geometrical, thermal and flow boundary conditions in the following papers: [Subbotin, *et al*., 1961,1964,1967,1970], [Friedland, *et al*., 1961a, b], [Borishanskii and Firsova, 1963 and 1964], [Maresca and Dwyer, 1964], [Nimmo and Dwyer, 1965], [Kalish and Dwyer, 1967], [Borishanskii, *et al*., 1967, 1969], [Pashek, 1967], [Hlavac, *et al*., 1969], [Zhukov, *et al*. 1969a, b, 1978, 1982], [Marchese, 1972], [Gräber and Rieger, 1973], [Weinberg, 1975], [Möller and Tschöke, 1978]. The comprehensive overview by [Weinberg, 1975] on the experimental studies exhibits that the correlations obtained are extremely sensitive to depositions of impurities on the surface, the question of the wetting especially to heavy liquid metals and the surface roughness. As one of his conclusions he mentioned that reliable correlations are only available for very few cases. One of the problems associated with the heat transfer over rod bundles is according to [Rehme, 1987] that only in a few experiments the temperatures are measured locally at different rods and that the temperature differences are often due to the high thermal conductivities of the liquid metals so small that reliable Nusselt number correlations are difficult to derive from these data.

Most of the experiments were performed in triangular or hexagonal arrays or bundles, which arise from the design intended to use or used in fast breeder reactors. The pitch (P) to pin (D) ratio, where P is the distance between the center of two neighbouring fuel rods and D is its diameter, ranges from $1.0 \le P/D \le 1.95$ and the Peclet number from $2 \le Pe \le 4.5 \cdot 10^3$. In this context rod bundles from 7 to 37 pins were investigated. Only one experiment is available in square arrays with 9 heated rods in a cluster of 25 by [Ushakov, *et al*., 1963]. The problem of the turbulent Prandtl number for the calculation of the Nusselt number has been already discussed in Subsection 10.7.4 in the context of the closure methods for the turbulent heat flux.

For the liquid metal heat transfer in rod bundles and the case of vanishing Prandtl number [Zhukov, *et al*., 1973] and [Ushakov, *et al*., 1974] derived a general correlation. This correlation was first published by [Subbotin, *et al*., 1975] and extensions were reported by [Ushakov, *et al*., 1976, 1977 and 1979]. This general correlation was checked against numerous results, both experimental data and theoretical predictions and can be recommended for rod bundles arranged in a triangular or hexagonal arrangement and reads to:

$$Nu = Nu_{lam} + \frac{3.67}{90(P/D)^2}\left[1 - \frac{1}{\frac{1}{6}\left[(P/D)^{30} - 1\right] - \sqrt{1.24\varepsilon_K + 1.15}}\right] \cdot Pe^{m_1} \tag{10.119}$$

$$\text{with } m_1 = 0.56 + 0.19\frac{P}{D} - 0.1\left(\frac{P}{D}\right)^{-80} \text{ and}$$

$$Nu_{lam} = \left(7.55\frac{P}{D} - \frac{6.3}{(P/D)^{17(P/D)(P/D-0.81)}}\right)\left(1 - \frac{3.6P/D}{(P/D)^{20}\left(1 + 2.5\varepsilon_K^{0.86}\right) + 3.2}\right)$$

The laminar Nusselt number Nu_{lam} was originally proposed by [Subbotin, 1974]. The thermal modelling parameter ε_K takes into account the effects of heat conduction in the fuel (λ_1), the cladding (λ_2) and the fluid (λ_3) and can be estimated by:

$$\varepsilon_K = \frac{\lambda_2}{\lambda_3}\frac{1 - \Lambda_0(r_1/r_2)}{1 + \Lambda_0(r_1/r_2)} \quad \text{with } \Lambda_0 = \frac{\lambda_2 - \lambda_1}{\lambda_2 + \lambda_1} \tag{10.120}$$

where r_1 and r_2 denotes the distances of the fuel rod rows from the centre of the bundle. The limiting case of ε_K are 0.01 for peripherally constant heat flux and infinity for peripherally constant temperature. Eq. (10.119) is valid in the ranges from $1.0 \le P/D \le 2.0$ and the Peclet number from $1 \le Pe \le 4{\cdot}10^3$ and $0.01 \le \varepsilon_K < \infty$. In Figure 10.7.7 the Nusselt number calculated after Eq. (10.119) is shown as a function of the Peclet number for different *P/D*.

Figure 10.7.7. Nusselt numbers in fully developed flow in rod bundles arranged in a triangular array as a function of the Peclet number *Pe* and *P*/*D* for constant wall heat flux

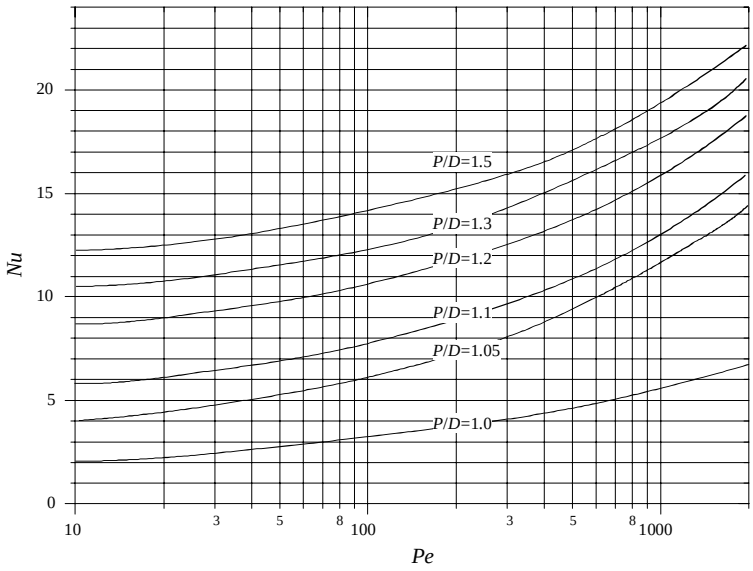

In case P/D grows beyond 1.3 the effect of ε_K diminishes and Eq. (10.119) reduces to:

$$Nu = 7.55\frac{P}{D} - 20\left(\frac{P}{D}\right)^{-13} + \frac{3.67}{90(P/D)^2}Pe^{0.19(P/D)+0.56} \tag{10.121}$$

It is valid for $1.0 \le P/D \le 2.0$ and from $1 \le Pe \le 4{\cdot}10^3$. The thermal hydraulic design is usually performed by subchannel codes, which compute fluid and surface temperatures averaged over each subchannel. Therefore, it is important to know the peripheral variations of the rod surface temperatures superimposed on the average temperature. The dimensionless peripheral variation of the surface temperature is correlated by [Subbotin, 1974 and 1975] and [Ushakov, 1979] and reads to Eq. (10.122). Eq. (10.122) is valid in the ranges from $1.0 \le P/D \le 1.15$, $1 \le Pe \le 2{\cdot}10^3$and $\varepsilon_K > 0.2$. $\Delta T_{max,lam}$ is the maximum temperature variation of the fully developed laminar flow in a bundle. [Rehme, 1987] found that the agreement between Eq. (10.122) and most of the experimental data is better than 10%. Correlations of the Nusselt numbers for heat transfer to liquid metals for design purposes which are only of approximate nature can be taken from [Todreas and Kazimi, 1993], [Kazimi and Carelli, 1976] or [Tang, *et al*., 1978]. In some ranges they are very pessimistic and according to [Rehme, 1987] they should not be used for the design.

$$\Delta T_{max} = \frac{\Delta T_{max,lam}}{1+\gamma Pe^{\beta}} \quad \text{with} \tag{10.122}$$

$$\gamma = 0.008\left(1+0.03\varepsilon_K\right) \quad \text{and} \quad \beta = 0.65 + \frac{51\cdot\log_{10}(P/D)}{(P/D)^{20}} \quad ,$$

$$\Delta T_{max} = 2\lambda_3\frac{T_w^{max} - T_w^{min}}{q_w D} \quad \text{and}$$

$$\Delta T_{max,lam} = \frac{0.022}{(P/D)^{3(P/D-1)^{0.4}}} - 0.99\left[1 - \tanh\left(\frac{1.2\exp\left(-26.4(P/D-1)\right) + \ln\varepsilon_K}{0.84 + 0.2\left(\frac{P/D-1.06}{0.06}\right)^2}\right)\right]$$

In case of thermally developing flows along rod bundles the Nusselt number values may significantly deviate from the circular duct because of the strong geometric non-uniformity of the subchannels. If the coolant area per rod is taken to define an equivalent annulus with zero shear at its outer boundary, it is found that the Nusselt number predictions are accurate within ±10% for $P/D \ge 1.12$, see e.g. [Nijsing, 1972]. Especially, the entrance region is problematic since the entrance length is sensitive to Re, Pr and the geometry. For a hydraulically fully developed flow only one experiment is available by [Subbotin, 1975], where he detected that fully developed thermal conditions in sodium could not be reached for l_{th}/d_h below 200 (!) for $Pe > 10^2$. Their experimental data were obtained for a $P/D = 1.15$. For lower P/D ratios the thermal developing length is even larger, because the heat transfer between the subchannels is reduced. This has been confirmed by the measurement of [Möller and Tschöke, 1980] obtained in a 19-rod bundle with $P/D = 1.31$. For a corner subchannel and $Pe = 150$ a thermal entrance length of $l_{th}/d_h = 70$ was measured. The use of fins reduces the thermal entrance length considerably, since it leads to a better lateral mixing. In the textbook by [Stasiulevivius and Skrinska, 1988] different options for fins on the rods are discussed and optimisation guidelines are given.

10.8 Some final remarks

This report mainly focuses on the forced convective single phase heat transfer of liquid metals in smooth ducts. Although the author is aware that in many technical applications this rather idealised case will hardly appear. Thus, this chapter requires in the future an extension to the heat transfer appearing in mixed and purely buoyancy governed flows.

A few aspects also need a closer view in context with all kinds of heat transfer in liquid metals. In recent years, many papers addressed the question of wetting and the influence of surface roughness, which is sometimes taken as an explanation for a mismatch of data. Although many experimenters spend a lot of effort to avoid this issue, it obviously leads to severe effects in thermal-hydraulic components and as a consequence to lower Nusselt numbers. But, the data basis for a closed discussion on these two topics seemed to me too sparse either theoretically and experimentally to dedicate an individual chapter to it. The nature of this chapter based only on the experimental results would be rather of speculative nature.

A topic also not considered up to now is the flow and the heat transfer around obstacles, which occurs in many reactor and metal refinement processes. Although here a much broader data basis is available it is difficult to structure this rather complex context in a short paragraph. But since it is important for the experimental investigation of heat transport phenomena it should be integrated in a next step of the liquid metal handbook.

Many advanced reactor concepts make use of the gas lift principle by means of a convection enhancement injecting gas into the heavy liquid metal. The resulting two-phase flow is theoretically difficult to describe due to the large density differences and currently only limited accessible to the modelling. Nevertheless, also here a large variety of experiments exist, which were performed in the context of the specific technical configuration used for the individual technical application. Associated with the two-phase flow problem is the treatment of free liquid metal surfaces, as they may appear in free surface targets of accelerator driven systems or other metallurgical processes. Here, mainly turbulent flows appear and currently a lot of effort is spent on the modelling of these free surfaces. The next issue of the liquid metal should contain a chapter dedicated only to this problem.

REFERENCES

Abe, K., T. Kondoh, Y. Nagano (1995), "A New Turbulence Model for Predicting Fluid Flow and Heat Transfer in Separating and Reattaching Flows. II. Thermal Field Calculations", *Int. J. Heat Mass Transfer*, Vol. 38, pP. 1467-1481.

Addison, C.C. (1984), "The Chemistry of the Liquid Alkali Metals", J. Whiley & Sons, Ltd., ISBN 0471905089.

Anderson, D.A., J.C. Tannehill, R.H. Pletcher (1984), "Computational Fluid Mechanics and Heat Transfer", Hemisphere, New York.

Aoki, S. (1963), "A Consideration on the Heat Transfer in Liquid Metals", *Bull. Tokyo Inst. Tech*., Vol. 54, pP. 63-73.

Arien, B. (2004), *Assessment of Computational Fluid Dynamic Codes for Heavy Liquid Metals – ASCHLIM*, EC-Contract FIKW-CT-2001-80121-Final Report.

Arpaci, V.S., P.S. Larsen, "Convective Heat Transfer", Prentice-Hall, Englewood-Cliffs, N.J.

Azer, N.Z., B.T. Chao (1960), "A Mechanism of Turbulent Heat Transfer in Liquid Metals", *Int. J. Heat and Mass Transfer*, Vol. 1, p. 121 ff.

Azer, N.T., B.T. Chao (1961), "Turbulent Heat Transfer in Liquid Metals – Fully Developed Pipe Flow with Constant Wall Temperature", *Int. J. Heat and Mass Transfer*, Vol. 3, pp.77-83.

Baker, R.A., A. Sesonske (1962), "Turbulent Heat Transfer in Concentric Annuli of a NaK Heat Exchanger", *Nucl. Science Eng*., Vol. 13, p. 283ff.

Barenblatt, G.I., A.J. Chorin (1998), "Turbulence: An Old Challenge and New Perspectives", *Meccanica*, Vol. 33, pp. 445-468.

Barleon, L., K-J. Mack, R. Stieglitz (1996), *The MEKKA Facility – A Flexible Tool to Investigate MHD-flow Phenomena*, FZKA-Report FZKA-5821.

Batchelor, G.K. (1959a), "Small-scale Variation of Convected Quantities like Temperature in Turbulent Fluid Flows. Part 1. General Discussion and the Case of Small Conductivity", *J. Fluid Mech.*, Vol. 5, pp. 113-133.

Batchelor, G.K., I.D. Howells, A.A. Townsend (1959b), "Small-scale Variation of Convected Quantities like Temperature in Turbulent Fluid. Part 2. The Case of Large Conductivity", *Journal Fluid Mech*., Vol. 5, pp. 134-139.

Becker, H.L. (1956), "Heat Transfer in Turbulent Tube Flow", *Appl. Sci. Res.*, Ser. A, Vol. 6, pp. 147-191.

Beitz, W., K-H. Küttner (1986), "Dubbel-Taschenbuch des Maschinenbaus", Springer-Verlag, 15th Edition, ISBN 3-540-12418-7, p. 1358 ff (in German).

Benemann, J. (1996), "Status Report on Solar Through Power Plants", Pilkington Press.

Betchov, R., O.W. Criminale (1967), "Stability of Parallel Flows", Academic Press, New York.

Bird, R.B., W.E. Stewart, E.N. Lightfoot (1960), "Transport Phenomena", Wiley, New York.

Bhatti, M.S. (1985), *Fully Developed Temperature Distribution in a Circular Duct Tube with Uniform Wall Temperature*, Owens-Corning Fiberglas Corporation, Granville, Ohio.

Bhatti, M.S. (1985b) *Limiting Laminar Heat Transfer in Circular and Flat Ducts by Analogy with Transient Heat Transfer Problems*, Owens Corning Fiberglas Corporation, Granville, Ohio.

Bhatti, M.S., R.K. Shah (1987), "Turbulent and Transition Flow, Convective Heat Transfer in Ducts", Chapter 4, in Handbook of Single-phase Convective Heat Transfer, (Kakac, Shah and Aung eds.), John Wiley and Sons, New York, ISBN 0-471-81702-3.

Black, A.W., Sparrow, E.M. (1967) "Experiments on Turbulent Heat Transfer in a Tube with Circumferentially Varying Boundary Conditions", *J. Heat Transfer*, Vol. 89, pp. 258-268.

Boelter, L.M.K., G. Young, H.W. Iverson (1948), *An Investigation of Heaters XXVII – Distribution of Heat Transfer Rate in the Entrance Section of a Circular Tube*, NACA TN1451.

Borishanskii, M.V., E.V. Firsova (1963), "Heat Exchange in the Longitudinal Flow of Metallic Sodium Past a Tube Bank", *At. Energiya*, Vol. 14, pp. 584-585.

Borishanskii, M.V., E.V. Firsova (1964), "Heat Exchange in Separated Bundles of Rods with Metallic Sodium Flowing Longitudinally", *At. Energiya*, Vol. 16, pp. 457-458.

Borishanskii, M.V., M.A. Gotovskiy, E.V. Firsova (1967), "Heat Exchange when a Liquid Metal Flows Longitudinally Through a Bundle of Rods Arranged in a Triangular Lattice", *At. Energiya*, Vol. 22, pp. 318-320.

Borishanskii, M.V., M.A. Gotovskiy, E.V. Firsova (1969), "Heat Transfer in Liquid Metals Flowing Longitudinally in Wetted Rod Bundles", *At. Energiya*, Vol. 27, pp. 549-552.

Boston, N.E.J., R.W. Burling (1972), "An Investigation of High-wave Number Temperature and Velocity Spectra in Air", *J. Fluid Mech*., Vol. 55, pp. 473-492.

Boussinesq, J. (1877), "Theorie d'écoulement tourbillant", Mem. Pres. Acad. Sci, Paris, Vol. 23, p. 46ff.

Bremhost, K., L. Krebs (1992), "Experimentally Determined Turbulent Prandtl Numbers in Liquid Sodium at Low Reynolds Numbers", *Int. J. Heat Mass Transf.*, Vol. 35, pp. 351-359.

Brown, H.E., B.H. Amstead, B.E. Short (1957), "Temperature and Velocity Distribution and Transfer of Heat in a Liquid Metal", *Trans. Am. Soc. Mech. Engrs.*, Vol. 79, pp. 279-285.

Buhr, H.O. (1967), “Heat Transfer to Liquid Metals, with Observations of the Effect of Superimposed Free Convection in Turbulent Flow”, PhD Thesis, Univ. Cape Town, Cape Town, South Africa.

Buhr, H.O., A.D. Carr, R.E. Balzhiser (1968) “Temperature Profiles in Liquid Metals and the Effect of Superimposed Free Convection in Turbulent Flows”, *Int. J. Heat and Mass Transfer*, Vol. 11, pp. 641-654.

Buleev, N.I. (1959), “Problems of Heat Transfer”, Publishing house of the USSR Acad. Sci., Moscow.

Buleev, N.I. (1962), “Theoretical Model of the Mechanism of Turbulent Exchange in Fluid Flow”, Coll. Heat Trans. USSR Acad. Sci., pp. 64-98.

Burmeister, L.C. (1983), “Convective Heat Transfer”, Wiley-Interscience, New York.

Carteciano, L.N., D. Weinberg, U. Müller (1997), “Development and Analysis of a Turbulence Model for Buoyant Flows”, *4th World Conf. on Experimental Heat Transfer, Fluid Mechanics and Thermodynamics*, 2-6 , Brussels, Vol. 3, pp. 1339-1347.

Carteciano, L.N., G. Grötzbach (2003), *Validation of Turbulence Models in the Computer Code FLUTAN for a Free Hot Sodium Jet in Different Buoyancy Flow Regimes*, FZKA-Report, FZKA-6600.

Carteciano, L.N., G. Grötzbach (2003), *Validation of Turbulence Models for a Free Hot Sodium Jet with Different Buoyancy Regimes Using the Computer Code FLUTAN*, Forschungszentrum Karlsruhe FZKA-6600.

Cebeci. T. (1973), “A Model for Eddv Conductivitv and Turbulent Prandtl Number”, *ASME Journal of Heat Transfer*, Vol. 95, pp. 227-234.

Cebeci, T., P. Bradshaw (1977), “Momentum Transfer in Boundary Layers”, Hemisphere Publishers, Washington.

Chen, R.Y. (1973), “Flow in the Entrance Region at Low Reynolds Number”, *J. Fluids Engn*., Vol. 95, pp. 153-158.

Chen, C.J., J.S. Chiou (1981), “Laminar and Turbulent Heat Transfer in the Pipe Entrance Region for Liquid Metals”, *International Journal of Heat and Mass Transfer*, Vol. 24, pp. 1179-1189.

Chien, K.Y. (1982), “Prediction of Channel of Boundary Layer Flows with a Low Reynolds Number Turbulence Model”, *AIAA J*., Vol. 20(1), pp. 33-38.

Chou, P.Y., J. Chin (1940), “Wave Number Analysis in Turbulent Flow”, *J. Phys*., Vol. 4, p. 1ff.

Churchill, S.W. (1997a), “New Simplified Models and Formulations for Turbulent Flow and Convection”, *AIChE Journal*, Vol. 43, pp. 1125-1140.

Churchill, S.W. (1997b), “The Prediction of Turbulent Convection with Minimal Explicit Empiricism”, *Thermal Science and Engineering*, Vol. 5, pp. 13-30.

Churchill, S.W. (2000), “The Prediction of Turbulent Flow and Convection in a Round Tube”, *Advances in Heat Transfer*, Vol. 34, pp. 255-361.

Churchill, S.W., M. Shinoda, N. Arai (2000), "A New Concept of Correlation for Turbulent Convection", *Thermal Science and Engineering*, Vol. 3, pp. 49-65.

Cole, J.D. (1968), "Perturbation Methods in Applied Mathematics", Blaisdell Publishers, Waltham.

Danckwerts, P.V. (1951), "Significance of Liquid-film Coeffcients in Gas Absorption", *Ind. Engng. Chem.*, Vol. 43(6), pp. 1460-1467.

David, S. (2005), "Future Scenarios for Fission Based Reactors", *Nuclear Physics A*, Vol. 751, pp. 419-441.

Davies, F. (1969), "Eddy Viscosity and Eddy Conductivity: A Statistical Approach and Experimental Verification", PhD Thesis ETH-Zürich, No. 4107 (1969).

Deissler, R.G. (1952), "Analysis of Fully Developed Turbulent Heat Transfer in at Low Peclet Numbers in Smooth Tubes with Application to Liquid Metals", Res. Memo E52F05 US Nat. Adv. Comm. Aero.

Deng, B., W. Wu, S. Xi (2001), "A Near-wall Two-equation Heat Transfer Model for Wall Turbulent Flows", *Int. J. Heat Mass Transfer*, Vol. 44, pp. 691-698.

Durbin, P.A. (1993a), "A Reynolds Stress Model for Near-wall Turbulence", *J. Fluid Mech.*, Vol. 249, pp. 465-498.

Donaldson, C. (1972), "Calculation of Turbulent Shear Flows for Atmospheric and Vortex Motions", *AIAA J.*, Vol. 10, pp. 4-12.

Duchatelle, L., L. Vautrey (1964), "Determination des coefficients de convection dún alliage NaK en ecoulement turbulent emtre plasques plates paralleles", *Int. J. Heat and Mass Transfer*, Vol. 7, pp. 1017-1031.

Durbin, P.A. (1993b), "Application of Near-wall Turbulence Model to Boundary Layers and Heat Transfer", *Int. J. Heat Fluid Flow*, Vol. 14, pp. 316-323.

Dwyer, O.E. (1963), "Eddy Transport in Liquid Metal Teat Transfer", *A. I. Ch. E. J.*, Vol. 9, pp. 261-268.

Dwyer, O.E. (1965), "Heat Transfer Through Liquid Metals Flowing Turbulently Between Parallel Plates", *Nuc. Sci. Eng.*, Vol. 21, pp. 79-89.

Dwyer, O.E. (1966), "Recent Developments in Liquid Metal Heat Transfer", *Atomic Energy Review*, Wien, Vol. 4(1), pp. 3-94.

Dwyer, O.E. (1976), "Liquid Metal Heat Transfer", Sodium-NaK Engineering Handbook, Vol. 2, pp. 73-191.

Eckert, E.R.G., R.M. Drake (1972), "Analysis of Heat and Mass Transfer", McGraw-Hill Book Corporation, New York.

El Hadidy, M.A., F. Gori, D.B. Spalding (1982), "Further Results on the Heat Transfer to Low Prandtl Number Fluids in Pipes", *Num. Heat Transfer*, Vol. 5, pp. 107-117.

Faggiani, S., Gori, F. (1980), "Influence of Streamwise Molecular Heat Conduction of the Heat Transfer Coefficient for Liquid Metals in Turbulent Flow Between Parallel Plates", *J. Heat Transfer*, Vol. 102, pp. 292-296

Foust, O.J (1972), "Sodium-NaK Engineering Handbook", Vol. 1, Sodium Chemistry and Physical Properties, Gordon and Breach Science Publishers, ISBN0677030204.

Friedland, A.J., O.E. Dwyer, W.M. Maresca, C.F. Bonilla (1961a), "Heat Transfer to Mercury in a Parallel Flow Through Rod Bundles of Circular Rods", *Int. Dev. in Heat Transfer*, Am. Soc. Mech. Eng., New York, Part III, pp. 526-534.

Friedland, A.J., C.F. Bonilla (1961b), "Analytical Study of Heat Transfer Rates for Parallel Flow of Liquid Metals Through Tube Bundles. Part II", *AIChE J*., Vol. 7, pp. 107-122.

Fuchs, H. (1973), "Wärmeübergang an strömendes Natrium", Eidg. Institut für Reaktorforschung, Würelingen, Bericht Nr. 241, Schweiz.

Gardner, R.A. (1969), "Magneto Fluid Mechanic Pipe Flow in a Transverse Magnetic Field with and without Heat Transfer", PhD Thesis Purdue University, West Lafayette, Ind.

Gartner, D., K. Johannsen, H. Ramm (1974), "Turbulent Heat Transfer in a Circular Tube with Circumferrentially Varying Thermal Boundary Conditions", *Int. J. Heat and Mass Transfer*, Vol. 17, pp. 1003-1018.

Gebhardt, B. (1971), "Heat Transfer", MacGraw Hill Book Corp., New York.

Genin, L.G., E.V. Kudryavtseva, Yu.A. Pakhotin, V.G. Sviridov (1978), Temperature Fields and Heat Transfer for a Turbulent Flow of Liquid Metal on an Initial Thermal Section", *Teplofiz. Vysokikh. Temp*., Vol. 16 (6), pp. 1243-1249.

Gibson, C.H., W.H. Schwarz (1963a), "The Universal Equilibrium Spectra of Turbulent Velocity and Scalar Fields", *J. Fluid Mech*., Vol. 16, pp. 365-384.

Gibson, C.H., W.H. Schwarz (1963b), "Detection of Conductivity Fluctuations in a Turbulent Flow Field", *J. Fluid Mech*., Vol. 16, pp. 357-364.

Gilliland, E.R., R.J. Musser, W.R. Page (1951), "Heat Transfer to Mercury", *Gen. Disc. on Heat Transfer*, Inst. Mech. Eng. and ASME, London, pp. 402-404.

Gräber, H., M. Rieger (1973), "Experimentelle Untersuchung des Wärmeübergangs an Flüssigmetalle (NaK) in parallel durchströmten Rohrbündeln bei konstanter und exponentieller Wärmeflussdichteverteilung", *Atomkernenergie*, Vol. 19, pp. 23-40.

Graetz, L (1883), "Über die Wärmeleitungsfähigkeiten von Flüssigkeiten. Part 1", *Ann. Phys. Chem*., Vol. 18, pp. 79-94.

Graetz, L. (1885), "Über die Wärmeleitungsfähigkeiten von Flüssigkeiten, Part 2", *Ann. Phys. Chem*., Vol. 25, pp. 337-357.

Grant, H.L., B.A. Hughes, W.M. Vogel, A. Moilliet (1968), "The Spectrum of Temperature Fluctuations in Turbulent Flow", *J. Fluid Mech*., Vol. 34, pp. 423-442.

Grigull, U., Tratz, H. (1965), "Thermischer Einlauf in ausgebildeter laminarer Rohrströmung", *Int. J. Heat and Mass Transfer*, Vol. 8, pp. 669-678.

Grötzbach, G., M. Wörner (1992), "Analysis of Second Order Transport Equations by Numerical Simulation of Turbulent Convection in Liquid Metals", *Proc. 5th Int. Topical Meeting on Nuclear Reactor Thermal-hydraulics (NUETH-5)*, Am. Nuc. Soc., Vol. 2, pp. 358-365.

Grötzbach, G., A. Batta, C-H. Lefhalm, I. Otic (2004), "Challenges in Thermal and Hydraulic Analyses of ADS Target Systems", *6th Int. Conf. on Nuclear Thermal Hydraulics, Operations and Safety (NUTHOS6)*, Nara, Japan, 4-8 Oct. 2004, paper ID N6P005.

Guo, J., P.Y. Julien (2003), "Modified Log-wake Law for Turbulent Flow in Smooth Pipes", *Journal of Hydraulic Research*, Vol. 41, No. 5, pp. 493-501.

Hanjalic, K., B.E. Launder (1972), "A Reynolds Stress Model of Turbulence and its Application to Asymmetric Shear Flows", *J. Fluid Mech*., Vol. 52, pp. 609-638.

Harlow, F.H., P.I. Nakayama (1968), *Transport of Turbulent Energy Decay Rate*, Los Alamos Scientific Laboratory Report LA 3584.

Hartnett, J.P., T.F. Irvine (1957), "Nusselt Values for Estimating Liquid Metal Heat Transfer in Non-circular Ducts", *AIchE J*., Vol. 3, pp. 313-317.

Hatton, A.P., A. Quarmby (1963), "The Effect of Axially Varying and Unsymmetrical Boundary Conditions on Heat Transfer with Turbulent Flow Between Parallel Plates", *Int. J. Heat and Mass Transfer*, Vol. 6, pp. 903-914.

Hatton, A.P., A. Quarmby, I. Grundy (1964), "Further Calculations on the Heat Transfer with Turbulent Flow Between Parallel Plates", *Int. J. Heat and Mass Transfer*, Vol. 7, pp. 813-823.

Hausen, H. (1943), "Darstellung des Wärmeübergangs in Rohren durch verallgemeinerte Potenzbeziehungen", *VDI-Zeitung*, Suppl. "Verfahrenstechnik", No. 4, pp. 91-98.

Heng,L., C. Chan, S.W. Churchill (1998), "Essentially Exact Characteristics of Turbulent Convection in a Round Tube", *Chemical Engineering Journal*, Vol. 71, pp. 163-173.

Hennecke, D.K. (1968), "Heat Transfer by Hagen-Poiseulle Flow in the Thermal Development Region with Axial Conduction", *Wärme-und Stoffübertragung*, Vol. 1, pp. 177-184.

Hickman, H.J (1974), "An Asymptotic Study of the Nusselt-Graetz Problem, Part 1: Large x Behaviour", *Int. J. Heat and Mass Transfer*, Vol. 96, pp. 354-358.

Hlavac, P.J., O.E. Dwyer, M.A. Helfant (1969), "Heat Transfer to Mercury Flowing In-line Through an Unbaffled Rod Bundle: Experimental Study on the Effect of Rod Displacement on Rod-averaged Heat Transfer Coefficients", *J. Heat Transfer*, Vol. 91, pp. 568-580.

Hornbeck, R.W. (1964), "Laminar Flow in the Entrance Region of a Pipe", *Appl. Sci. Res*., Vol. A13, pp. 224-232.

Horsten, E.A. (1971), "Combined Free and Forced Convection on Turbulent Flow of Mercury", PhD Thesis, University of Cape Town, Cape Town, South Africa.

Hsu, C.J. (1965), “Heat Transfer in a Round Tube with Sinusoidal Wall Heat Flux Distribution”, *AIchE J*., Vol. 11, pp. 690-695.

Hsu, C.J. (1968), “Exact Solution to Entry Region of Laminar Heat Transfer with Axial Conduction and the Boundary Conditions of the Third Kind”, *Chem. Eng. Sci*., Vol. 23, pp. 457-468.

Jackson, J.D. (1983), “Turbulent Mixed Convection Heat Transfer to Liquid Sodium”, *Int. J. Heat Fluid Flow*, Vol. 4, pp. 107-111.

Jacoby, J.K. (1972), “Free Convection Distortion and Eddy Diffusivity Effects in Turbulent Mercury Heat Transfer”, MS Thesis, Purdue University, West Lafayette, Indiana.

Jenkins, R. (1951), “Variation of the Eddy Conductivity with Prandtl Modulus and its Use in Prediction of Turbulent Heat Transfer Coefficients”, *Proc. of the Heat Transfer and Fluid Mechanics Institute*, Stanford University Press, Stanford, CA.

Jischa, M., H.B. Rieke (1979), “About the Prediction of Turbulent Prandtl Numbers and Schmidt Numbers from Modelled Transport Equations”, *Int. J. Heat and Mass Transfer*, Vol. 22. pp. 1547-1555.

Jischa, M. (1982), “Konvektiver Impuls-, Wärme- und Stoffaustausch”, Vieweg Verlag, Braunschweig, ISBN 3-528-08144-9 (in German).

Jones, W.P., B.E. Launder (1972), “The Prediction of Laminarization with a Two-equation Model of Turbulence”, *Int. J. Heat and Mass Transfer*, Vol. 15, pp. 301-314.

Kalish, S., O.E. Dwyer (1967), “Heat Transfer to NaK Flowing Through Unbaffled Rod Bundles”, *Int. J. Heat and Mass Transfer*, Vol. 10, pp. 1533-1558.

Karcz, M., J. Badur (2005), “An Alternative Two-equation Turbulent Heat Diffusivity Closure”, *Int. J. of Heat and Mass Transfer*, Vol. 48, pp. 2013-2022.

Kasagi, N., Y. Tomita, A. Kuroda (1992), “Direct Numerical Simulation of Passive Scalar Field in a Turbulent Channel Flow”, *ASME J. Heat Transfer*, Vol. 144, pp. 598-606.

Kasagi, N., Y. Ohtsubo (1993), “Direct Numerical Simulation of Low Prandtl Number Thermal Field in a Turbulent Channel Flow”, in *Turbulent Shear Flows*, Vol. 8, Springer, Berlin, pp. 97-119.

Kawamura, H. (1995) “Direct Numerical Simulation of Turbulence by Finite Difference Scheme”, in *The Recent Developments in Turbulence Research*, International Academic Publishers, pp. 54-60.

Kawamura, H., K. Ohsaka, H. Abe, K. Yamamoto (1998), “DNS of Turbulent Heat Transfer in Channel Flow with Low to Medium-high Prandtl Number Fluid”, *Int. J. of Heat and Fluid Flow*, Vol. 19, pp. 482-491.

Kawamura, H., H. Abe, Y. Matsuo (1998), “DNS of Turbulent Heat Transfer in Channel Flow with Respect to Reynolds and Prandtl Number Effects”, *Int. J. of Heat and Fluid Flow*, Vol. 20, pp. 196-207.

Kays, W.M., E.Y. Leung (1963), “Heat Transfer in Annular Passages: Hydrodynamically Developed Turbulent Flow with Arbitrarily Prescribed Wall Heat Flux”, *Int. J. Heat and Mass Transfer*, Vol. 6, pp. 537-557.

Kays, W.M., M.E. Crawford (1993), "Convective Heat and Mass Transfer", 3rd Ed. McGraw-Hill, New York.

Kays, W.M. (1994), "Turbulent Prandtl Number – Where Are We?", *Trans. of the ASME,* Vol. 116, pp. 285-295.

Kazimi, M.S., M.D. Carelli (1976), "Heat Transfer Correlations for Analysis of CRBRP Assemblies", CRBRP-ARD-0034, Westinghouse Electric Corp., Madison, Penn.

Keenan, J. (1941), "Thermodynamics", Wiley, New York.

Kerr, R.M. (1990), "Velocity, Scalar and Transfer Spectra in Numerical Turbulence", *J. Fluid Mech*., Vol. 211, pp. 309-332.

Kim, J., P. Moin (1989), "Transport of Passive Scalars in a Turbulent Channel Flow", *Proc. 6th Int. Symp. on Turbulent Shear Flows*, Toulouse, 7-9 Sept. 1989, Springer Verlag Berlin-Heidelberg, pp. 85-96.

Kim, J., P. Moin (1989), "Transport of Passive Scalars in a Turbulent Channel Flow", in *Turbulent Shear Flows*, Vol. 6, Springer, Berlin, pp. 85-96.

Knudsen, J.G., D.L. Katz (1958), "Fluid Dynamics and Heat Transfer", MacGraw Hill Book Corp., New York.

Kowalski, D.J. (1974), "Free Convection Distortion in Turbulent Mercury Pipe Flow", M.S. Thesis, Purdue Univ., West Lafayette.

Kraichnan, R.H. (1971), "Inertial-range Transfer in Two- and Three-dimensional Turbulence", *J. Fluid Mech*., Vol. 47, pp. 525-535.

Kunz, H.R., S. Yerazunis (1969), "An Analysis of Film Condensation, Film Evaporation and Single Phase Heat Transfer for Liquid Prandtl Numbers from 10^{-3} to 10^{4}", *J. Heat Transfer*, Vol. 91C, pp. 413-420.

Lamb, H. (1945), "Hydrodynamics", Dover, New York.

Lau, S.C., E.M. Sparrow, J.W. Ramsey (1981), "Effect of Plenum Length and Diameter on Turbulent Heat Transfer in a Downstream Tube and on Plenum Related Pressure Losses", *J. Heat Transfer*, Vol. 103, pp. 415-422.

Launder, B.E., D.B. Spalding (1974), "The Numerical Computation of Turbulent Flows", *Comp. Meth. Appl. Mech. Eng*., Vol. 3, pp. 269-289.

Launder, B.E., G.J. Reece, W. Rodi (1975), "Progress in the Development of a Reynolds Stress Turbulence Closure", *J. Fluid Mech*., Vol. 68, pp. 537-566.

Lee, S.L. (1983), "Liquid Metal Heat Transfer in Turbulent Pipe Flow with Uniform Heat Flux", *Int. J. Heat and Mass Transfer*, Vol. 26, pp. 349-356.

Lefhalm, C.H., N.I. Tak, G. Groetzbach, H. Piecha, R. Stieglitz (2003), "Turbulent Heat Transfer Along a Heated Rod in Heavy Liquid Metal Flow", *Proceedings of the 10th International Topical Meeting on Nuclear Reactor Thermal Hydraulics (NURETH-10)*, Seoul, Korea, 5-9 October 2003.

Lefhalm, C-H., N-I. Tak, H. Piecha, R. Stieglitz (2004), "Turbulent Heavy Liquid Metal Heat Transfer Along a Heated Rod in an Annular Cavity", *Journal of Nuclear Materials*, Vol. 335, pp. 280-285.

Leslie, D.C. (1977), "A Recalculation of Turbulent Heat Transfer to Liquid Metals", *Lett. Heat and Mass Transfer*, Vol. 4, pp. 25-33.

Leveque, M.A. (1928), "Le lois de la transmission de chaleur par convection", *Ann. Mines*, Mem., Ser. 12, Vol. 13, pp. 201-299, pp. 305-362, pp. 381-415.

Lin, C.C. (1961), "The Theory of Hydrodynamic Stability", Cambridge University Press.

Lin, B.S., C.C. Chang, C.T. Wang (2000), "Renormalization Group Analysis for Thermal Turbulent Transport", *Physical Review E*, Vol. 63, pp. 16304-16311.

Lubarski, B., S.J. Kaufman (1955), *Review of Experimental Investigations of Liquid Metal Heat Transfer*, NACA Technical Note, TN-3336.

Lykoudis, P.S., Y.S. Touloukian (1958), "Heat Transfer in Liquid Metals", *Trans. Am. Soc. Mech. Engnrs*., Vol. 80, pp. 653-666.

Lyon, R.N. (1949), *Forced Convection Heat Transfer Theory and Experiments with Liquid Metals*, USAEC Report, ORNL-361, Oak Ridge National Laboratory.

Lyon, R.N. (1951), "Liquid Metal Heat Transfer Coefficients", *Chem. Engng. Progr*., Vol. 47 (2), pp. 75-79.

Lyon, R.N. (1952), "Liquid Metals Handbook", Navexos P-733, 2nd ed.

Lyons, S.L., T.J. Hanratty, J.B. McLaughlin (1991), "Direct Numerical Simulation of Passive Heat Transfer in a Turbulent Channel Flow", *Int. J. Heat Mass Transfer*, Vol. 34, pp. 1149-1161.

Malang, S., L. Barleon, L. Bühler, H. Deckers, S. Molokov, U. Müller, P. Norajitra, J. Reimann, H. Reiser, R. Stieglitz (1992), "MHD Work on Self-cooled Liquid-metal Blankets Under Development at the Nuclear Research Center Karlsruhe", *Perspectives in Energy*, Vol. 2, pp. 303-312.

Manceau, R., S. Parneix, D. Laurence (2000), "Turbulent Heat Transfer Predictions Using the v^2–f Model on Unstructured Grids", *Int. J. Heat Fluid Flow*, Vol. 21, pp. 320-328.

Marchese, A.R. (1972), "Experimental Study of Heat Transfer to NaK Flowing In-line Through a Tightly Packed Rod Bundle", *13th Nat. Heat Transfer Conf*., Denver, Col., AIChE Paper No.36, Am. Inst. Chem. Eng.

Maresca, M.W., O.E. Dwyer (1964), "Heat Transfer to Mercury Flowing In-line Through a Bundle of Circular Tubes", *J. Heat Transfer*, Vol. 86, pp. 180-196.

Martinelli, R.C. (1947), "Heat Transfer to Molten Metals", *Trans. of the ASME*, Vol. 69, p. 947ff.

Michelson, M.L, J. Villadsen (1974), "The Graetz Problem with Axial Heat Conduction", *Int. J. Heat and Mass Transfer*, Vol. 17, pp.1391-1402.

Mills, A.F. (1962), "Experimental Investigation of Heat Transfer in the Entrance Region of a Circular Conduit", *J. Mech. Eng. Sci*., Vol. 4, pp. 63-77.

Mizushina, T., T. Sasano (1963), "The Ratio of the Eddy Diffusivities of Heat and Momentum and its Effect on the Liquid Metal Heat Transfer", *Int. Dev. Heat Trans*., pp. 662-668.

Mizushina, T., R. Ito, F. Ogina, H. Muramoto (1969), "Eddy Diffusivities for Heat in the Region Near the Wall", *Mem. Fac. Engng. Kyoto Univ*., Vol. 31, pp. 169-181.

Möller, R., H. Tschöke (1978), "Local Temperature Distributions in the Critical Duct Wall Zones of LMFBR Core Elements. A Status of Knowledge, Unsettled Problems and Possible Solutions", *Proc. ANS/ASME Int. Top. Meet. Nuc. Reac. Thermal Hydraulics*, Saratoga, NY, Vol. 3, pp. 1871-1881.

Molki, M., E.M. Sparrow (1983), "In-tube Heat Transfer for Skewed Inlet Flow Caused by Competition Among Tubes Fed by the Same Plenum", *J. Heat Transfer*, Vol. 105, pp. 870-877.

Nagano, Y., C. Kim (1988), "A Two-equation Model for Heat Transport in Wall Turbulent Shear Flows", *Trans. ASME, J. Heat Transfer*, Vol. 110, p. 583ff.

Nagano, Y., M. Shimada, M.S. Youssef (1994), "Progress in the Development of a Two-equation Heat Transfer Model Based on DNS Data Bases", *Proc. Int. Symp. on Turbulence, Heat and Mass Transfer*, Lisbon, 9-12 Aug. 1994, pp. 3.2.1-3.2.6

Nagano,Y., M. Shimada (1995), "Rigorous Modeling of Dissipation-rate Equation Using Direct Simulations", *Jpn. Soc. Mech. Eng. Int. J. Ser. B*, 38, p. 51.

Nagano, Y. (2002), "Modelling Heat Transfer in Near-wall Flows", in *Closure Strategies for Modelling Turbulent and Transitional Flows*, B.E. Launder, N.D. Sandham (Eds.), Cambridge University Press, Cambridge.

Ng, K.H., D.B. Spalding (1972), "Turbulence Model for Boundary Layers Near Walls", *Phys. Fluids*, Vol. 15, pp. 20-30.

Nimmo, B., O.E. Dwyer (1965), "Heat Transfer to Mercury Flowing In-line Through a Rod Bundle", *J. Heat Transfer*, Vol. 87, pp. 312-313.

Nimmo, B., O.E. Dwyer (1966), "Experimental Study on Turbulent Flow of Mercury in Annuli", *Nuc. Sci. Eng*., Vol. 19, p. 48ff.

Nijsing, R. (1972), *Heat Exchange and Heat Exchangers with Liquid Metals*, AGRD-LS-57-12, AGRD Lecture Series No. 57, on Heat Exchangers by J.J. Ginoux.

Notter, R.H. (1969), "Two Problems in Turbulence", PhD Thesis, University of Washington, Seattle.

Notter, R.H., C.H. Sleicher (1972), "A Solution to the Turbulent Graetz-Problem III Fully Developed and Entrance Region Heat Transfer Rates", *Chem. Eng. Sci*., Vol. 27, 2073-2093.

Ooi, A., G. Iaccarino, P.A. Durbin, M. Behnia (2002), "Reynolds Averaged Simulation of Flow and Heat Transfer in Ribbed Ducts", *Int. J. Heat Fluid Flow*, Vol. 23, pp. 750-757.

Otic, I., G. Grötzbach, M. Wörner (2005), "Analysis and Modelling of the Temperature Variance Equation in Turbulent Natural Convection for Low-Prandtl-number Fluids", *J. Fluid Mech*., Vol. 525, pp. 237-261.

Pashek, M. (1967), *Study of Local Heat Transfer and Thermal Fields in a Seven Rod Bundle with Axial Flow of Sodium*, UJV-1815, Nuc. Res. Inst., CSSR.

Petrovichev, V.I. (1959), "Heat Transfer in Concentric Annuli", *Atomn. Energ*., Vol. 7, pp. 366-369.

Piller, M., E. Nobile, T.J. Hanratty, (2002), "DNS Study of Turbulent Transport at Low Prandtl Numbers in a Channel Flow", *J. Fluid Mech*., Vol. 458, pp. 419-441.

Prandtl, L. (1928), "Bemerkungen über den Wärmeübergang in einem Rohr", *Phys. Z*., Vol. 29, pp. 487-489.

Quarmby, A., R.K. Anand (1970), "Turbulent Heat Transfer in the Thermal Entrance Region of Concentric Annuli with Uniform Wall Heat Flux", *Int. J. Heat and Mass Transfer*, Vol. 13, pp. 395-411.

Quarmby, A., R. Quirk (1972), "Measurements of the Radial and Tangential Eddy Diffusivities of Heat and Mass in Turbulent Flow in a Plain Tube", *Int. J. Heat and Mass Transfer*, Vol. 15, pp. 2309-2327.

Quarmby, A., R. Quirk (1974), "Axisymmetric and Non-axisymmetric Turbulent Diffusion in a Plain Circular Tube at High Schmidt Number", *Int. J. Heat and Mass Transfer*, Vol. 17, pp. 143-148.

Ramm, H., K. Johannsen (1973), "Radial and Tangential Turbulent Diffusivities of Heat and Momentum in Liquid Metals", *Prog. Heat and Mass Transfer*, Vol. 7, pp. 45-58.

Reed, C.B. (1987), "Convective Heat Transfer in Liquid Metals", Chapter 9 from *Handbook of Single-phase Convective Heat Transfer*, S. Kakac, R. Shah, W. Aung (Eds.), John Wiley & Sons, ISBN 0471-817-02-3.

Rehme, K. (1987), "Convectvie Heat Transfer Over Rod Bundles", Kakac, Shah, Aung (Eds.), John Wiley & Sons, New York, ISBN 0-471-81702-3.

Rensen, Q. (1981), "Experimental Investigation of the Turbulent Heat Transfer to Liquid Sodium in the Thermal Entrance Region of an Annulus", *Nuc. Eng. Design*, Vol. 68, pp. 397-404.

Reynolds, W.C. (1963), "Turbulent Heat Transfer in a Circular Tube with Variable Circumferential Heat Flux", *Int. J. Heat and Mass Transfer*, Vol. 6, pp .445-454.

Reynolds, W.C. (1976), "Computation of Turbulent Flows", *Ann. Rev. Fluid Mech*., Vol. 8, pp. 183-208.

Roberts, A., H. Barrow (1967), "Turbulent Heat Transfer in the Vicinity of the Entry of an Internally Heated Annulus", *Proc. Inst. Mech. Engnrs*., Vol. 182, Pt3H, pp. 269-276.

Rodi, W. (1980), *Turbulence Models and Their Application in Hydraulics*, Monograph Int. Association of Hydraulic Research, Delft, The Netherlands.

Rodi, W. (1981), “Progress in Turbulence Modelling for Incompressible Flows”, *AIAA*, Paper 81-0045.

Roshenow, W.M., L.S. Cohen (1960), *Turbulent Transfer of Heat*, MIT Heat Transfer Lab Report.

Rohsenow, W.M., H. Choi (1961), “Heat, Mass and Momentum Transfer”, Prentice Hall, Englewood-Cliffs, New Jersey.

Rotta, J.C. (1972), “Turbulente Strömungen”, B.G. Teubner Stuttgart.

Sakakibara, M., K. Endo (1976), “Analysis of Heat Transfer for Turbulent Flow Between Parallel Plates”, *Int. Chem. Eng.*, Vol. 18, pp. 728-733.

Sakakibara, M. (1982), “Analysis of Heat Transfer in the Entrance Region with Fully Developed Turbulent Flow Between Parallel Plates – The Case of Uniform Wall Heat Flux”, Mem. Fac. of Eng. Fukui Univ., Vol.30 (2), pp. 107-120.

Schlichting, H., Truckenbrodt (1960), “Aerodynamik des Flugzeugs”, Springer Verlag, Berlin.

Schlichting, H., (1979), “Boundary Layer Theory”, 7th ed., McGraw-Hill, New York.

Schrock, S.L. (1964), “Eddy Diffusivity Ratio in Liquid Metals”, PhD Thesis, Purdue Univ., West Lafayette, Ind.

Schulz, B. (1986), *Thermophysical Properties in the System LiPb*, KfK-4144.

Shikazono, N., N. Kasagi (1996), “Second-moment Closure for Turbulent Scalar Transport at Various Prandtl Numbers”, *Int. J. Heat Mass Transfer*, Vol. 39, pp. 2977-2987.

Seban, R.A. (1950), “Heat Transfer Through a Fluid Flowing Turbulently Between Parallel Walls with Asymmetric Wall Temperatures”, *Trans. ASME*, Vol. 72, pp. 789-795.

Seban, R.A., T.T. Shimazaki (1951), “Heat Transfer to a Fluid Flowing Turbulently in a Smooth Pipe with Walls at Constant Temperature”, *Trans. ASME*, Vol. 73, pp. 803-809.

Senechal, M. (1968), “Contribution to Convection Theory for Liquid Metals”, Thèse 3e cycle, Paris.

Shah, R.K., A.L. London (1978), “Laminar Flow Forced Convection in Ducts”, Supplement 1 to *Advances in Heat Transfer*, Academic, New York.

Shah, R.K., R.S. Johnson (1981), “Correlations for Fully Developed Turbulent Flow Through Circular and Non-circular Channels”, *Proc. 6th Int. Heat and Mass Transfer Conf.*, Indian Inst. of Techn., Madras, India, D75-D95.

Sheriff, N., D.J. O’Kane (1981), “Sodium Eddy Diffusivity and Heat Measurements in a Circular Duct”, *Int. J. Heat Mass Transfer*, Vol. 24, pp. 205-211.

Shibani, A.A., M.N. Özisik (1977), “A Solution to Heat Transfer in Turbulent Flow Between Parallel Plates”, *Int. J. Heat and Mass Transfer*, Vol. 20, pp. 565-573.

Siegel, R., E.M. Sparrow, T.M. Hallman (1958), “Steady Laminar Heat Transfer in a Circular Tube with Prescribed Wall Heat Flux”, *Appl. Sci. Res.*, Vol. A7, pp. 386-392.

Skupinski, E., J. Tortel, L. Vautrey (1965), “Determination des coefficients de convection d’un allage sodium-potassium dans un tube circulaire”, *Int. J. Heat and Mass Transfer*, Vol. 8, pp .937-951.

Sleicher, C.A., M. Tribus (1956), “Heat Transfer in a Pipe with Turbulent Flow and Arbitrary Wall Temperature Distributions”, 1956 Heat Transfer and Fluid Mechanics Institute, Stanford Univ. Press, Stanford, CA, pp. 59-78.

Sleicher, C.A., M. Tribus, Jr. (1957), “Heat Transfer in a Pipe with Turbulent Flow and Arbitrary Wall Temperature Distribution”, *Trans. ASME*, Vol. 79, pp. 789-797.

Sleicher, C.A. (1958), “Experimental Velocity and Temperature Profiles for Air in a Turbulent Pipe Flow”, *Trans. Am. Soc. Mech. Engns*., Vol. 80, pp. 693-703.

Sleicher, C.A., A.S. Awad, R.H. Notter (1973), “Temperature and Eddy Diffusivity Profiles in NaK”, *Int. J. Heat and Mass Transfer*, Vol. 16, pp. 1565-1575.

Sleicher, C.J., M.W. Rouse (1975), “A Convenient Correlation for Heat Transfer to Constant and Variable Property Fluids in Turbulent Pipe Flow”, *Int. J. Heat Mass Trans*., Vol. 18, pp. 677-683.

Smith, D.L., *et al*. (1984), *Blanket Comparison and Selection Study*, Final report; ANL/FPP-84-1, Vol. 2, Chapter 6.

Sommer, T.P., R.M. So, Y.G. Lai (1992), “A Near-wall Two-equation Model for Turbulent Heat Fluxes, *Int. J. Heat Mass Transfer*, Vol. 35, pp. 3375-3387.

Sparrow, E.M., S.H. Lin (1963), “Turbulent Heat Transfer in a Tube with Circumferentially Varying Temperature and Wall Heat Flux”, *Int. J. Heat and Mass Transfer*, Vol. 6, pp. 866-867.

Sparrow, E.M., S.V. Patankar, H. Shahrestani (1978), “Laminar Heat Transfer in a Pipe Subjected to Circumferentially Varying External Heat Transfer Coefficients”, *Num. Heat Transfer*, Vol. 1, pp. 117-127.

Sparrow, E.M., K.K. Moram, M. Charmchi (1980), “Heat Transfer and Pressure Drop Characteristics Induced by a Slat Blockage in a Circular Tube”, *J. Heat Transfer*, Vol. 102, pp. 64-70.

Sparrow, EM., J.E.O. O’Brien (1980), “Heat Transfer Coefficients on the Downstream Face of an Abrupt Enlargement or Inlet Constriction in a Pipe”, *J. Heat Transfer*, Vol. 102, pp. 408-414.

Sparrow, E.M., M. Molki, S.R. Chastain (1981), “Turbulent Heat Transfer Coefficients and Fluid Flow Patterns on the Surface of a Centrally Positioned Blockage in a Duct”, *Int. J. Heat and Mass Transfer*, Vol. 24, pp. 507-519.

Sparrow, E.M., L.D. Bosmans (1983), “Heat Transfer and Fluid Flow Experiments with a Tube Fed by a Plenum Having Non-aligned Inlet and Exit”, *J. Heat Transfer*, Vol. 105, pp. 56-63.

Sparrow, E.M., U. Gurdal (1983), “Heat Transfer at an Upstream Facing Surface Washed by Fluid En Route to an Aperture in the Surface”, *Int. J. Heat and Mass Transfer*, Vol. 24, pp. 851-857.

Sparrow, E.M., A. Chaboki (1984), “Swirl Affected Turbulent Fluid Flow and Heat Transfer in a Circular Tube”, *J. Heat Transfer*, Vol. 106, pp. 766-773.

Speziale, C.G., R.M.C. So (1998), "Turbulence Modelling and Simulation", in *The Handbook of Fluid Dynamics*, R.W. Johnson (Ed.), CRC Press LLC, Boca Raton, Florida, pp. 14.1–14.111.

Stasiulevivius, J., A. Skrinska (1988), "Heat Transfer of Finned Tube Bundles in Crossflow", Hemisphere Publishing Corporation, ISBN-0-89116-360-3.

Subbotin, V.I., P.A. Ushakov, B.N. Gabrianovich, A.V. Zhukov (1961), "Heat Exchange Through the Flow of Mercury and Water in a Tightly Packed Rod Pile", *Sov. At. Energy*, Vol. 9, pp. 1001-1009.

Subbotin, V.I., A.K. Papovyants, P.L. Kirillov, N.N. Ivanovskii (1962), "A Study of Heat Transfer to Molten Sodium in Tubes", *At. Energiya* (USSR), Vol. 13, pp. 380-382.

Subbotin, V.I., P.A. Ushakov (1964), "Heat Removal from Reactor Fuel Elements Cooled by Liquid Metals", *Proc. 3rd Int. Conf. of Peaceful Uses of Atomic Energy*, Geneva, Vol. 8, United Nations, New York, pp. 192-203.

Subbotin, V.I., P.A. Ushakov, A.V. Zhukov, V.D. Talanov (1967), "The Temperature Distribution in Liquid Metal Cooled Fuel Elements", *At. Energiya*, Vol. 22, pp. 372-378.

Subbotin, V.I., P.A. Ushakov, A.V. Zhukov, E.Y. Sviridenko (1970), "Temperature Fields of Fuel Elements in the BOR Reactor Core", *Sov. At. Energy*, Vol. 28, pp. 620-621.

Subbotin, V.I. (1974), "Heat Exchange and Hydrodynamics in Channels of Complex Geometry", *Proc. 5th Int. Heat Transfer Conf.*, Tokyo, Vol. 6, pp. 89-104.

Subbotin, V.I., P.A. Ushakov, A.V. Zhukov, N.M. Matyukhin, Y.S. Jur´év, L.K. Kudryatseva (1975) "Heat Transfer in Cores and Blankets of Fast Breeder Reactors – A Collection of Reports", *Symp. of CMEA Countries: Present and Future Work on Creating AES with Fast Reactors*, Obninsk, Vol. 2.

Subbotin, V.I., M.K. Ibragimov, M.N. Ivanovskii, M.N. Arnolbov, E.V. Nomofilov (1992), "Heat Transfer from the Turbulent Flow of Heavy Liquid Metals in Tubes", *The Soviet Journal of Atomic Energy*, Vol. 11 (1), pp. 769-775.

Tang, Y.S., R.D. Coeffield, R.A. Markley (1978), "Thermal Analysis of Liquid Metal Fast Breeder Reactors", *Am. Nuc. Soc*.

Taylor, G.I. (1915), "Transport of Vorticity and Heat Through Fluids in Turbulent Motion", *Phil. Trans. Roy. Soc. London*, A215, pp. 1-16.

Tien, C.L. (1961), "On Jenkins Model of Eddy Diffusivities for Momentum and Heat", *J. Heat Transfer*, Vol. 83C, pp. 389-390.

Todreas, N.E., M.S. Kazimi (1993), "Thermalhydraulic Fundamentals – Nuclear Systems I", Francis and Taylor, ISBN 0-89116-935-0.

Tricoli, V. (1999), "Heat Transfer in Turbulent Pipe Flow Revisited – Similarity Law for Heat and Momentum Transport in Low Prandtl Number Fluids", *International Journal of Heat and Mass Transfer*, Vol. 31, pp. 1535-1540

Tyldesley, J.R., R.S. Silver (1968), "The Prediction of Transport Properties of a Turbulent Fluid", *Int. J. Heat and Mass Transfer*, Vol. 11, pp. 1325-1340.

Tyldesley, J.R. (1969), "Trasnport Phenomena in Free Turbulent Flows", *Int. J. Heat and Mass Transfer*, Vol. 12, pp. 489-496.

Ushakov, P.A., V.I. Subbotin, B.N. Gabrianovich, V.D. Talanov, E.Y. Sviridenko (1963), "Heat Transfer and Thermalhydraulic Resistance in Tightly Packed Corridor Bundle of Rods", *Sov. At. Energy*, Vol. 13, pp. 761-768.

Ushakov, P.A. (1974), "Calculation of the Temperature Fields of Bundles of Fuel Elements in Axial Turbulent Flows of Heat Transfer Media with Vanishing Small Prandtl Number", *High Temp*., Vol. 12, pp. 677-685.

Ushakov, P.A, A.V. Zhukov, N.M. Matyukhin (1976), "Thermal Fields of Rod-type Fuel Elements Situated in Rectangular Lattices Streamlined by a Heat Carrier", *High Temp*., Vol. 14, pp. 482-488.

Ushakov, P.A, A.V. Zhukov, N.M. Matyukhin (1977), "Heat Transfer to Liquid Metals in Regular Arrays of Fuel Elements", *High Temp*., Vol. 15, pp. 868-873.

Ushakov, P.A. (1978), "Problems of Fluid Dynamic and Heat Transfer in Cores of Fast Reactors", *COMECON Symp*., Teplofizika I gidrodynamika aktivnoi zony I parogeneratov dlya bystrykh reaktorov, Marianske Lazne, CSSR, Paper ML78/01, pp. 14-35.

Ushakov, P.A. (1979), "Problems of Heat Transfer in Cores of Fast Breeder Reactors", *Heat Transfer and Hydrodynamics of Single-phase Flow in Rod Bundles*, Izd. Nauka, Leningrad (in Russian).

Van Driest, E.R. (1956), "On Turbulent Flow Near a Wall", *J. Aerosp. Sci*., Vol. 23, pp. 1007-1011.

Van Dyke, M. (1977), "Perturbation Methods in Fluid Mechanics", Parabolic, Stanford.

Van Vylen, G.J., R.E. Sonntag, "Fundamentals of Classical Thermodynamics", 2nd edition, Wiley, New York.

Von Karman (1931), "Mechanische Ähnlichkeit und Turbulenz", *Nachr. Ges. Wiss. Göttingen, Math. Phy. Klasse*, No. 5, pp. 58-76.

Walz, A. (1966), "Strömungs- und Temperaturgrenzschichten", G. Braun Verlag Karlsruhe (in German).

Wassel, A.T., I. Catton (1973), "Calculation of Turbulent Boundary Layers Over Flat Plates with Different Phenomenological Theories of Turbulence and Variable Turbulent Prandtl Number", *Int. J. Heat and Mass Transfer*, Vol. 16, pp. 1547-1563.

Weigand, B. (1996), "An Extract Analytical Solution for the Extended Turbulent Graetz Problem with Dirichlet Wall Boundary Conditions for Pipe and Channel Flows", *Int. J. Heat Mass Transfer*, Vol. 39 (8), pp. 1625-1637.

Weinberg, D. (1975), *Temperaturfelder in Bündeln mit Na-Kühlung- Thermo- und Fluiddynamische Unterkanalanalyse der Schnellbrüter-Brennelemente und ihre Relation zur Brennstabmechanik*, Kernforschungszentrum Karlsruhe, KfK-2232.

Wesley, D.A., E.M. Sparrow (1976), "Circumferentially Local and Average Heat Transfer Coefficients in a Tube Downstream of a Tee", *Int. J. Heat and Mass Transfer*, Vol. 19, pp. 1205-1214.

White, F.M. (1974), “Viscous Fluid Flow”, McGraw-Hill Comp., New York.

Wilcox, D.C., R.M. Traci (1976), “A Complete Model of Turbulence”, *AIAA*, Paper 76-351, San Diego. CA.

Wilcox, D.C. (1986), “Multiscale Model for Turbulent Flows”, *24th Aerospace Science Meetings*, American Institute of Aeronautics and Astronautics.

Yakhot, V., S.A. Orszag, A. Yakhot (1987), “Heat Transfer in Turbulent Fluids Pipe Flow”, *Int. J. Heat Mass Transfer*, Vol. 30, pp. 15-22.

Yu, B., H. Ozoe, S.W. Churchill (2001), “The Characteristics of Fully Developed Turbulent Convection in a Round Tube”, *Chemical Engineering Science*, Vol. 56, pp. 1781-1800.

Zagarola, M.V. (1996), “Mean-flow Scaling of Turbulent Pipe Flow”, PhD Dissertation, Princeton University, N.J.

Zagarola, M.V., A.J. Smits (1997), “Scaling of the Mean Velocity Profile for Turbulent Pipe Flow”, *Physical Review Letters*, Vol. 78, No. 2, pp. 239-242.

Zhi-quing, W. (1982), “Study of Correction Coefficients of Laminar and Turbulent Entrance Region Effect in Round Pipe”, *Appl. Math. Mech*., Vol. 3 (3), pp. 433-446.

Zhukov, A.V., V.I. Subbotin, P.A. Ushakov (1969a), “Heat Transfer from Loosely Spaced Rod Clusters to Liquid Metal Flowing in the Axial Direction”, *Liquid Metals*, Engl. Translation, NASA Rep. NASA-TT-F522, pp. 149-169.

Zhukov, A.V., L.K. Kudryatseva, E.Y. Sviridenko, V.I. Subbotin, D.V. Talanov, P.A. Ushakov (1969b), “Experimental Studies of Temperature Fields Using Models”, *Liquid Metals*, Engl. Translation, NASA Rep. NASA-TT-F522, pp. 170-189.

Zhukov, A.V., M.N. Matyukhin, A.B. Muzhanov, Y.Y. Sviridenko, P.A. Ushakov (1973), *Methods of Calculating Heat Exchange of Liquid Metals in Regular Lattices of Fuel Elements and Some New Experimental Data*, FEI-404, Inst. of Physics and Energy, Obninsk, AEC-TR-7549.

Zhukov, A.V., M.N. Matyukhin, E.V. Nomofilov, A.P. Sorokin, V.S. Yurev (1978), “Temperature Distribution in Non-standard and Deformed Fuel Pin Grids of Fast Reactors”, *COMECON Symp*. Teplofizika I gidrodynamika aktivnoi zony I parogeneratov dlya bystrykh reaktorov, Marianske Lazne, CSSR, Paper ML78/11.

Zhukov, A.V., M.N. Matyukhin, Y.Y. Sviridenko (1982), *Einfluss von Geometriestörungen auf die Temperaturfelder und den Wärmeübergang in den Unterkanälen von Brennelementbündeln Schneller Reaktoren*, FEI-979, Fiziko-energeticheskii Institut Obninsk. German Translation: KfK-Tech. Rep. 675.